FINAL REPORT

PROTECTIVE COATINGS FOR CHROMIUM ALLOYS

by

Marvin Negrin
Allan Block

prepared for

NATIONAL AERONAUTICS AND SPACE ADMINISTRATION

July 13, 1967

CONTRACT NAS 3-7273

Technical Management
NASA Lewis Research Center
Cleveland, Ohio
Robert Oldrieve, Project Manager
S.J. Grisaffe, Research Advisor

TABLE OF CONTENTS

TABLE OF CONTENTS (Cont.)

TABLE OF CONTENTS (Cont.)

TABLE OF CONTENTS (Cont.)

LIST OF ILLUSTRATIONS

LIST OF ILLUSTRATIONS (Cont.)

LIST OF ILLUSTRATIONS (Cont.)

LIST OF ILLUSTRATIONS (Cont.)

LIST OF ILLUSTRATIONS (Cont.)

LIST OF ILLUSTRATIONS (Cont.)

LIST OF TABLES

FOREWORD

This is the Final Summary Report on National Aeronautics and Space Administration Contract No. NAS 3-7273 administered by the Lewis Research Center, Cleveland, Ohio. The NASA Project Manager for this contract has been Mr. Robert Oldrieve and the NASA Research Advisor was Salvatore Grisaffe. This report covers the period from November 1, 1965 to July 13, 1967

Chromalloy personnel contributing to the experimental work and to the writing of this report were:

- Allan Noetzel — Mgr. Metallurgical Services
- Leonard Maisel — Technical Director, Chromalloy Division
- Dr. Harry Brill-Edwards — Technical Director, Turbine Support Division
- Martin Epner — General Manager, Turbine Support Division
- Richard Hines
- John Garcia
- T. Milidantri — Research Technicians

PROTECTIVE COATINGS FOR CHROMIUM ALLOYS

By

M. NEGRIN and A. BLOCK

ABSTRACT

A variety of aluminum-base coatings were deposited by pack-cementation methods on a prototype chromium base alloy Cr-5W-Y The coatings were of both the simple and modified aluminum types. Promising systems were examined in great detail by cyclic and continuous oxidation, ductile-brittle-transition testing, metallography, and electron beam microprobe techniques.

Of the systems studied, a simple aluminum (Cr_5Al_8-type) and iron-aluminum [$(Fe\text{-}Cr)_xAl_y$ type] produced the best results. Under static oxidation (cyclic-static) these systems survived >1000 hours at 2100°F and approximately 200 hours at 2400°F. Under dynamic conditions coating failures appeared in much shorter periods of time. Protectiveness of these systems is closely related to $AlCr_2O_4$, and $FeO \cdot Al \cdot Cr_2O_4$ type spinel formation. Life of these systems is further limited to a point where nitrogen penetration of the substrate is observed.

Moderate increases in DBTT were noted after coating. However, far greater increases were noted after oxidation exposure.

1

INTRODUCTION

1.1 GENERAL

Through the years gas turbine engine manufacturers have sought to sophisticate their engines and minimize operating costs by increasing the thrust - to - weight ratio and necessarily decreasing the specific fuel consumption. To this end more stringent demands have been made of ancillary technologies i.e. lubricants, fuels, materials, etc. The key to increasing specific fuel consumption lies in increasing the thermal efficiency of the gas turbine engine by increasing the turbine inlet temperature.

Engine manufacturers and alloy producers have thus concentrated their efforts on the development of turbine blade and stator alloys with high temperature properties superior to those of current generation nickel and cobalt base alloys. However, for application at material temperatures in excess of 2000° F., the use of alloy systems of nickel and cobalt appear prohibitive due to their strength, rigidity, melting point, and corrosive attack limitations. As a result of the latter, a solution to the existing problem must be found in using ceramic materials, composite (i.e. fiber and/or dispersion strengthened) materials and/or refractory metals. However, there are many limitations possessed by these materials and they are well known. However, dispersion and/or fiber reinforced materials e.g. TD nickel and TD - nickel - chromium, may in fact represent some potential use for the aforementioned requirements.

A survey of all those materials capable of withstanding the anticipated severe conditions of new - generation turbine engines cannot discount the extremely attractive properties of chromium.

Several investigators have demonstrated quite clearly that chromium base alloys maintain an outstanding degree of resistance to deformation (creep) and oxidation at elevated temperatures. Further, its high melting point (3500°F), low density (relative to the refractory metals and superalloys) and high strength at temperatures in excess of 2000°F surely place it in a position of extreme promise. Although this list of chromium's attractiv properties is impressive, another list enumerating its inherent deficiencies would be almost equal in size. The most significant of these deficiencies are those of low temperature brittleness and severe nitrogen diffusion (and subsequent embrittlement) at elevated temperature. Since it was the goal of this development contract to retain the pre-exposure ductility of chromium after high temperature air exposure, the immediate aims were necessarily the development of coating systems capable of:

Inhibiting the diffusion of nitrogen into the program designated Cr-5W-.02Y alloy (a prototype alloy chosen to establish a state-of-the-art for coating Cr alloys).

Increasing the oxidation resistance in the range 2100-2400°F while not causing embrittlement due to any chemical reactions resulting from the coating process.

Minimizing chromium losses due to its high vapor pressure at temperature in excess of 2100°F.

This contract encompassed the development and evaluation of aluminum coatings on the designated Cr-5W-Y alloy, with the ultimate goal being the protection of the substrate for 3000 hours at 2400°F. The coating systems under development consisted of:

1. Spinel forming coatings:

   Al-Fe, Al-Co, Al-Fe-Co.

2. Simple Aluminum and solid solution tetravalent types:
   Al, Al-Ti
3. Spinel - tetravalent element types:
   Al-Fe-Co, Al-Co-Ti, Al-Fe-Ti
4. Any and/or all of the above with an incorporated glassy phase.

1.2 LITERATURE REVIEW

Concomitant with the actual experimental work early in the program, a brief literature review was conducted so as to obtain a better understanding of the oxidation-nitrification kinetics of chromium. The results of the literature review are summarized and presented below:

There are numerous reports in the literature that chromium can form oxides of the type Cr_2O_3, Cr_3O_4, CrO and CrO_3 and nitrides of the type Cr_2N and CrN. However, only Cr_2O_3 and Cr_2N have been observed in the products resulting from the corrosion of chromium in air at elevated temperatures. Since the oxide Cr_2O_3 is thermodynamically more stable than the nitride, then the presence of the latter in the corrosion products of chromium must indicate an over-riding influence of kinetic control in the corrosion reactions. It is, therefore, essential that at least a partial understanding of the mass transport mechanisms operative during these reactions be acquired if corrosion resistant coatings for chromium and its alloys are to be developed on a scientific rather than an empirical basis.

In order to expand on the mechanisms of chromium corrosion in air, it is convenient to consider the oxidation and nitrification processes separately.

1.2.1 Mechanism of Chromium Oxidation

It has been conclusively established by inert marker experiments that the oxidation of chromium progresses by the outward diffusion of Cr^{3+} from the substrate through the Cr_2O_3 lattice and reaction with oxygen at the Cr_2O_3/gas interface. (Ref. 1, 2 & 3). This mechanism of growth has been corroborated by independent measurements of cationic and anion mobilities in the Cr_2O_3 lattice which have indicated that the cationic diffusion is some 10,000 times greater than that of anionic diffusion. (Ref. 3). These results are contrary to those reported for Al_2O_3 and Fe_2O_3 (both of which are isomorphous with Cr_2O_3) in which growth is controlled by anionic diffusion through the oxide lattice.

Invariably cation transfer mechanisms can be readily explained in terms of ionic disorder within the oxide lattice (e.g. NiO). However, in the case of Cr_2O_3 the exact nature of the equilibrium defect structure is considerably more complex than most oxide lattices and as yet has not been fully resolved. It has been indicated from electronic property studies that the oxide is a "p" type semi-conductor, (Ref. 3), and attempts have been made to explain the ionic transfer properties by a simple cation vacancy model i.e. $Cr^{3+}_{(2-2x}$ $Cr_xv_xO_3$, where v = vacancy. However, neither of these models can fully explain the observed properties of Cr_2O_3 and it now appears necessary to reconsider the defect lattice in terms of both cation vacancies and interstials, and possibly less mobile anion defects (Ref. 3). The unfortunate outcome of this complex ionic disorder is that the effect of divalent and tetravalent metal ions in the

lattice on the growth rate of Cr_2O_3 cannot be predicted. It has been tentatively suggested, however, that the Ti^{4+} ions in the Cr_2O_3 lattice would reduce the oxidation rate of chromium.

From a protection point of view, the simple fact that Cr^{+3} diffusion is the rate controlling step during the oxidation of chromium (as exemplified by the parabolic growth characteristics [Ref. 5]) is sufficient to indicate the approach that should be taken in developing an oxidation resistant coating. Clearly, the coating should have inherently poor cationic mobility particularly for the relatively large Cr^{+3} ion, and should also be fairly resistant to inward diffusion of oxygen ions to the coating/chromium interface.

In addition to the high propensity of Cr_2O_3 for cation mobility, it has several other inherent properties which are not conducive to efficient corrosion protection as indicated below:

1) Cr_2O_3 is fairly volatile above 2100° F. (Ref. 7) particularly in wet oxygen atmospheres. At such temperatures volatilization will reduce still further the limited protection afforded by the relatively slow diffusion of Cr^{+3} through the Cr_2O_3, and eventually a dynamic equilibrium scale of constant thickness would be established. Clearly, the rate at which this is achieved and the thickness will depend on the partial pressure of the oxygen atmosphere.

2) By virtue of its rhombohedral (considered on hexagonal axes) lattice structure and its ionic nature, dislocation movement within the Cr_2O_3 lattice is severely restricted by both electrostatic and geometric considerations. These restrictions give rise to dislocations of high Burgers vector, and consequently extremely

high energy, with the result that deformation usually proceeds by breakdown into "partials" and stacking faults. The implication of this restricted dislocation probability is that the oxide is inherently brittle even at elevated temperature, and consequently is unable to relieve stress induced during growth or thermal cycling other than by micro-failure. The anisotropic nature of the oxide alone indicates that such expansion and contraction stresses will be induced during thermal cycling, and the high Pilling-Bedworth volume ratio $Cr_2O_3/Cr=2.03$ indicates that severe compressive stresses must also be developed during growth of the oxide. From the point of view of the latter, it is advantageous that the oxide is formed at the Cr_2O_3/oxygen interface, as this will permit a certain degree of stress relief due to the larger periphery of the component.

1.2.2 Intergranular Oxidation of Chromium

Under certain conditions chromium becomes prone to intergranular oxidation with consequential catastrophic failure. From the results of relatively recent work (Ref. 4), it appears that this preferential attack is associated with grain boundary migration during grain growth and recrystallization. It is proposed that oxygen in solution in the chromium is swept up by the grain boundary as it moves until local saturation occurs. At this stage either Cr_2O_3 or Cr_3O_4 will precipitate and restrict further migration of the boundary.

1.2.3 Effect of Alloying on the Oxidation of Chromium

To date there has been relatively little quantitative data published concerning the effect of alloy additions on the oxidation rate of

chromium. However, there have been tentative reports (Ref. 6) that the solid solution strengthening elements, except for molybdenum and vanadium, have little effect on the oxidation rate of chromium in air up to about 1800° F.

Also, there is evidence available (Ref. 7 & 9) which indicates that the resistance of chromium alloys to oxidation can be improved by the addition of small amounts of selected elements such as Th, Ce, and other rare earths. This improvement has been partially attributed to the lower vapor pressure of the Cr_2O_3 formed, and the alloying of the chromite spinels (e.g. NiO Cr_2O_3), (Ref. 6).

Alloy additions can also be effective in reducing the rate at which chromium is lost by direct evaporation from a surface, a process which under certain conditions can by-pass the rate controlling Cr^{+3} diffusion mechanism, (Ref. 9). Aluminum appears to be effective in directly lowering vapor pressure of chromium, and any Al_2O_3 scale formed at the surface further reduces the tendency to evaporate. As previously described, Cr_2O_3 is ineffective in this latter respect.

1.2.4 Mechanism of Chromium Nitrification

Cr_2N, unlike Cr_2O_3, exhibits a high degree of covalent bonding, and consequently its growth is more likely to be controlled by the interstitial diffusion of atomic nitrogen rather than by an ionic diffusion process. This hypothesis is supported by the experimental observation that Cr_2N forms at the existing Cr_2N/Cr interface, which also suggests that the interstitial diffusion of nitrogen is the rate controlling step. (Ref. 8 & 2). Cr_2N has a far greater tendency for accelerated grain boundary growth than Cr_2O_3. This has been demonstrated by parallel oxidation-nitrification tests, in which the

oxide grew in a topochemical fashion (i.e. governed by the specimen surface contour) while the nitride rapidly developed large grain boundary intrusions. This result is to be expected since the rate controlling step during oxidation is diffusion in the oxide, whereas in the nitrification it is in the diffusion in the substrate which will inevitably be more rapid along the grain boundary regions of the disordered lattice.

It follows from the above that a coating which is to provide adequate protection of chromium in air must incorporate a physical diffusion barrier to atomic nitrogen. It has been found in practice that Cr_2O_3 fulfills this requirement to a limited degree, (Ref. 1 & 2) but the porous nature of such oxide layers can give rise to intensified intergranular nitrification. This has been illustrated by hot corrosion tests in oxygen/nitrogen atmospheres of low oxygen potential. Under such conditions a continuous Cr_2O_3 film could not form, and consequently N_2 absorption proceeded relatively unhindered.

It may be inferred from the above that adequate nitrogen protection may well be possible after a pre-oxidation treatment in the absence of nitrogen.

1.2.5 Effect of Alloying on the Nitrification of Chromium

As in the case of oxidation, the literature contains little data on the effect of alloy additions on the nitrification of chromium. However, Sully & Heal (Ref. 8) have studied the corrosion of Cr-Co and Cr-Mn alloys in air, and reported that the large quantities of nitride formed on melting were pure chromium nitrides. These results are at variance with those of Carlile & Hume-Rothery, (Ref. 8), who stated that the nitrides in Cr/Mn alloys were alloy

nitrides of the type $(CrMn)_2N$.

1.2.6 Mixed Oxygen - Nitrogen Corrosion of Chromium

The Cr_2N oxidation and Cr_2O_3 nitrification experiments conducted by Seybolt & Haman (Ref. 2), have contributed significantly towards understanding the nature of the atmospheric corrosion of chromium at elevated temperatures.

This work indicated that the rate of oxidation of a pure chromium surface was the same as that of a nitrided chromium surface. This implies that the rate controlling step in both instances was the same, that is the diffusion of Cr^{3+} through the Cr_2O_3 oxide layer. In addition, it was observed that oxidation of a relatively uniform Cr_2N layer resulted in breakdown of the layer and extensive intergranular intrusion of Cr_2N towards the center of the specimen. The resultant structure closely resembled that observed by Sully & Heal in air melted chromium. This profound change in Cr_2N morphology has been attributed to the liberation of free nitrogen as the more stable Cr_2O_3 is formed.

That is:-

$$2Cr_2N+3O_2 \rightarrow 2Cr_2O_3+N_2$$

This reaction develops a high nitrogen potential at the nitride surface which promotes accelerated diffusion of nitrogen into the core of the specimen. This diffusion, as indicated previously, can occur more rapidly along the structural discontinuities of the grain boundary regions until saturation is achieved and Cr_2N is precipitated.

Contrary to the above, nitrification of a pre-oxidized chromium surface resulted in a relatively uniform Cr_2N layer below the oxide which was basically parallel to the specimen contour. In this case,

the nitrogen potential at the Cr_2N interface was low due to restricted atomic nitrogen diffusion through the oxide.

1.2.7 Protection of Chromium From Mixed Gas Corrosion

It is evident from this brief survey that two independent mass transport mechanisms are operative during the corrosion of chromium in air, on one hand the cationic diffusion of chromium towards the oxide/gas interface, and on the other, the interstitial diffusion of nitrogen towards the free chromium substrate. Clearly a coating system must provide adequate barriers to both of these diffusion processes.

It is inevitable that aluminum must be considered as a potential coating. There is sufficient data available to indicate that Al_2O_3 effectively reduces the diffusion of Cr compared with Cr_2O_3. However, there is no evidence to suggest that it also provides a suitable barrier to nitrogen diffusion other than the fact that AlN is more stable than Cr_2N and, hence, likely to form preferentially. To be effective in these respects, an aluminum containing coating must be applied which retains a high Al content at the surface. This may prove to be difficult to achieve, owing to the high solubility of Al in chromium, and its rapid diffusion at the appropriate coating temperatures.

Even if chromium coatings were effective in restricting Cr^{3+} and N_2 diffusion, it would still be necessary to alloy the surface with a bivalent metal ion in order to form a spinel aluminate of superior plasticity to Al_2O_3.

REFERENCES

1) The Selective Oxidation of Chromium in an Iron-Chromium-Nickel Alloy
R.P. Abeadroth
Trans. A.I.M.E. 1964 Volume 230, P. 1735

2) Oxidation - Nitrification of Chromium at 1000°C
A.N. Seybolt & D.H. Haman
Trans. A.I.M.E. Volume 230, 1966 P. 1294

3) Oxidation of Chromium at 890 - 1200 C
D. Caplan, A. Harvey, M. Cohen
Corrosion Science 1963 Volume 3 P.P. 161 - 175

4) The Occurrence & Partitioning of Impurity Phases in Recrystallized Chromium
R.E. Hook, H.J. Garrett & A.M. Adair
Trans. A.I.M.E. Volume 227 1963 P. 145

5) Oxidation of Chromium
V.I. Arkharov, V.N. Koner, I.S. Traktenberg & S.V. Shumilira
Fiz Metal Metallored Akad Nauk S.S.S.R. Ural S. 190 1951

6) The Status of Chromium-Base Alloy Development
D.M.I.C. Memorandum 6 January 1959

7) Oxidation of Nickel & Cobalt Base Superalloys
D.M.I.C. Report 214 March 1965
C.H. Lund & H.J. Wagner

8) Discussion:- "A note on the effect of nitrogen on the structures of certain alloys of chromium & manganese, & the existence of an intermediate nitride".
Journal of the Institute of Metals 1949-So. Volume 76
P. 719

9) "Oxidation of Nickel-Base Alloys at Elevated Temperatures".
Journal of the Institute of Metals 1966 February P. 24

2

MATERIALS AND PROCEDURES

2.1 SUBSTRATE MATERIAL

Four shipments of 0.0625" thick Cr-5W-Y sheet alloy were delivered to the Chromalloy Division from General Electric's Cleveland facility between 16 December 1965, and 13 July 1967. The material was from four separate heats and the chemical analyses reported by NASA* are shown in Table I below:

TABLE I

CHEMICAL ANALYSES OF NASA-FURNISHED Cr-5W-Y SHEET

		ELEMENT (WITH BALANCE CHROMIUM)							
Heat No.	Form	W %	Y %	C ppm	O ppm	N ppm	H ppm	S ppm	P ppm
57-100	INGOT	4.82	0.085	90	88	30	2	40	20
57-100	SHEET	4.72	0.140	58	94	57	4	30	50
58-100	INGOT	4.78	0.054	80	136	49	1	40	20
58.100	SHEET	4.86	0.070	79	82	44	1	20	<10
64-100	INGOT	4.86	0.120	20	116	23	2	20	50
64-100	SHEET	4.82	0.110	80	49	35	8	50	10
67-100	INGOT	4.83	0.11	80	90	17	1	40	<10
67-100	SHEET	4.90	0.12	<10	41	30	5	70	20

Chromalloy Division also received from General Electric 0.250" thick Cr-5W-Y plate which was employed in the fabrication of the final wedge specimens.

*Reference: "The Pilot Production and Evaluation of Chromium Alloy Sh & Plate", L.J. Goetz, J.R. Hughes, & W.F. Moore, NASA CR-72184, 3/15/6

Cutting and edge preparation of the 0.250" plate was performed by the Battelle Memorial Institute under Sub Contract Number 67-5.

The average results obtained from bend transition (4t radius punch) tests conducted by General Electric on the four heats of material are shown in Table II:

TABLE II

SUMMARY OF BEND TRANSITION TESTS OF Cr-5W-Y SHEET (0.0625" THICK) ALLOY

Heat No.	Longitudinal	Transverse	Average Bend Transition Temperature (°F)
57-100	392°F	842°F	617 (325°C)
58-100	887°F	1067°F	975 (525°C)
64-100	437°F	482°F	458 (237°C)
67-100	302°F	617°F	458 (237°C)

2.2 SUBSTRATE SHEET PREPARATION

2.2.1 Cutting

The sheet material was cut to size using a silicon-carbide cut off wheel with a very heavy coolant (water) flow. The room temperature brittleness of this material was such that it could tolerate no chatter without cracking.

2.2.2 Edge Preparation

After cutting, all corners and edges were radiused

using rubberized abrasive wheels. It has been shown that use of these wheels allows for very rapid preparation of refractory-metal and chromium test specimens.

2.2.3 Cleaning

Following the radiusing procedure, all specimens were washed in running water, degreased in acetone and air-dried.

2.2.4 Identification

Although extremely soft (R_A62) the room temperature brittleness of the substrate precluded the use of metal stamping techniques. However, it was found that if extreme care was taken, a diamond tipped vibratool was adequate to the task.

2.3 RAW MATERIALS

Several metals powders, energizers and metal halides were employed. Table III shows a listing of the materials used:

TABLE III

LISTING OF METAL POWDERS, ENERGIZERS, METAL-HALIDES AND CHEMICALS EMPLOYED IN COATING EXPERIMENTS

Material	Mesh Size
Al Powder	-325
Cr Powder	-100
Al_2O_3 Powder Tabular	-325
Ti Powder	-325
Co Powder	-325
Fe Powder	-325
Ta Powder	-325
$CoBr_2$ Powder	-
$FeBr_2$ Powder	-
K_2SiF_6 Powder	-
I Powder	-
CoI_2 Powder	-
FeI_2 Powder	-
TiH_2	-325

2.4 COATING PROCEDURES

All coatings were deposited by pack cementation methods. Although most procedures employed a halide to act as both a purge and a carrier, many coatings were deposited in a halide-argon atmosphere. Early experiments showed that no nitrogen embrittlement was noted when aluminizing in packs containing iodine as the purge and carrier. However, later experiments

indicated that the addition of argon was necessary to inhibit oxidation and corrosive attack at the surface of parts coated with iron and/or cobalt.

2.4.1 Retorts

Two types of retorts were employed in the program. Figure 2-1 shows a sketch of the retort used in those experiments where a halide was employed as the purge while Figure 2-2 shows a sketch of the assembly used for deposition where argon was employed. It should be noted that all inner boxes were chromized prior to the coating experiments to eliminate the possibility of any interfering chemical reactions associated with the walls (mild steel) of the retort.

2.5 METALLOGRAPHY AND MICROHARDNESS TESTING

Metallographic evaluations were made on all coating systems after both coating and oxidation exposure, where applicable. After coating, specimens were degreased and nickel (nickel sulfamate bath) plated for edge preservation. Oxidation tested specimens were sprayed with graphite so that they could be subsequently nickel plated. Specimens were mounted in bakelite or fiber-filled diallyl phthalate, a thermal-setting resin capable of excellent adherence. Lack of good adherence to the specimen can cause serious problems as manifested by inaccurate results and outgassing during micro-probe analyses. It should be noted that the specimens were not cut prior to mounting so that the problems of cracking, brittle constituent

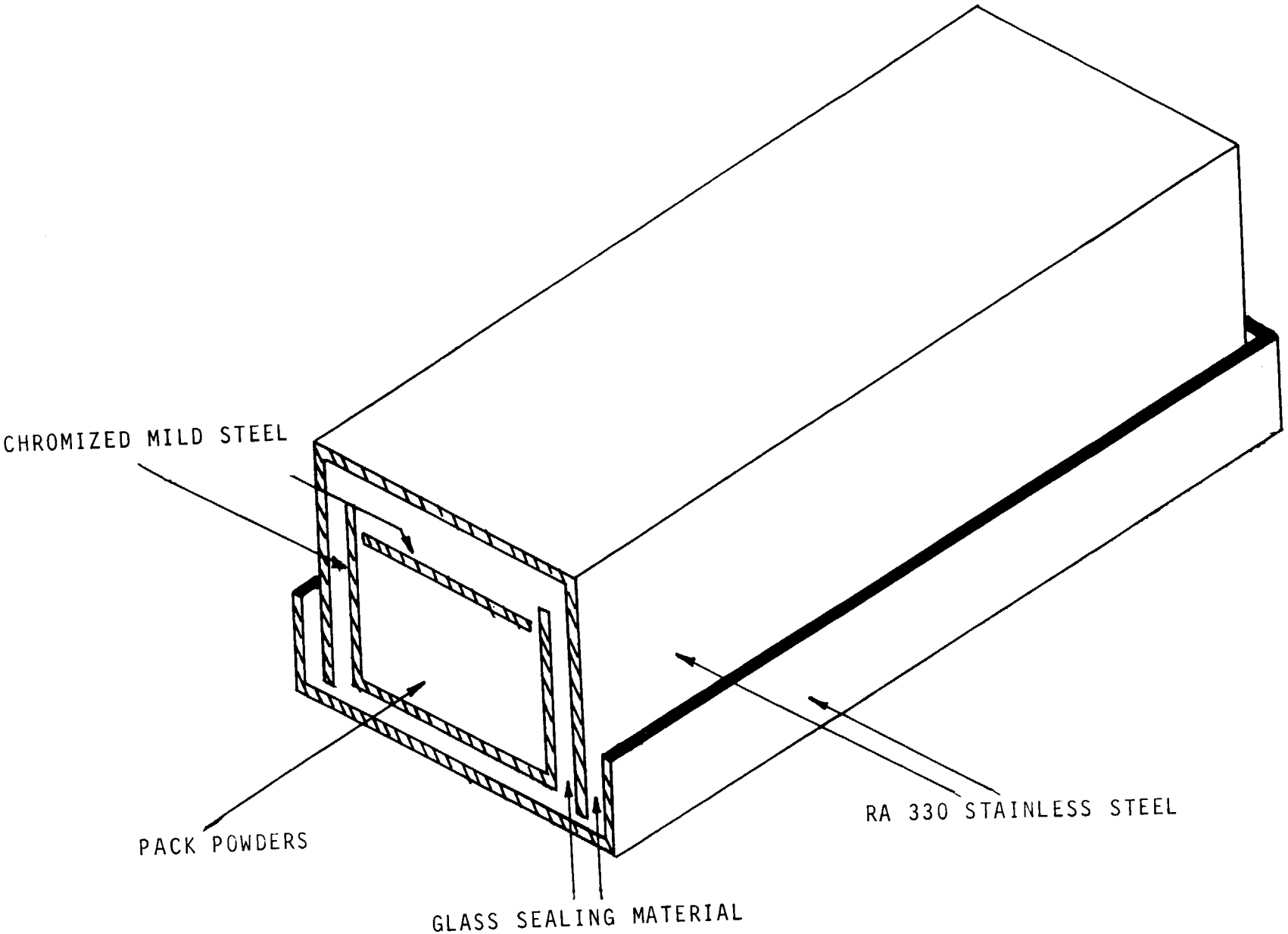

FIGURE 2-1 Schematic Diagram of Pack Cementation-Type Retort

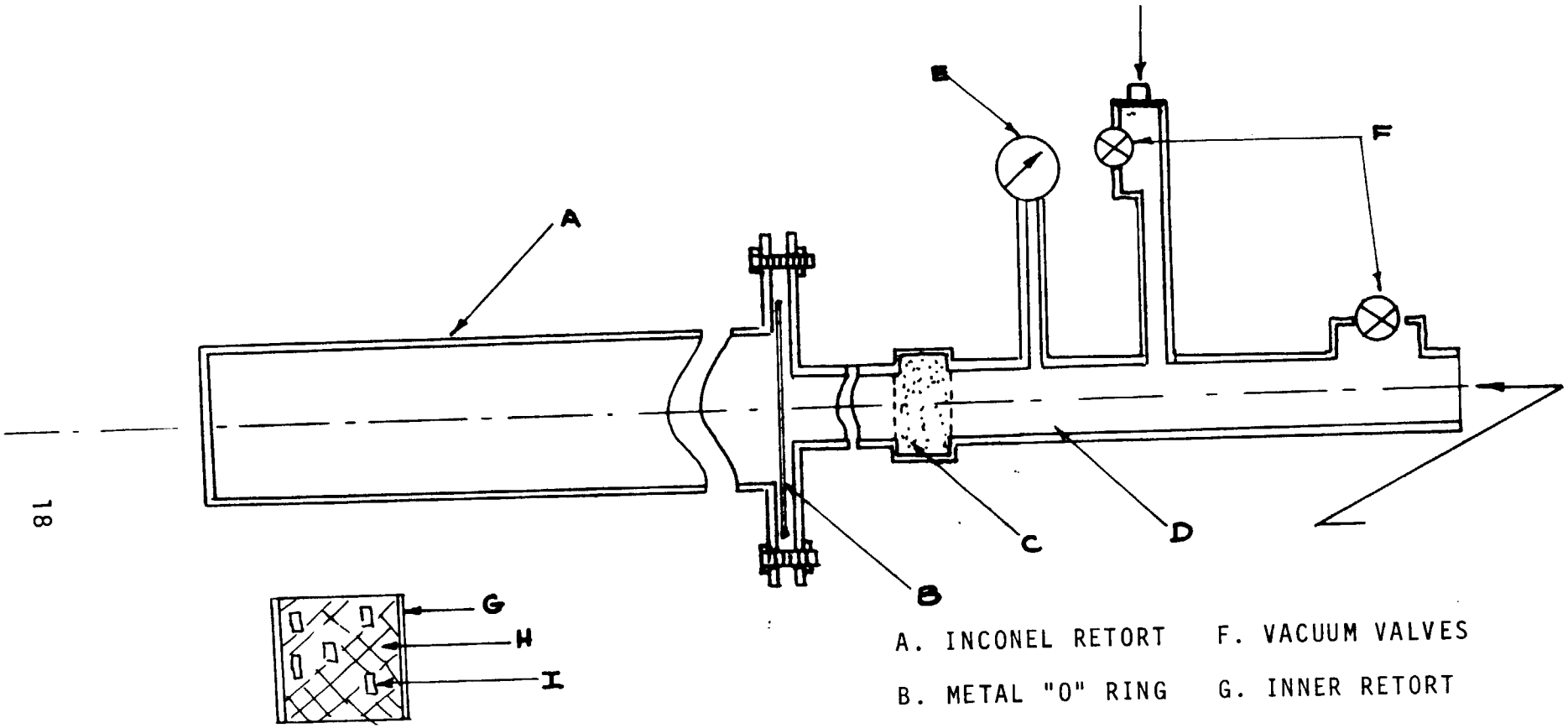

A. INCONEL RETORT
B. METAL "O" RING
C. SILFRAX FILTER
D. EVACUATION TUBE
E. PRESSURE GAGE
F. VACUUM VALVES
G. INNER RETORT
H. PACK POWDERS
I. SAMPLES

FIGURE 2-2

SCHEMATIC DIAGRAM OF PACK-CEMENTATION-TYPE RETORT EMPLOYED WITH INERT OR VACUUM ATMOSPHERES

removal etc. were negated. After mounting, specimens were ground by hand through 600 grit silicon carbide paper and polished successively through 0.3 and 0.05 micron aluminum oxide powders. When microprobe analyses were to be conducted, preparation was altered to employ 6 and 1/4 micron diamond paste followed by final polishing with magnesium oxide. The latter procedure was adopted so as to preclude any effects attributed to the polishing media when analyzing for aluminum in the coatings.

Microhardness determinations were made on a Model AK Riehle-Kentron microhardness tester. Loads of 10 and 25 grams were employed using a Vickers indenter.

2.6 ELECTRON BEAM MICROPROBE ANALYSIS

All analyses were conducted at Chromalloy Division facilities on a Model 400 MAC (Materials Analyses Company) Electron Microprobe Analyzer. This instrument has two spectrometers, minimum beam size of 0.5 microns, electron beam scanning capabilities and ability to analyze for any element down to and including atomic number eleven (sodium).

2.7 BEND TRANSITION TESTING

Bend transition testing equipment was fabricated according to specifications in MAB 192-M (National Academy of Sciences, National Research Council). A nichrome wound resistance furnace (6" x 4" x 3") capable of reaching temperatures of 2000° F. was used for heating. To eliminate the possibility of any deleterious effects due to oxidation, both the die and punch (4t radius)

H-12 steel were coated. One set was aluminized and another chromized (to form chromium - carbide) to eliminate any oxidation and/or galling. Both sets were further heat treated to a hardness of Rc 52.

2.8 OXIDATION TESTING

All oxidation testing performed during the program was accomplished in glow-bar box (7"W x 4"H x 8 1/4"D) and tube (1 1/2" diam.) furnaces. Subsequent to initial weighing, all specimens were individually placed on end in uncovered recrystallized Al_2O_3 crucibles (box furnace) or on Al_2O_3 boats (tube furnace). During cooling all capsules and boats were covered with transite sheet to minimize any weight losses due to spalling, exfoliation, etc.

2.9 EROSION RIG TESTING

Specimens 1" x 4" were tested in a Chromalloy designed, converging burner rig with kerosene employed as the fuel. Flame velocities were approximately Mach 0.5 and the parts rotated at 350 rpm. Temperatures in excess of 2100°F were obtainable. Figure 2-3 shows a photograph of the burner rig in a typical operation.

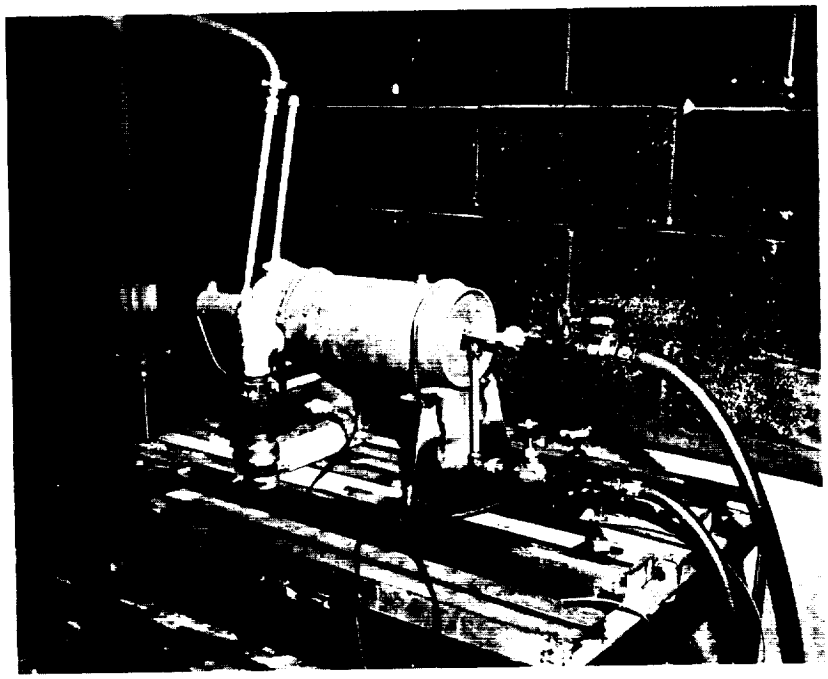

2.10 CONTINUOUS WEIGHT CHANGE OXIDATION TESTING

The tests were conducted using an Ainsworth AU-1 recording balance with the specimen suspended from quartz (in the upper areas of the set-up) and platinum (in hot zone) wire. Further, the tabs were placed in a recrystallized alumina crucible so as to retain any of the oxidation products which spalled or exfoliated during exposure. A stainless steel assembly was employed above the furnace to minimize the effects of exterior air currents while also allowing for a minimum convection current influences. The stainless steel assembly was connected (with air-tight seals) to a mullite tube which was inserted into a platinum-rhodium wound furnace capable of attaining 3000°F temperatures.

3

EXPERIMENTAL RESULTS

3.1 GENERAL

Since some ten different coating systems were evaluated along with bare material, it is most advantageous to present the data developed for each coating system separately. To further simplify all the data obtained the best of each of the coating systems investigated will often be compared (on the basis of oxidation and bend tests) against each other.

3.2 BARE MATERIAL

Concurrent with the initial screening tests conducted on several of the coating systems, base-line oxidation data was necessarily developed on the bare Cr-5W-Y sheet.

Figure 3-1 shows a typical photomicrograph of as-received Cr-5W-Y sheet. A heavily worked microstructure was noted along with some non-metallic inclusions. It is not known whether the cracks seen resulted from metallographic preparation or were in fact prevalent in the as-received material. However, there were repeated cases of observed substrate cracking (throughout the program) in the as-received sheet prior to metallographic preparation.

Figures 3-2 and 3-3 show photomicrographs of the bare material after 100 and 1350 hour exposures (10 hour cycles) at 2100°F., while Figure 3-4 shows the relative effects of exposure to 100 hours at 2100°F and 2400°F. It should be noted that these oxidation tests were conducted such that weight changes were recorded every 10 hours (to 100 hours) and every 24 hours subsequently. Microhardness data (direct reading-10 gram Vickers) are indicated on the photographs. Note the

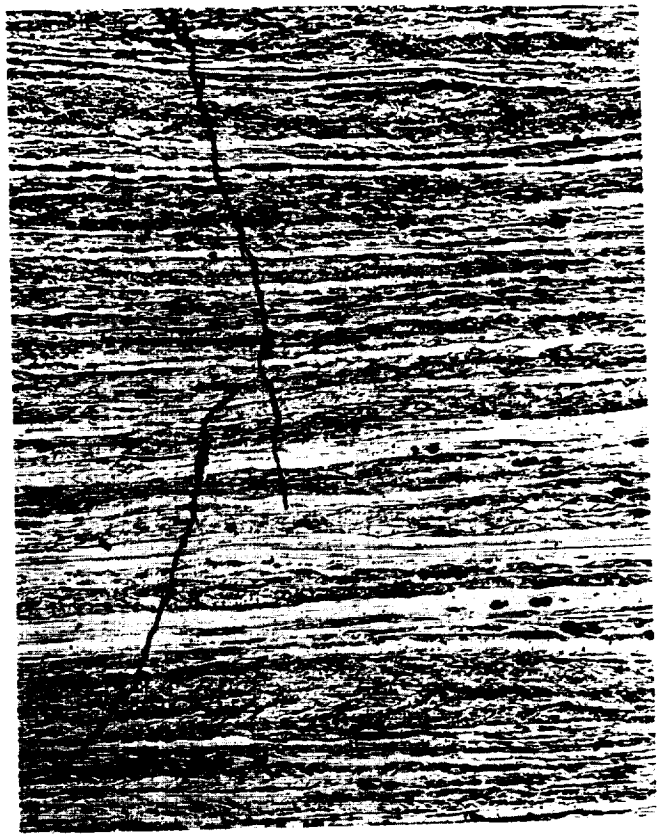

FIGURE 3-1 AS RECEIVED Cr-5W-Y SUBSTRATE SHOWING HEAVILY WORKED STRUCTURE, TRANSGRANULAR CRACKING AND A HIGH INCLUSION (NON-METALLIC) DENSITY

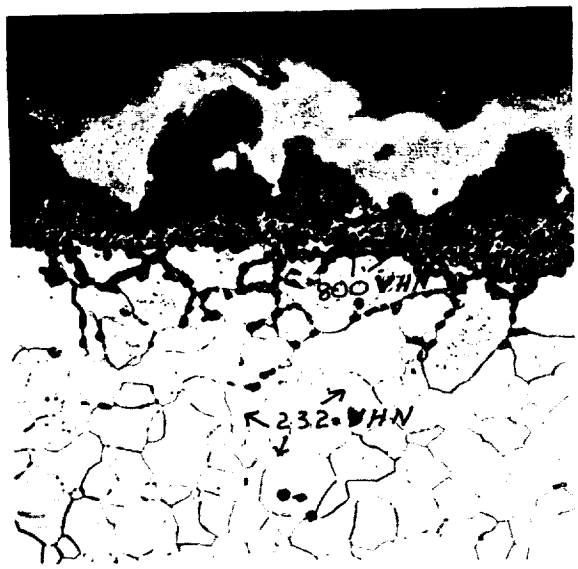

ETCH: 10% OXALIC ACID MAG: 250X

FIGURE 3-2 2100°F/100 HRS

ETCH: 10% OXALIC ACID MAG: 250X

FIGURE 3-3 2100°F/1350 HRS

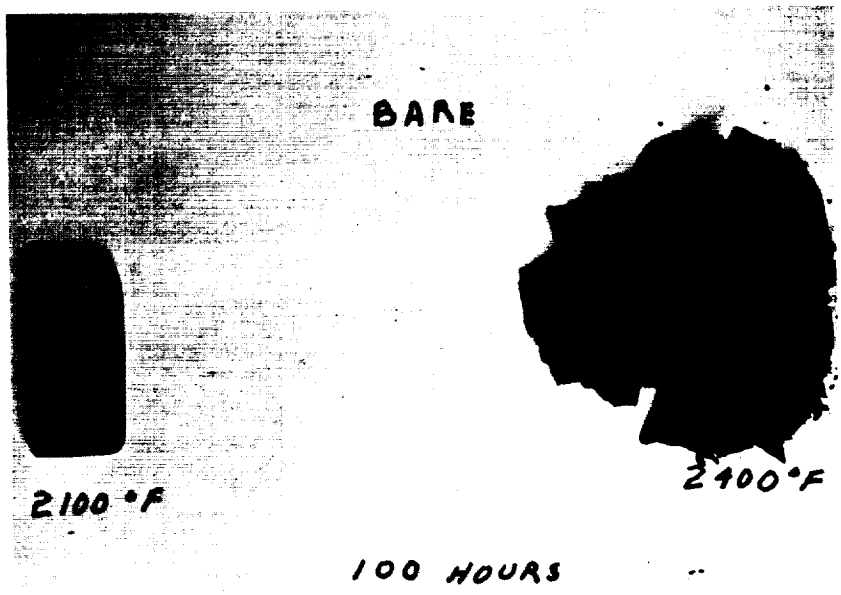

FIGURE 3-4

PHOTOMICROGRAPHS OF BARE Cr-5W-Y ALLOY AFTER EXPOSURE AT 2100°F AND 2400°F FOR VARYING LENGTHS OF TIME. NOTE EXTENT OF INTERGRANULAR NITROGEN ATTACK SHOWN IN FIGURE 3-3 AND EXTENT OF TOTAL ATTACK IN FIGURE 3-4.

severity of the attack on the specimen exposed at 2400°F and, although nitrogen has diffused extensively, the lack of surface spalling and exfoliation on the bare material tested at 2100°F. The adherence of the scale is usually attributed to the formation of an Y-Cr_2O_3- type spinel which according to many investigators inhibits cation (Cr^{+3}) diffusion.

Figure 3-5 shows oxidation curves for bare material tested at 1800, 2100 and 2400°F. These data were developed using cyclic-tests i.e., insertion into a hot furnace for 2 hours, removal and re-insertion four times with weight changes recorded every ten hours. Figure 3-6 shows the results of continuous weight change oxidation tests on the bare Cr-5W-Y alloy. Observed weight changes for a given length of time were less than seen in any of the non-continuous tests. These differences are due to both

a) the lack of any cycling and

b) the more finite supply of air in the relatively closed system.

It would also appear that a parabolic oxidation rate was seen at 2100°F. Figures 3-7, 3-8 and 3-9 show photomicrographs of specimens exposed 100 hours at 1800, 2100 and 2400°F respectively. Note the differences in substrate, grain size, and quantities of nitrogen ingression in the three photographs. Nitrogen attack was seen only after the 2400°F exposure.

Additional work conducted on bare material will be reported on succeeding sections. This work was designed to determine the effect of both the coating thermal cycle and thermal exposure (in inert atmosphere) on the DBTT of bare material.

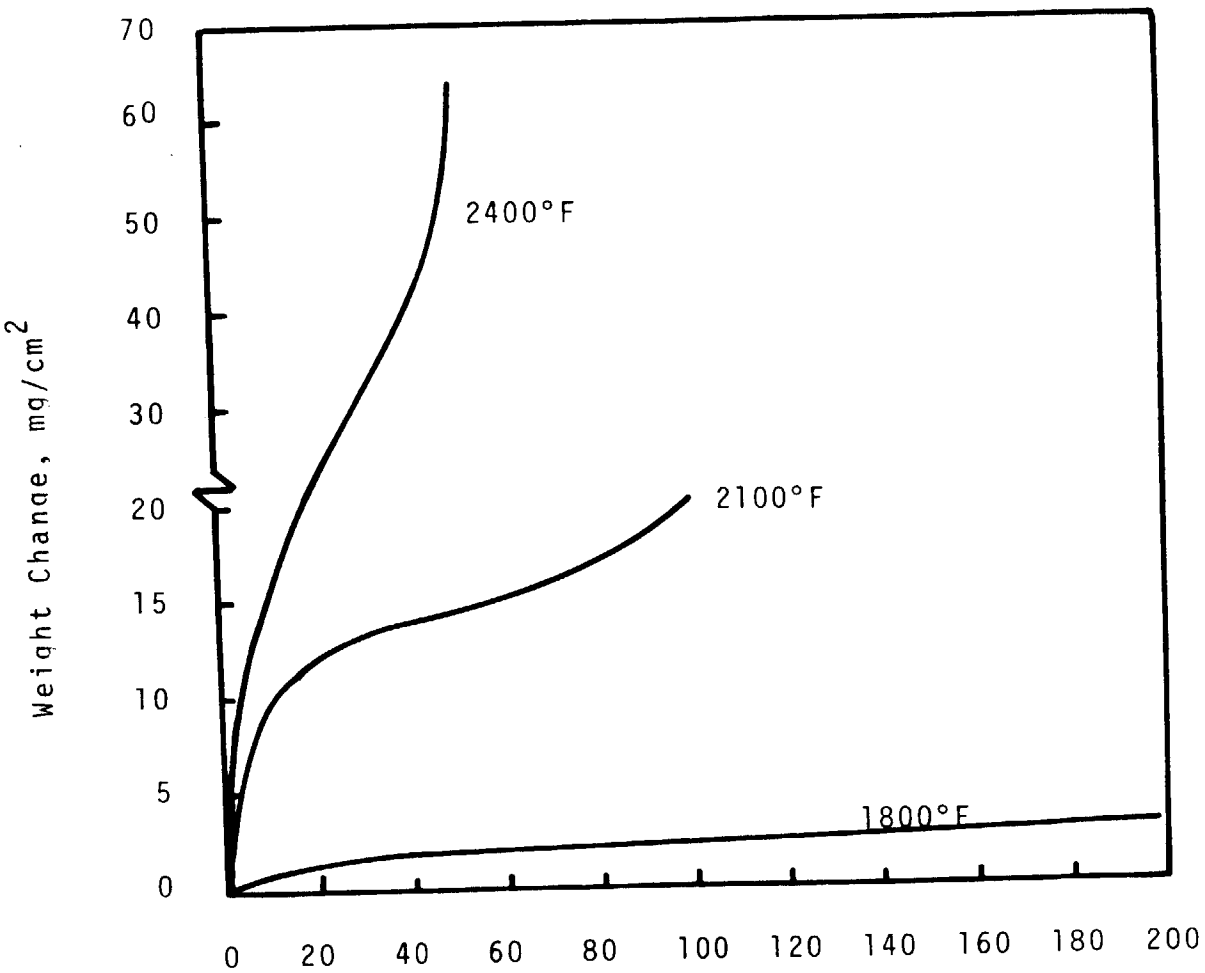

Figure: 3-5

CYCLIC OXIDATION CURVES OF THE
BARE Cr-5W-Y ALLOY

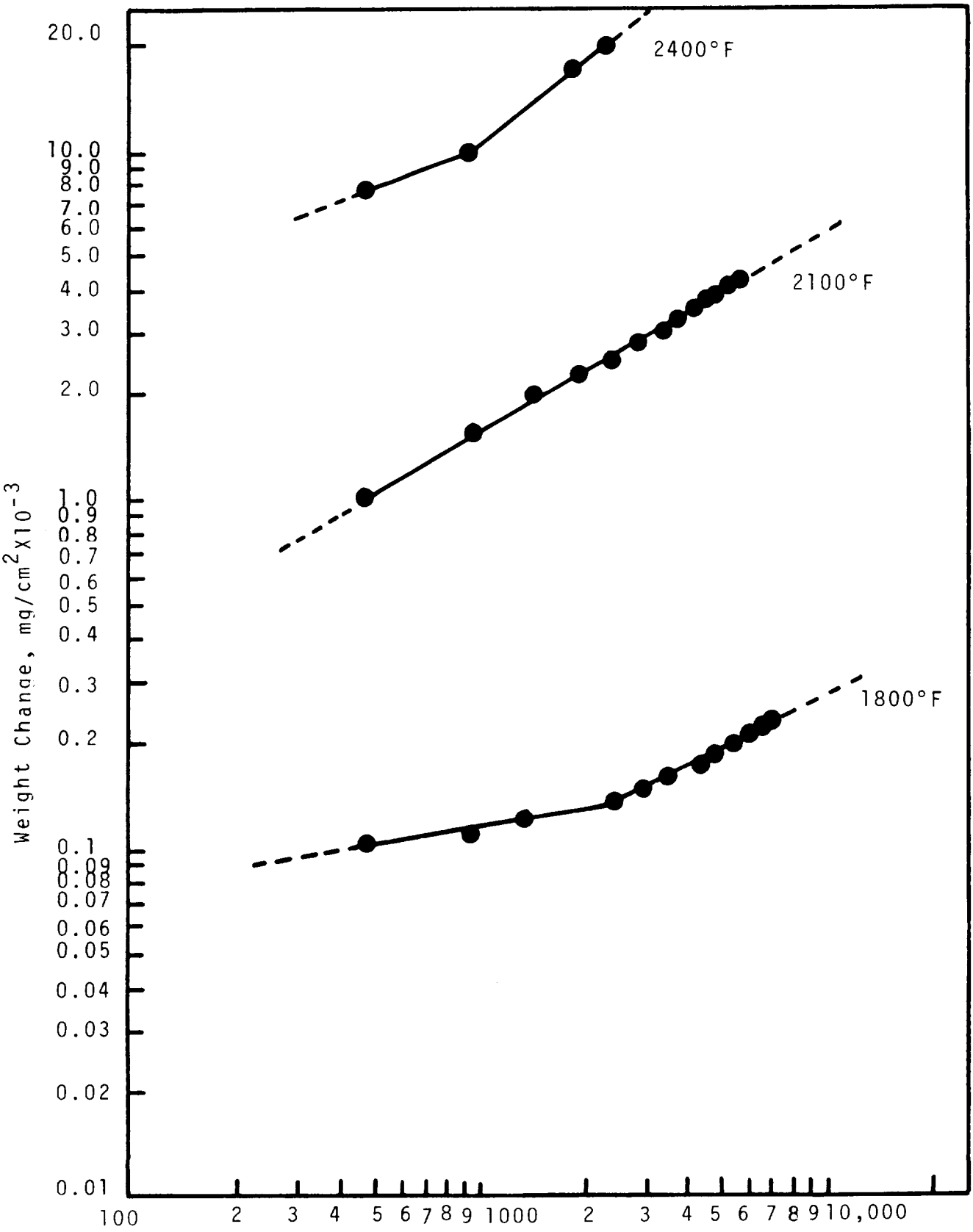

Figure: 3-6

CONTINUOUS OXIDATION CURVES OF THE BARE Cr-5W-Y ALLOY EXPOSED AT 1800, 2100, AND 2400°F

Figure 3-7

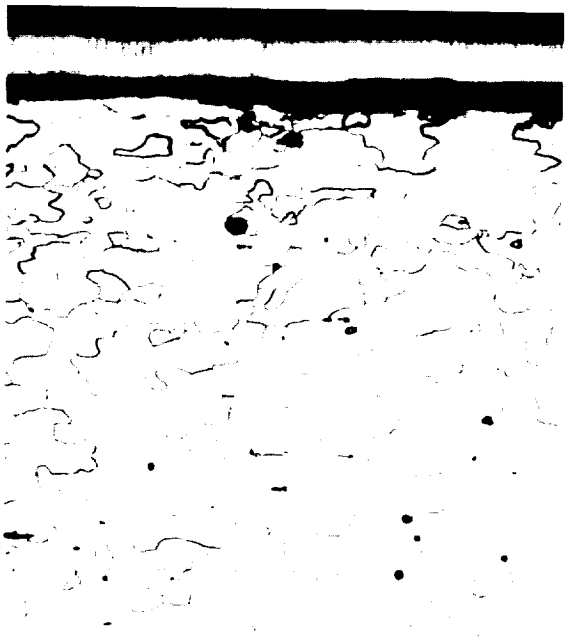

158 VHN

Etch: 10% Oxalic Acid MAG: 250X
1800°F/100 Hrs.

Figure 3-8

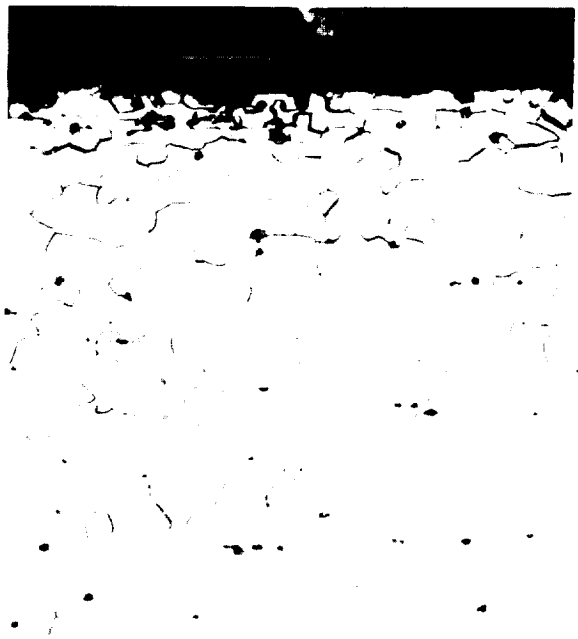

141 VHI

Etch: 10% Oxalic Acid MAG:250X
2100°F/100 Hrs.

Figure 3-9

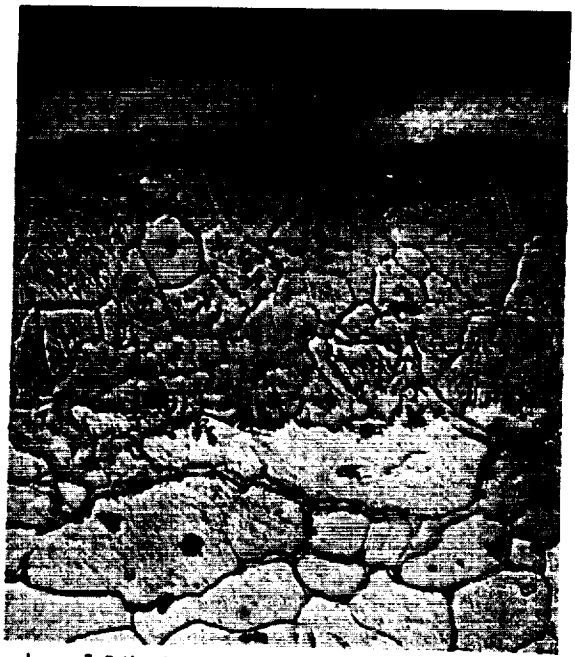

1232 VHN

179 VHN

Etch: 10% Oxalic Acid MAG: 250X
2400°F/100 Hrs.

PHOTOMICROGRAPHS OF BARE Cr-5W-Y ALLOY
AFTER EXPOSURE AT 1800°F, 2100°F AND 2400°F
IN CONTINUOUS OXIDATION

3.3 SIMPLE ALUMINUM SYSTEMS

3.3.1 General

It was inevitable that aluminum be considered as a potential coating for chromium-base alloys, since there is sufficient data available to indicate the following:

Al_2O_3 is a far more effective retardant to chromium diffusion (cation - outward) than is Cr_2O_3.

AlN is more stable thermodynamically than is Cr_2N, suggesting that it would form preferentially.

Aluminum is effective in directly lowering the vapor pressure of chromium while the formation of an Al_2O_3 scale reduced the tendency to evaporate even further.

High chromium bearing alloys of nickel and iron coated with aluminum have shown excellent resistance to corrosive attack at elevated temperatures. It should, however, be noted that alloys of the above type are not usually susceptible to the type of nitrogen ingression seen in chromium alloys, and in fact form spinel aluminates upon exposure at elevated temperatures.

3.3.2 Experimental Coating Trials and Screening Evaluation

Initial pack compositions employed for deposition of the simple-aluminum systems were in most cases derivations of those specifically developed by the Chromalloy Division during some earlier, unreported work on protective systems for chromium bas alloys. Table IV summarizes the experiments on simple-aluminum

TABLE IV
SIMPLE-ALUMINUM-SYSTEM EXPERIMENTAL COATING TRIALS ON Cr-5W-Y ALLOY

GR.	(1) XP #	PACK COMPOSITION Al_2O_3	Al	Cr	--	PROCESSING °F/Hrs	WEIGHT CHANGE mg/cm^2	COATING THICKNESS mils	COMMENTS
	19007	70%	22%	8%	1/4%I_2	1850/10	+2.71	1.5(2)	Adherent, Bright Diffusion Coating
	19013	"	"	"	"	2000/10	+4.87	1.96(2)	" " " "
I	19029	"	"	"	"	1750/10	+1.72	1.0	" " " "
	19049	"	"	"	"	1750/10	+2.79	1.0	" " " "
	19057	"	"	"	"	1850/10	+2.70	1.2	Pack used for 2nd time
	19008	60%+2%Si	30%	"	"	1850/10	+2.4	0.8-1.0	Adherent, Bright Diffusion Coating
II	19011	" "	"	"	"	1800/10	+1.92	0.8	" " " "
	19014	" "	"	"	"	2000/10	+4.79	2.0-2.4	" " " "
	19009	70%	22%	8%	1/4%K_2SiF_6	1850/10	+3.66	1.4-1.7(2)	Adherent, Bright Diffusion Coating
	19010	"	"	"	"	1850/10	+3.65	" "	" " " "
	19012	"	"	"	"	2000/10	+4.87	2.6	" " " "
	19018	"	"	"	"	1850/10	+3.55	1.4	" " " "
	19028	"	"	"	"	1750/10	+1.78	0.8-1.0	" " " "
III	19030	"	"	"	"	1850/10	+3.74	1.4-1.6	" " " "
	19039	"	"	"	"	1850/10	+5.19	---	Heavy Powder"Stick-On"Observed
	19043	"	"	"	"	1850/10	+3.97	1.6	Adherent, Bright Diffusion Coating
	19048	"	"	"	"	1750/10	+2.70	1.0	" " " "
	19050	"	"	"	"	1850/10	+4.21	1.7-1.9	Powder "Stick-On" Observed
	19056	"	"	"	"	1850/10	+3.41	1.2	Pack Used For 2nd Time

TABLE IV (continued)

GR.	(1) XP #	PACK COMPOSITION Al_2O_3	Al	Cr	--	PROCESSING °F/Hrs	WEIGHT CHANGE mg/cm^2	COATING THICKNESS mils	COMMENTS
	19024	87%	3%	10%Ta	1/4%I_2	2000/10	4.88	2.2	Adherent, Bright Diffusion Coating
IV	19040	"	"	"	"	2000/10	6.0-10.0	2.8	Excessive Powder "Stick-On"
	19047	"	"	"	"	2000/10	6.42	2.6	Some Powder "Stick-On" Observed
	19044	92%	8%	0%	"	1850/10	23.16	4.8-5.0	Two Phase Coating Observed
	19055	"	"	"	"	1850/10	19.53		" " " "
	19058	"	"	"	"	1750/10	12.65	3.2	" " " "
V	19059(3)	"	"	"	"	2000/10	29.15	8.6	" " " "
	19062(3)	91	"	1%	"	2000/10	27.84	6.4	" " " "
	19060(3)	90	"	2%	"	2000/10	25.74	6.4	" " " "
	19061(3)	88	"	4%	"	2000/10	21.20	5.2	" " " "

(1) XP # = EXPERIMENT NUMBER

(2) DETERMINED BY MICROPROBE TRACE

(3) XP'S 19059, 19060, 19061, 19062 RUN SIMULTANEOUSLY

systems conducted during the course of this contract. As can be seen from this table, five basic coating systems were attempted and evaluated and are listed as Groups I to V. Within each system, the variable studied most closely was that of processing temperature. This was studied to evaluate the effect on oxidation resistance of different coating thicknesses.

It should be noted that small additions of chromium to the 2ϕ pack were found to result in poorer oxidation resistance. These data were reported in the first semi-annual report issued under this contract. In fact the oxidation was poorer, the greater the chromium additions.

It should be noted that all coating runs made on material to be used during the advanced testing phases are not included in the preceding table (Table IV). The results obtained on these runs (for advanced testing) are included in the text of the report.

From all the data (oxidation, microprobe, etc.) gathered on the systems shown in Table IV, it was decided that two coating systems would be taken into advanced testing. The two systems chosen were to be processed as were experiments XP 19012 and XP 19044, as indicated in Table IV. Figures 3-10 and 3-11 show typical oxidation weight change curves on the two systems selected. A complete discussion of these coating systems is given in the sections which follow.

FIGURE: 3-10

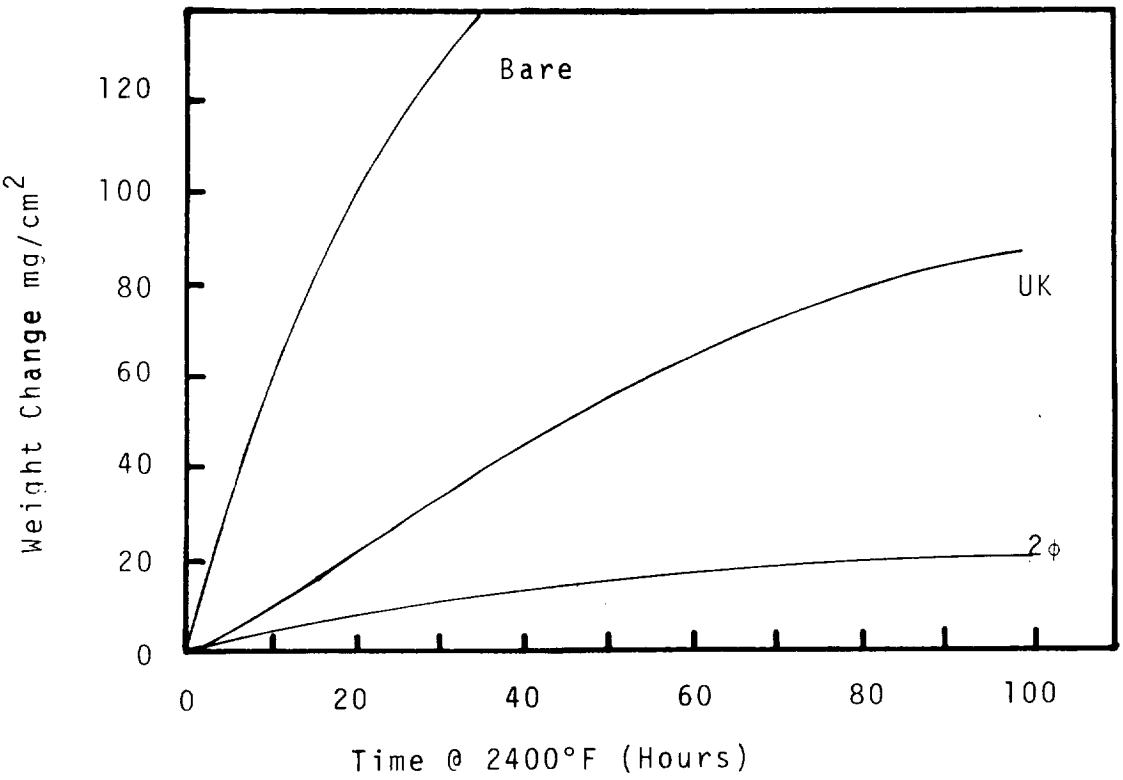

FIGURE: 3-11

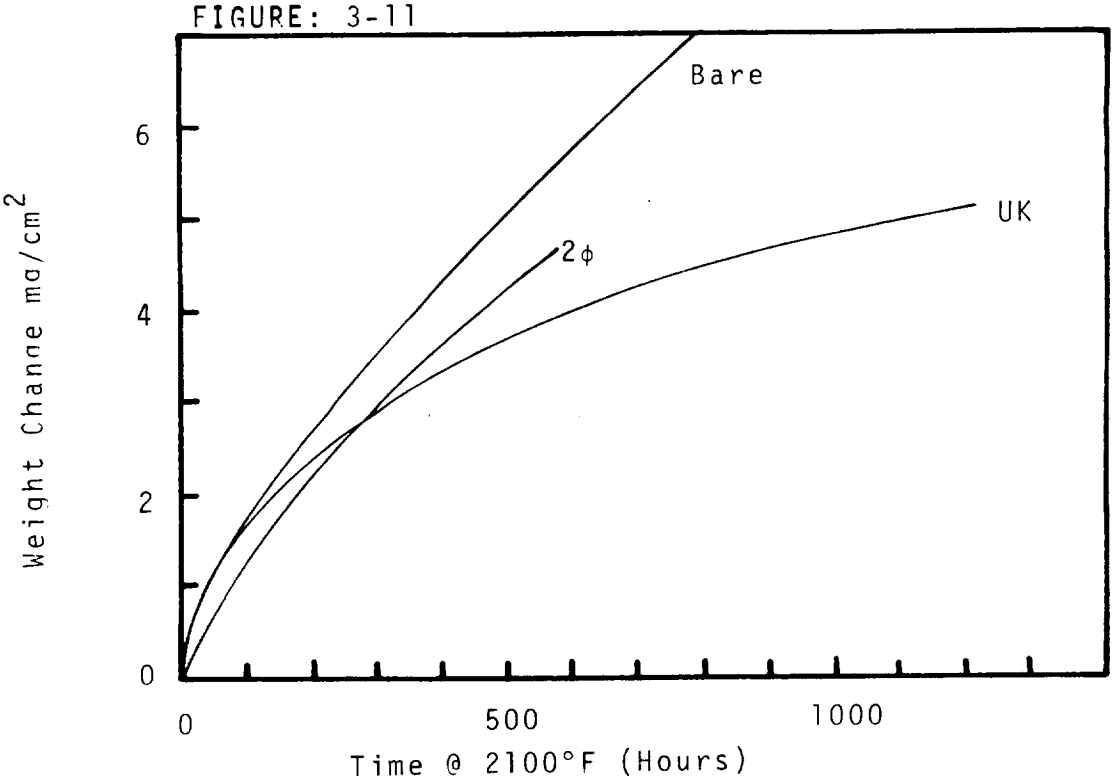

OXIDATION CURVES AT 2100°F AND 2400°F FOR SIMPLE ALUMINUM COATINGS ON Cr-5W-Y ALLOY

3.3.2.1 UK Coatings

The photomicrographs seen in Figures 3-12 to 3-14 are typical of one coating system (XP 19012) chosen for advanced testing. This system was designated "UK" and will be thus referred to throughout the remainder of the report. This series of photographs (Figure 3-12 to 3-14) illustrate metallographically some of the best oxidation resistance seen of all the systems tested. Note the low hardness readings (lower than as-received material) after coating; indicating no interstitial contamination (O, N) during processing. These lower readings are due to the softening accompanying recrystallization. It should be noted, however, that these specimens did not for the most part show the effects of formation and subsequent oxidation of Cr_2N as was noted in some of the more inferior coatings evaluated.

The effect of this formation and oxidation of Cr_2N could be seen (on other coated specimens) as manifested by nitrogen intrusion into the substrate grain boundaries (as hypothesized and partially proven in References 1, 2 and 8, Section 1) in the following sequence:

FIGURE 3-12

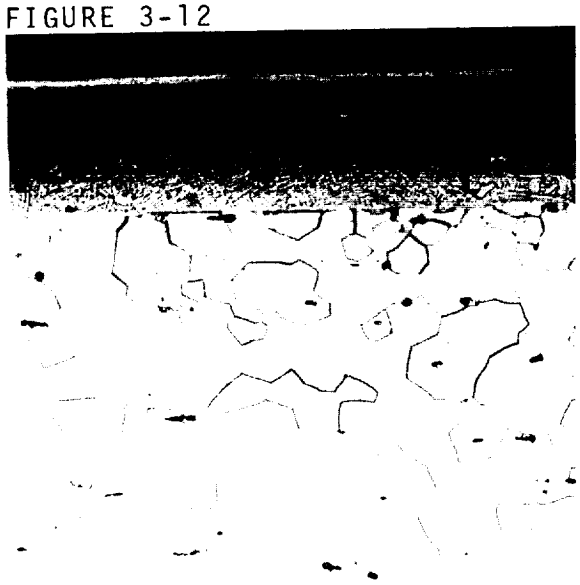

ETCH: 10% OXALIC ACID MAG: 250X
AS COATED

FIGURE 3-13

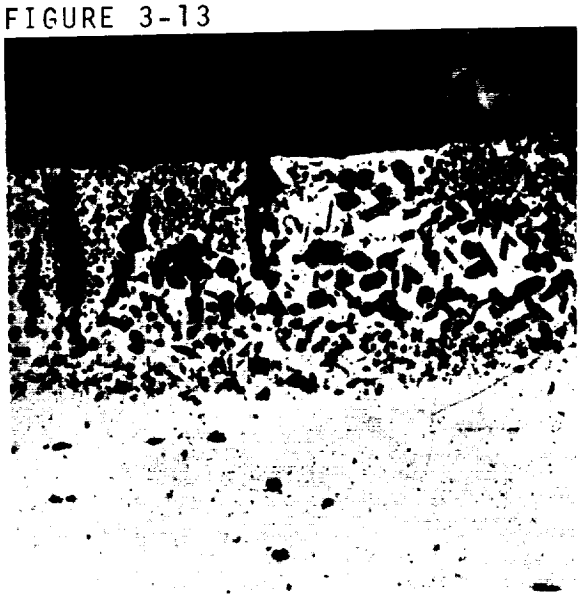

ETCH: 10% OXALIC ACID MAG: 250X
2100°F/1150 HRS.

FIGURE 3-14

ETCH: 10% OXALIC ACID MAG: 250X
2400°F/100 HRS.

TYPICAL UK, (SIMPLE-ALUMINUM) COATED SPECIMENS IN VARIOUS CONDITIONS. PROCESSED AT 2000°F. NOTE EXTENT OF INTERNAL OXIDATION AND INTERGRANULAR NITRIDE ATTACK.

A. Oxidation of the chromium (by cation diffusion) to form Cr_2O_3. (The outer layer seen in Figure 3-15).

B. Ingress of nitrogen through the Cr_2O_3 (a defect lattice) to form massive Cr_2N. (Seen as second layer in Figure 3-15).

C. Oxidation of the Cr_2N by the reaction;

$$2\ Cr_2N + 3O_2 \longrightarrow 2\ Cr_2O_3 + N_2$$

D. Intergranular diffusion of N_2 into the grain boundaries forming Cr_2N. (Figure 3-16)

E. Precipitation of acicular Cr_2N in the substrate matrix upon saturation of N_2 in the grain boundaries. (Figure 3-16)

It should further be noted that although the presence of an aluminum rich coating retards the above sequence, the defect-type lattice structure of Cr_2O_3 (see Section 1.2) coupled with the depletion of aluminum from the surface, (by inward diffusion and surface oxidation) creates an even more favorable condition for nitrogen penetration. Thus, the sequential model of oxidation-nitrification for bare chromium holds also for coated material if sufficient time in an oxidizing atmosphere is seen.

As can be noted from the photographs shown, the oxidation-nitrification resistance of the various simple aluminum coating systems was easily compared (one against

FIGURE: 3-15 MAG: 250X

1211 VHN

708 VHN

969 VHN

215 VHN

OXIDATION AND NITRIFICATION OF Cr_2N IN THE Cr-5W-Y ALLOY

another) during screening on the basis of metallographic evaluation. Further, evaluation of the simple aluminum coatings during the screening work indicated that oxidation-nitrification resistance was dependent upon total aluminum content of the coating. It is for this reason that several coating thicknesses were attempted with identical pack compositions. Figure 3-17 shows the effects of coating temperature on both weight change and thickness. The UK coating chosen for advanced testing showed a large weight change relative to most other systems evaluated. Figure 3-18 shows quantitative electron-beam microprobe analyses of UK coated material. As has been described above, the system chosen for further testing was deposited at 2000°F. In summary the data indicated that the effect of increasing the coating temperature while employing the same basic UK pack composition results in:

1. Increasing the coating thickness.
2. Increasing the resistance to oxidation/nitrification attack.
3. Lower aluminum concentration at the surface but greater total aluminum content of the coating.

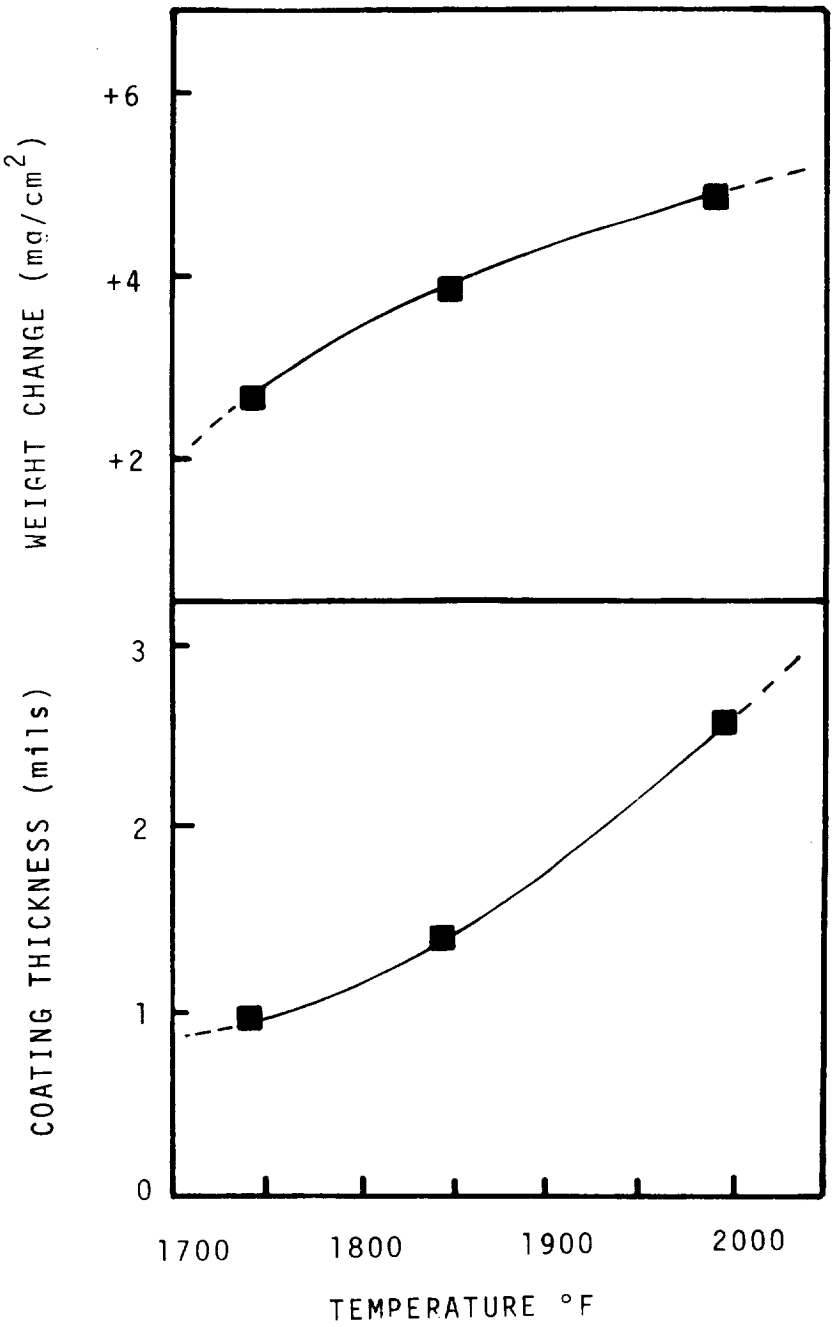

FIGURE 3-17 COATING THICKNESS AND WEIGHT CHANGE VS COATING TEMPERATURE. TIME HELD CONSTANT AT 10 HOURS FOR ALL RUNS.

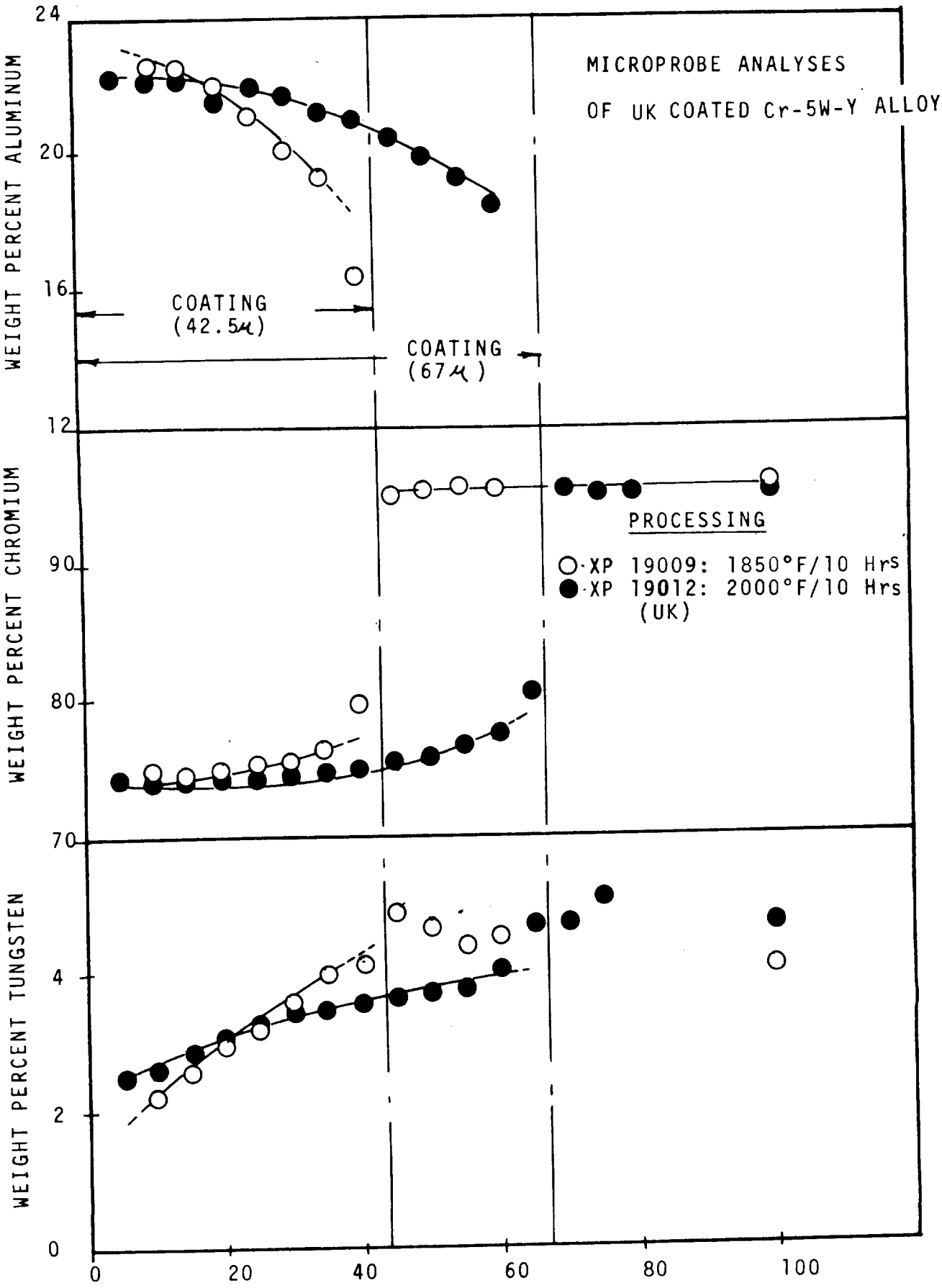
MICROPROBE ANALYSES
OF UK COATED Cr-5W-Y ALLOY
WEIGHT PERCENT ALUMINUM
WEIGHT PERCENT CHROMIUM
WEIGHT PERCENT TUNGSTEN
COATING (42.5μ)
COATING (67μ)
PROCESSING
XP 19009: 1850°F/10 Hrs
XP 19012: 2000°F/10 Hrs (UK)
DISTANCE FROM EDGE, MICRONS

FIGURE 3-18

3.3.2.2 2ϕ Coatings

As indicated in the previous section, coatings of higher aluminum composition were more resistant to corrosive attack. To this end, aluminizing from packs richer in aluminum were attempted. Figure 3-19 shows a photomicrograph typical of the 2ϕ coating (XP19044). It is most significant to observe that this coating consists of two distinct phases in the as-coated condition. Figure 3-20 shows 2ϕ coating after exposure of 140 hours at 2400°F. Although the diffusion of aluminum into the substrate has extended approximately 0.016 inches, no nitrogen contamination of the substrate was observed. The striations and inclusions examined by microprobe scanning techniques proved to be high in aluminum. This necessarily suggests internal oxidation of the aluminum to Al_2O_3. Figure 3-21 shows quantitative Electron-beam microprobe analyses of an as coated (2ϕ) specimen from the above experiment. As can be seen, the aluminum content in the outer phase is much higher (40%) than that of the UK coating (22%). Examination of the Cr-Al phase diagram shown in Figure 3-22 reveals that according to the microprobe trace the outer phase seen in this coating conforms to the η or η^1 phase (Cr_5Al_8) while the inner phase falls within the solid solution field. It is of further interest to note that the chemical analysis (by probe techniques) of this inner phase is equivalent to that obtained on the UK system (solid solution of Al in Cr).

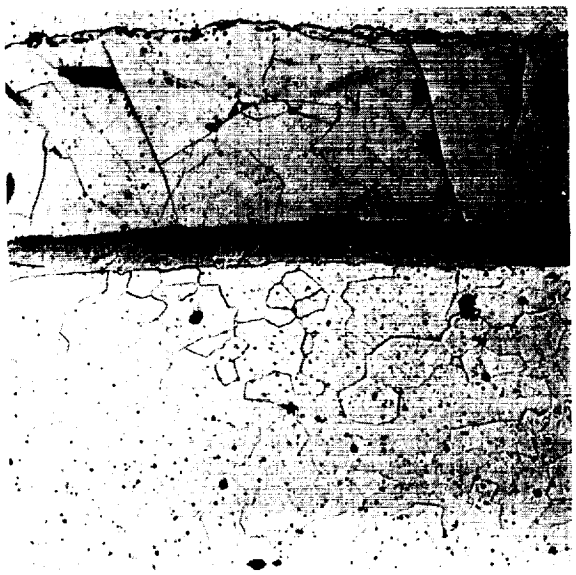

ETCH: 10% OXALIC ACID MAG: 250X

AS COATED

FIGURE 3-20

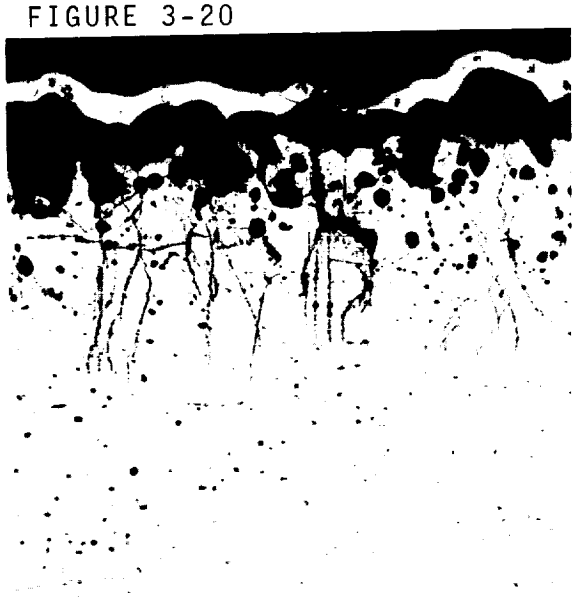

ETCH: 10% OXALIC ACID MAG: 100X

2400°F/140 HRS.

SIMPLE-ALUMINUM COATED SYSTEM (GROUP V). PACK CONTAINED Al, Al_2O_3, AND I_2 PROCESSED AT 1850°F NOTE TWO PHASES (FIG. 3-41) AS COATED AND EXTENT OF DIFFUSION AFTER 140 HOURS AT 2400°F. NO NITRIDE ATTACK WAS NOTED.

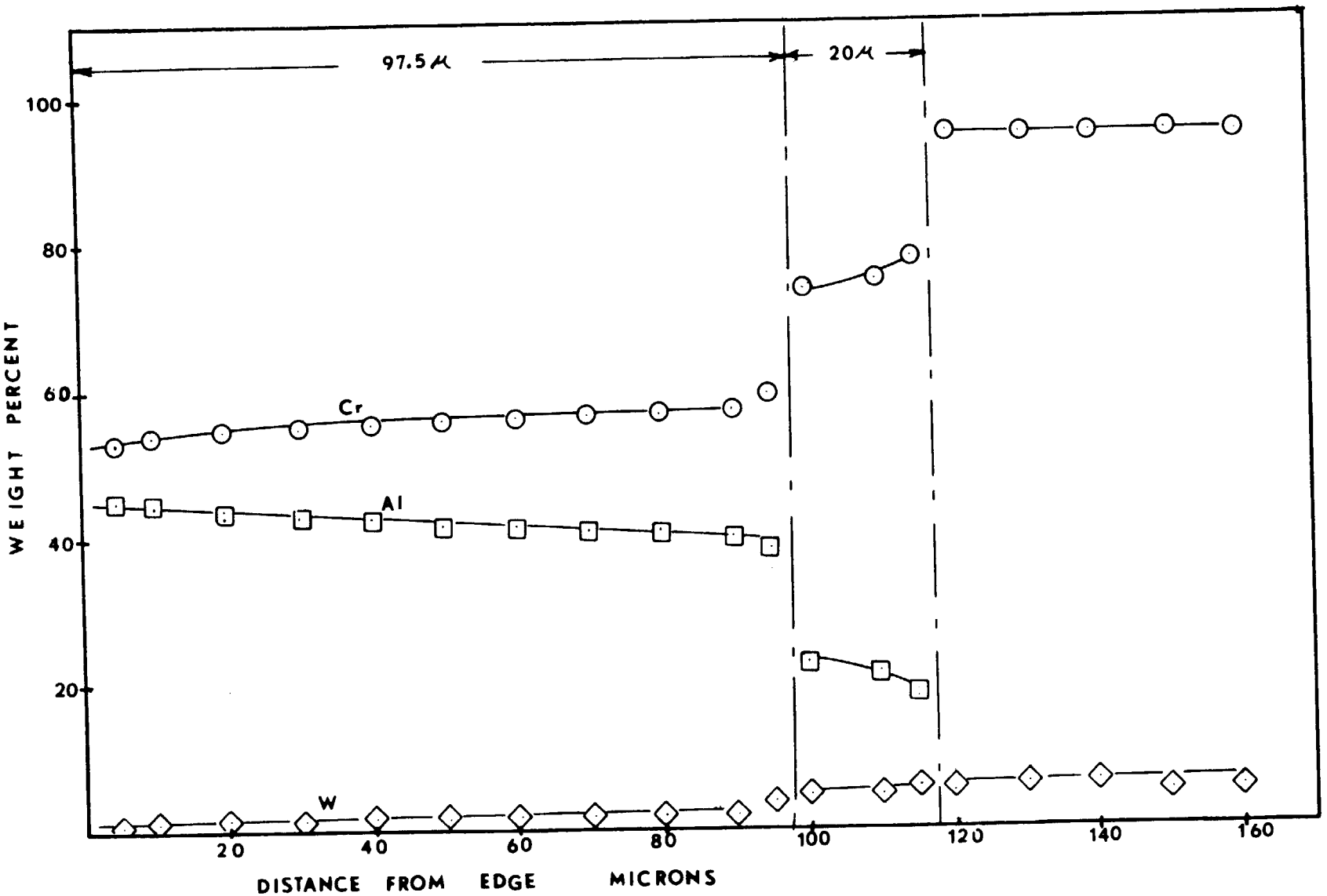

FIGURE 3-21

ELECTRON-BEAM MICROPROBE TRAVERSE OF TWO PHASE ALUMINUM COATED (XP19044) Cr-5W-Y PROCESSED AT 1850°F WITH Al, Al_2O_3 AND I_2 IN PACK.

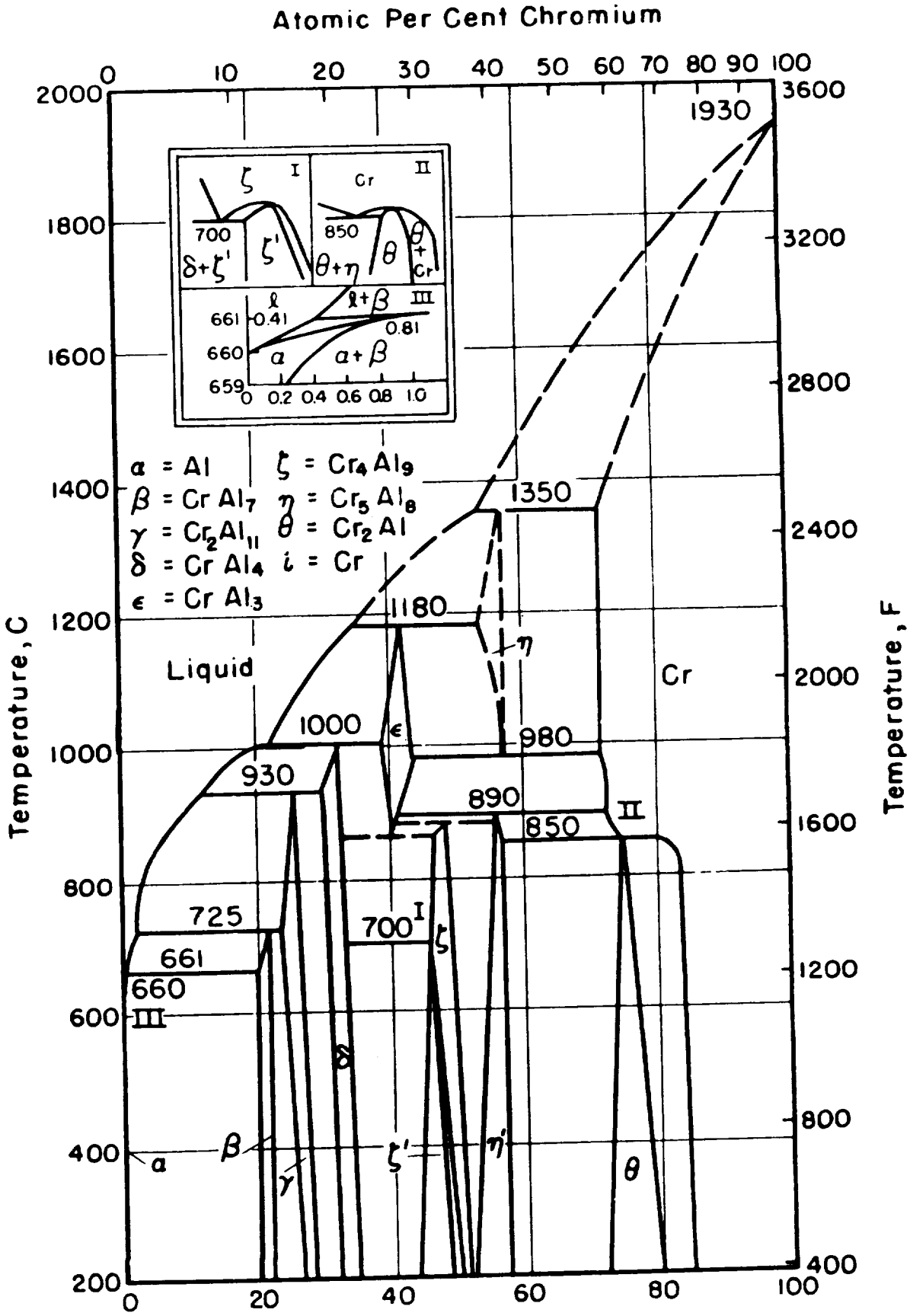

FIGURE 3-22 Chromium-aluminum system.[18]

It should be noted that although weight changes indicated during oxidation are larger than those seen with the previously described single phase aluminum coating, the rate of oxidation appears lower. Further, no nitrogen attack was noted (Figure 3-20) and the appearance of the usually seen green Cr_2O_3 at 2400°F. was not noted. The prevalent oxide seen in specimens of this coating type is initially white (indicative of Al_2O_3) and after approximately 50 hours at 2400°F. a lavender (indicative of solutioning of Cr in Al_2O_3) color.

In summary, it was shown conclusively that higher aluminum content coatings show superior resistance to oxidation-nitrification especially under 2400°F exposure conditions.

Since both the UK and 2ϕ coatings showed attractive properties, it was decided to include both in the advanced testing portion of the work.

3.3.3 Advanced Testing and Coating Evaluation 2ϕ and UK Coatings

3.3.3.1 General

As previously mentioned, it was decided that two simple-aluminum systems be taken through the advanced testing phase of the program. However, due to the lesser oxidation resistance of the UK coating, this system was eliminated from long-term oxidation tests. The description of the test

and the results obtained from the advanced testing phase of the program are presented below.

3.3.3.2 Cyclic Oxidation

The test employed five 2-hour cycles at 1800°F, 2100°F and 2400°F i.e., insertion into hot furnace for 2 hours at temperature, removal, cool to room temperature and re-insertion, with the weight changes recorded every 10 hours (five cycles) to 100 hours and every 20 hours (ten cycles) to 200 hours.. The weight change curves obtained are shown in Figure 3-23. Several conclusions were drawn from these tests and are listed below:

A. No failures of any type at 1800°F were seen on any of the specimens.

B. No visual failures of either coating system were seen at 2100°F, with the bare specimen failing after 100 hours, much sooner than in the previously run screening tests. It should be noted, however, that the screening test involved fewer test cycles.

C. At 2400°F the bare and UK coated specimens failed visibly in less than 100 hours. The 2ϕ coated specimens did not visibly fail during the 200 hour test.

D. The oxidation rates at 1800°F and 2100°F appear parabolic, while those seen at 2400°F appeared to be of a higher order.

FIGURE 3-23

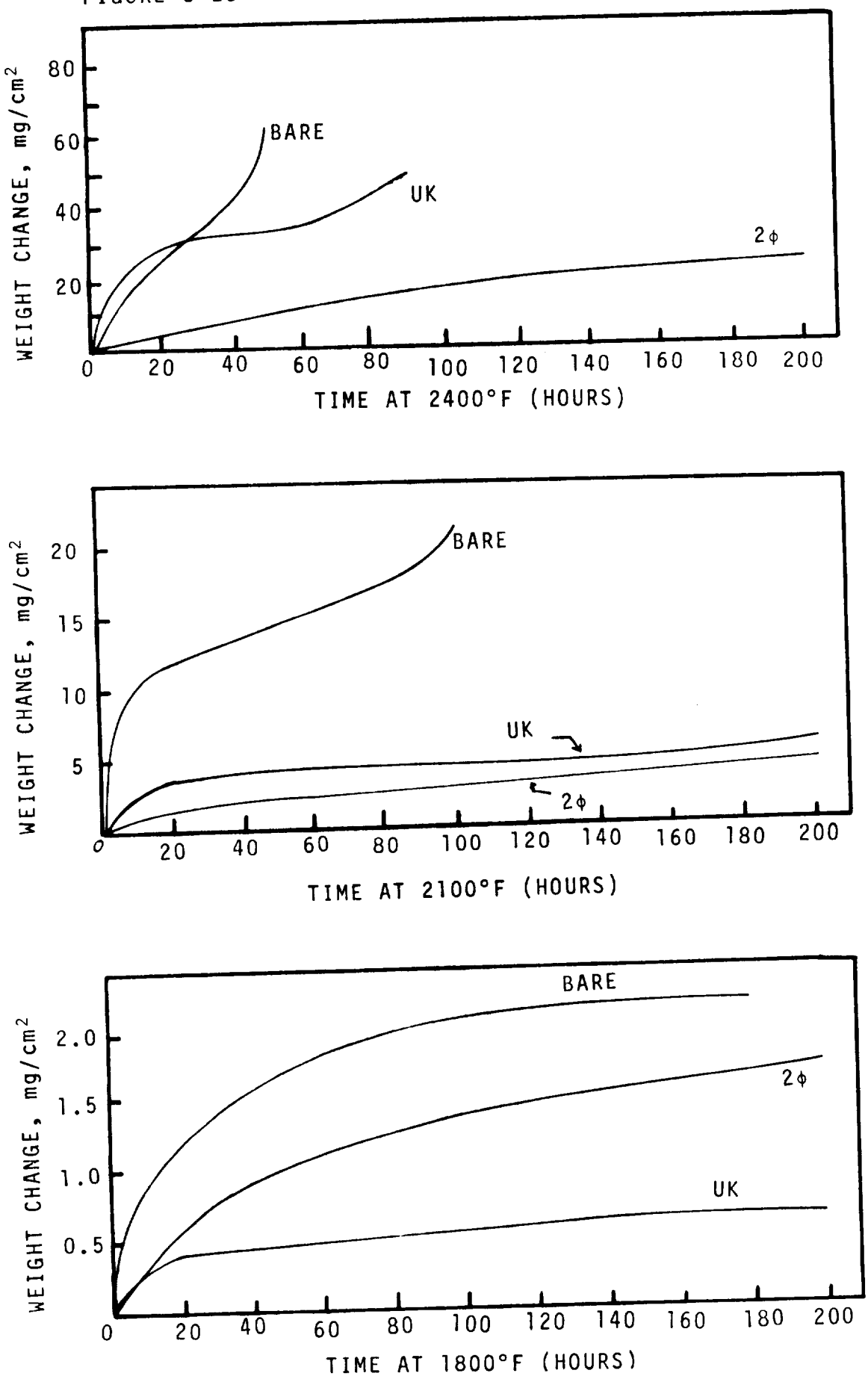

ADVANCED CYCLIC OXIDATION CURVES OF THE BARE, K_2SiF_6 ENERGIZED ALUMINUM COATED AND TWO PHASE ALUMINUM COATED TEST SPECIMENS.

E. Visual appearance of the specimens after intermittent exposure gave virtually no indication as to any nitrogen ingression through the coating or substrate. The only pertinent information obtainable was that of possible coating break-through and substrate oxidation. These observations were manifested by the appearance of the characteristic green Cr_2O_3.

3.3.3.3 Long-Term Oxidation

Long-term oxidation employed twenty hour cycles to 600 hours or failure at 2100°F and 2400°F and was so designed as to determine if the differences, if any, in coating degradation could be noted and if noted, attributed to the differences in the number of thermal cycles performed. These data, although not shown, proved conclusively that the life of the 2ϕ coating system was decreased as the number of cycles increased, i.e., a 5 mg/cm^2 weight change was noted after 200 hours (2100°F) in cyclic oxidation while the same weight change took 600 hours in the less cycled long-term oxidation test. Visual examination of the 2ϕ coated Cr-5W-Y alloy revealed this coating system to still be protective (i.e. no Cr_2O_3 formation) after 600 hours at 2100°F. After 225 hours at 2400°F, edge cracking and the formation of the "lavender (ruby) Al_2O_3 phase" appeared. Intermittent failure of this coating occurred after 300 hours at the 2400°F temperature with total failure occurring after 340 hours of testing.

FIGURE: 3-24

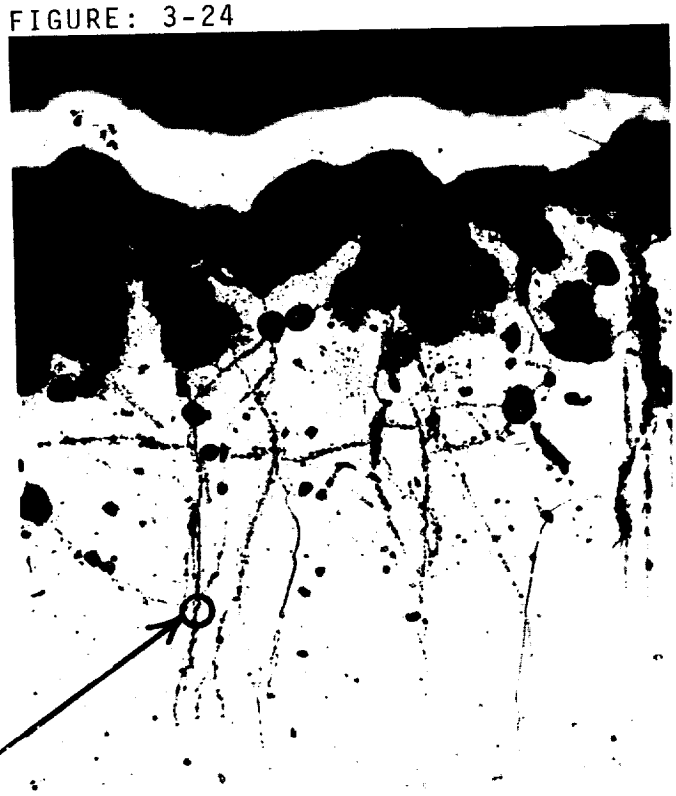

MAG: 400X

FIGURE: 3-25

MAG: 10,000X

LIGHT AND ELECTRON MICROPHOTOGRAPHS OF A 2ϕ COATING AFTER 140 HOURS @ 2400^{o}F SHOWING NEEDLE-LIKE STRUCTURE PROBABLY $AlCrO_4$

X-Ray diffraction patterns, using CuKα radiation, showed the 2ϕ coating to be characteristic of Cr_5Al_8 as had been predicted earlier by EBMP techniques. The 2100°F patterns (long-term oxidation) were essentially identical with the predominant phase being alpha Al_2O_3. Also detected was a cubic spinel-type phase, probably $AlCr_2O_4$.

Although several coated specimens were examined by use of electron microscopy, few instances revealed anything significant. Figure 3-24, 3-25 shows both electron and light microscopic photographs of the 2ϕ coating after 140 hours at 2400°F. The needle-like structure seen in Figure 3-25 is probably $AlCr_2O_4$.

3.3.3.4 Continuous Weight Change Oxidation Testing

Continuous weight change oxidation data was developed for both the UK and 2ϕ coatings at 1800°F, 2100°F and 2400°F. Figures 3-26 and 3-27 show continuous weight change curves for both the UK and 2ϕ coatings. Most significant in the results seen was a decrease in oxidation rate (as compared to cyclic testing) noted on all specimens tested. This decrease in rate was due to:

a) The lack of induced thermal shock cycling and its usual attendant spalling, and

b) The fact that only a limited supply of air is available within the tubular furnace.

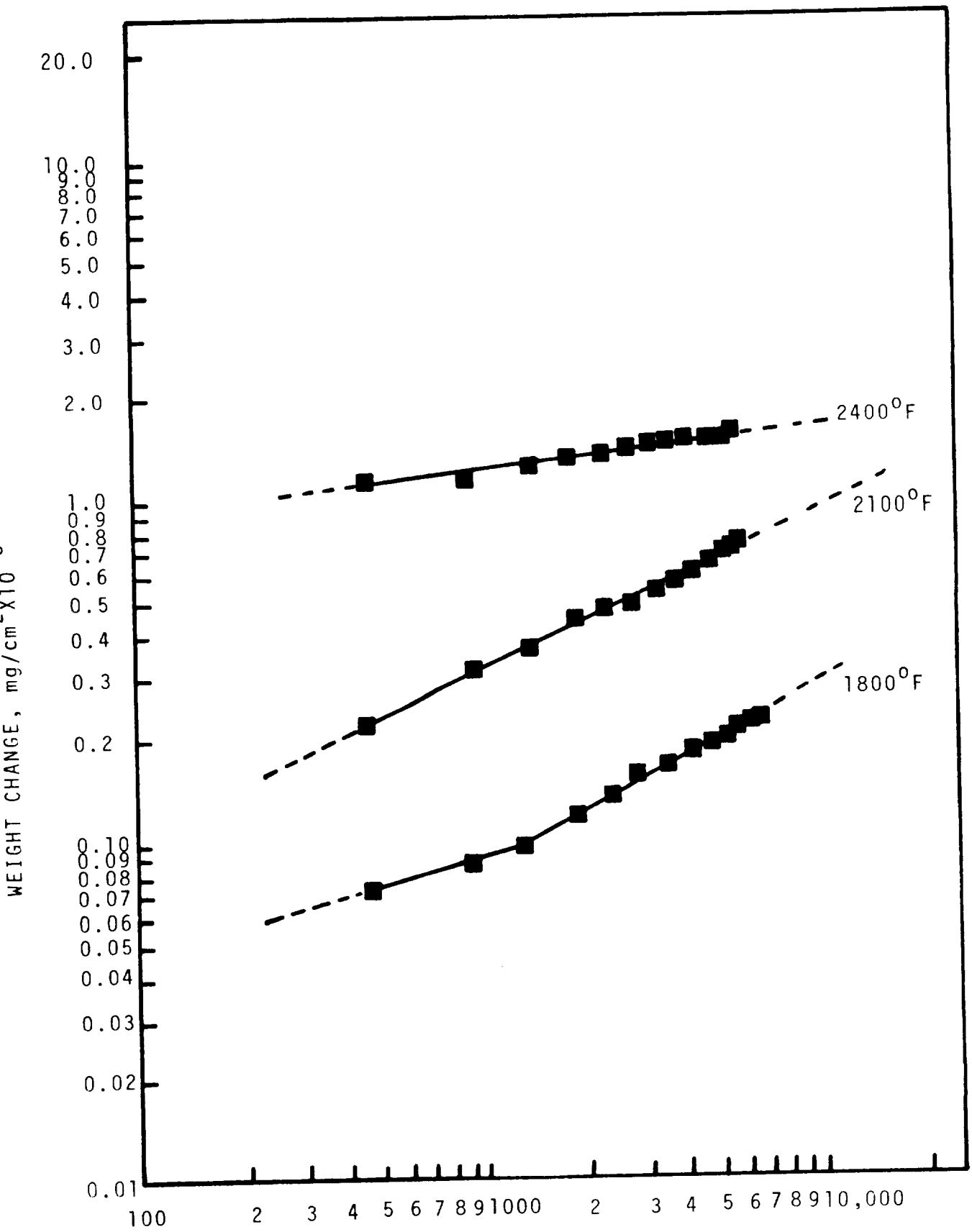

FIGURE: 3-26

CONTINUOUS OXIDATION CURVES OF THE "UK" COATED Cr-5W-Y ALLOY EXPOSED @ 1800, 2100, AND 2400°F.

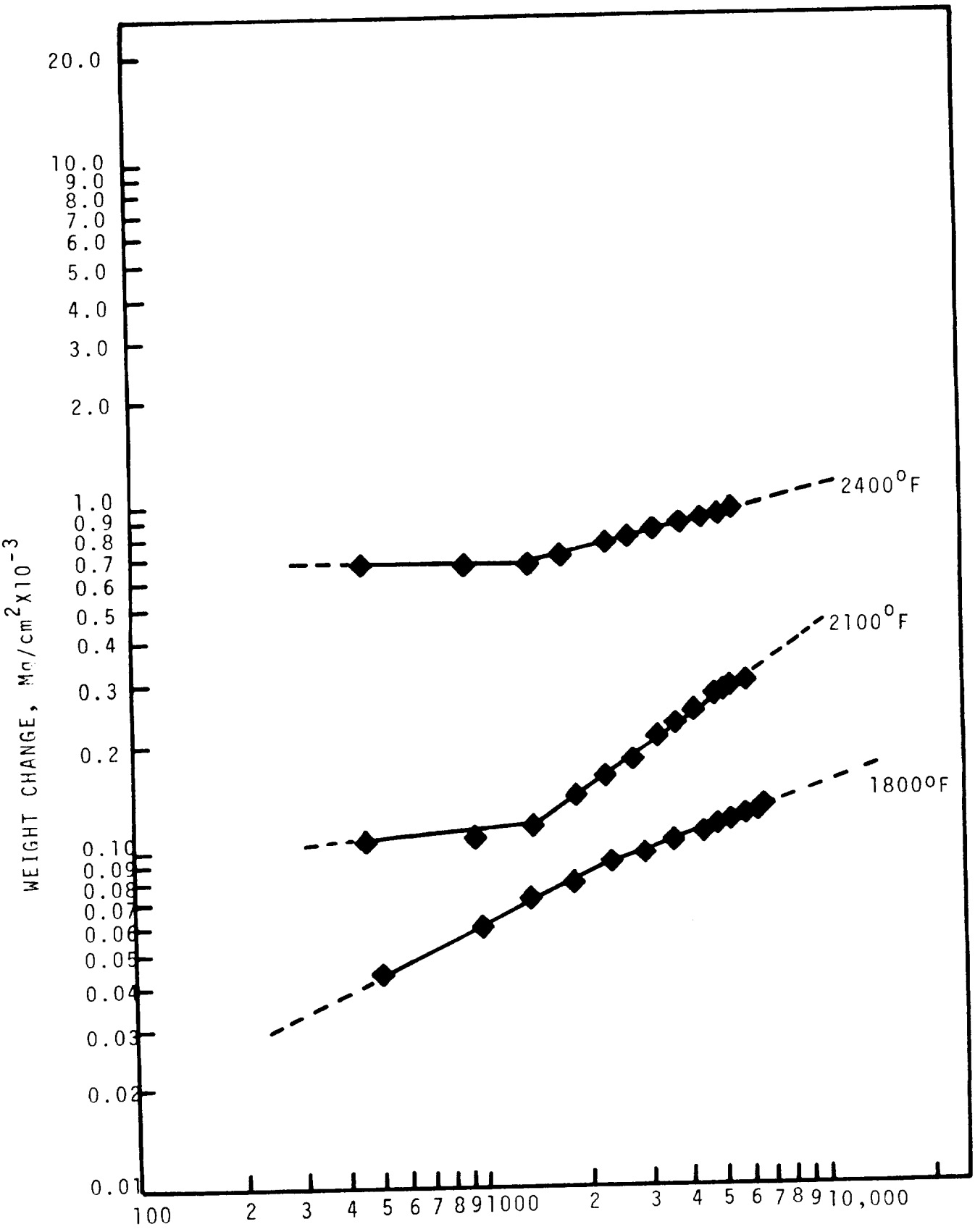

FIGURE: 3-27

CONTINUOUS OXIDATION CURVES OF THE 2ϕ COATED Cr-5W-Y ALLOY EXPOSED @ 1800, 2100 AND 2400°F

It appears that the oxidation-nitrification kinetics still could not be totally explained on the basis of the curves developed. However, the deviations from linearity seen in the 2ϕ coating might be attributable to the differences in oxidation rate of the outer Cr_5Al_8 and inner Cr-Al solid solutions. The linearity seen at 1800°F was apparently due to the far greater diffusion stability of this system. Longer times at 1800°F might possibly show deviations from linearity.

3.3.3.5 Oxidation Erosion Testing

Testing was performed in an oxidation-erosion rig as described in Section 2.1. Specimens 4"x1"x.065" were UK and 2ϕ coated and inserted in a specimen holder as shown in Figure 3-28. Although testing at both 2100°F and 2400°F was originally called for, the geometry of the specimens chosen precluded attainment of the higher temperatures. Several attempts were made, however, to reach temperatures in excess of 2100°F and although the use of radiation shields did yield surface temperatures of 2230°F, it was decided to test only at the lower temperatures (2100°F). The decision was based on the extensive difficulties that would be encountered in rig modifications.

The brittleness of Cr-5W-Y alloy further created extreme difficulty in specimen removal as manifested by edge cracking

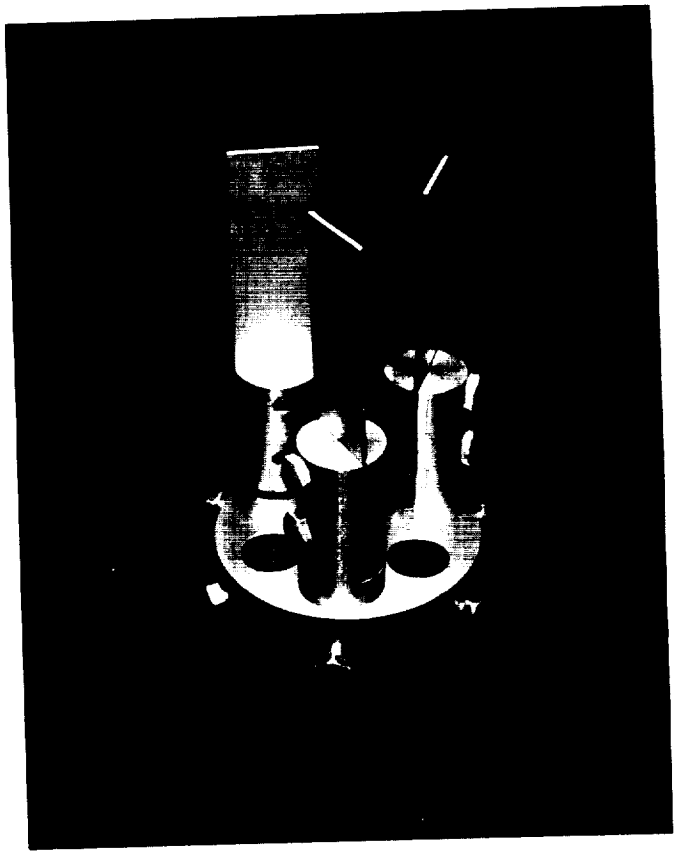

FIGURE: 3-28

Erosion Rig Specimen Holder And Specimens

and fracture in several locations. Because of this problem it was decided to discard weight change measurements and rely solely on visual examination every ten hours. It should be noted also that the thermal-fatigue-type cycle originally scheduled proved impractical due to observed substrate susceptibility to thermal cracking in preliminary tests where specimens showed severe substrate cracking with a 10-hour cyclic test.

Figure 3-29 shows a UK coated specimen after 60 hours at 2100 F, while Figure and 3-31 show photomicrographs as taken from the leading (i.e., closest to flame) and trailing edges. As can be seen the leading edge shows considerable gas-erosion likely due to its proximity to the flame. It was further noted that no substrate nitrogen attack commenced (Figure 3-30). This was in contrast to the nitride precepitation seen in a specimen from the trailing edge, which shows complete saturation of the coating with corrosive products and subsequent precipitation on the substrate. It is felt that the differences in protectiveness was due to:

1) The greater erosion and oxide flaking at the leading edge, and
2) The higher temperature (approximately 100-150^{o}F) obtained at the trailing edges due to heat build-up in the center of the holder employed.

This phenomena is commonly observed and has been reported

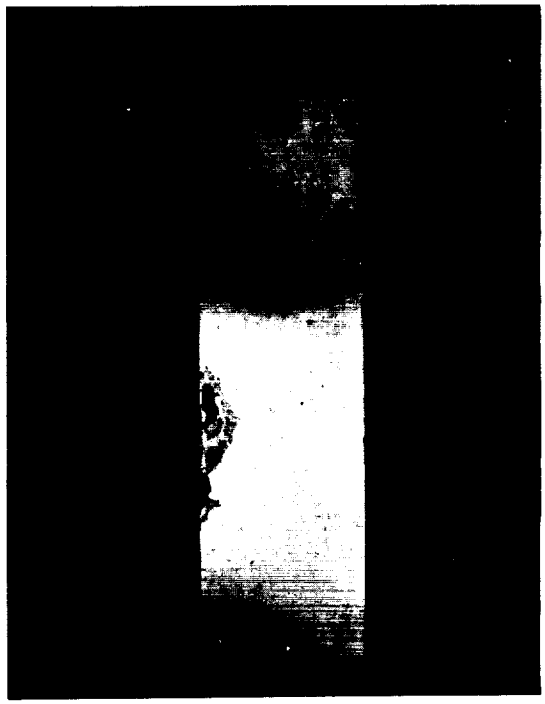

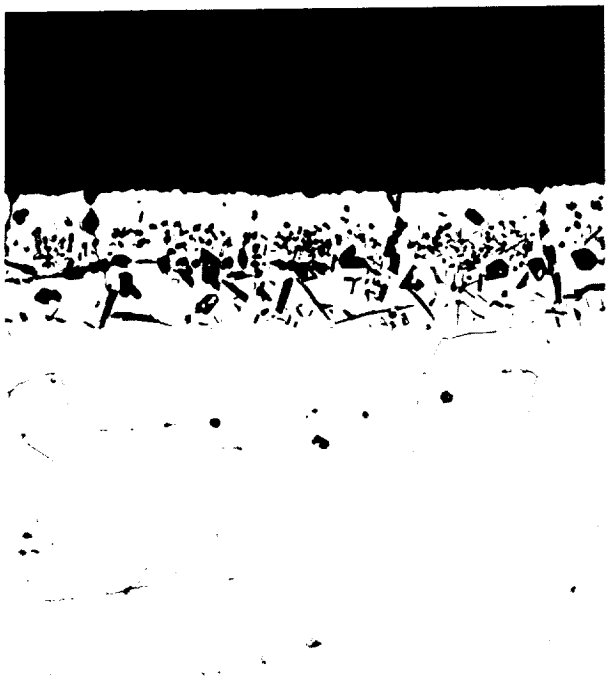

FIGURE 3-30 250X

LEADING EDGE

FIGURE: 3-31 250X

TRAILING EDGE

UK COATED EROSION TEST SPECIMEN AFTER 60 HOURS AT 2100°F. NOTE OXIDE FORMATION AT LEADING EDGE (3-30) AND NITRIDE PRECIPITATE (3-31) WITHIN THE MATRIX OF Cr-5W-Y ALLOY.

by several investigators employing similar facilities. Figures 3-32 to 3-34 show similar illustrations for 2ø coated specimens tested 160 hours at 2100°F. As can be seen, this system although more oxidation-nitrification resistant than the UK coating, also shows more pronounced coating attack at the trailing edge. However, no nitrogen attack of the substrate was noted.

The observations made during these tests clearly confirmed all published information regarding the lack of correlation between static and dynamic oxidation tests. It thus becomes clear that the life of these coatings under static conditions is much longer than under dynamic environments. Further, the superiority of the 2ø coating was again clearly demonstrated.

3.3.3.6 Ductile-Brittle Bend Transitition Testing

All testing was performed according to Materials Advisory Board MAB 192-M and described in Section 2.7. DBTT testing of the UK coating was not included in this series of tests. Tests conducted early in the program showed the DBTT to increase greatly after only short exposures under oxidizing atmospheres. Necessarily additional cycles were formulated in an effort to determine the cause of this increase in transition temperature. It was however speculated that the diffusion of interstitials into the coating con-

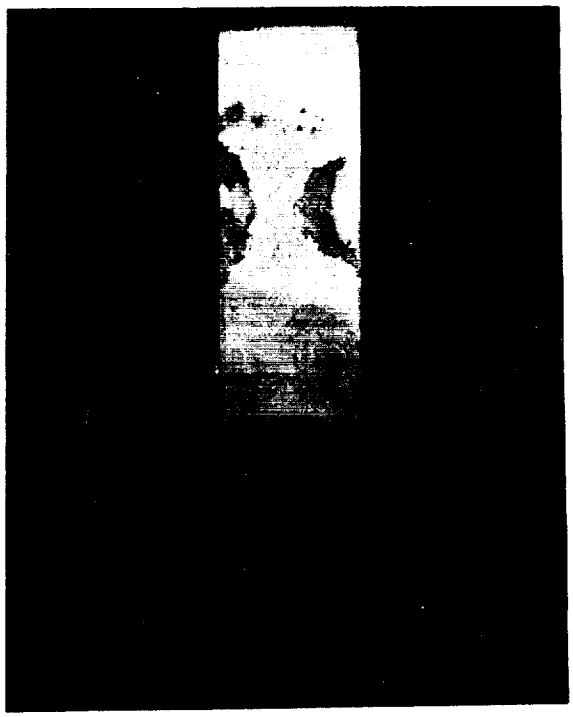

FIGURE: 3-32

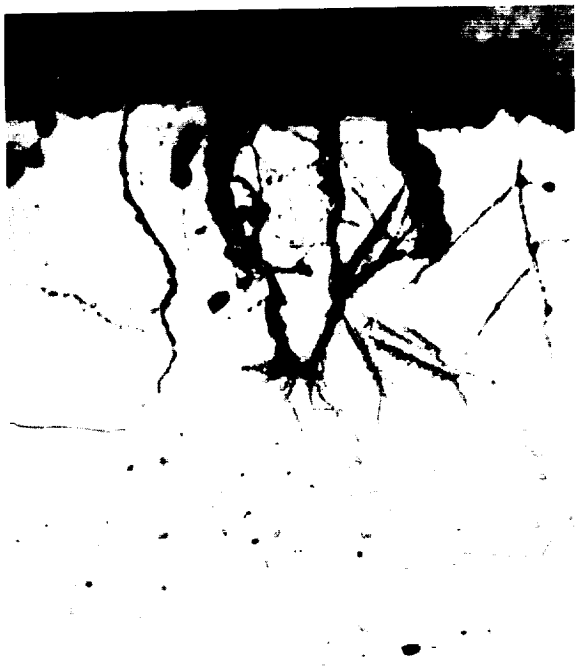

FIGURE 3-33 250X

LEADING EDGE

FIGURE: 3-34 250X

TRAILING EDGE

2ø COATED EROSION SPECIMEN AFTER 160 HOURS AT 2100°F

NOTE OXIDE FORMATION WITHIN THE COATING (3-34)

comitant with the diffusion of aluminum into the substrate produced a brittle phase which cracked upon testing. This crack thus originated, would then propagate into an already brittle (due to recrystallization) substrate.

The first three conditions seen in Table V show results obtained earlier in the program. As can be seen, the DBTT was greatly increased after exposure. The tests subsequently run were designed to determine the changes in DBTT as a function of the following:

A. Al or nitrogen diffusion

B. Coating thermal cycle

C. Cyclic - thermal - stressing

D. Oxidation Testing Thermal Cycle

All DBTT data obtained are shown in Table V. It should be noted that two criteria were considered in the evaluations. The first criteria employed, considered that any specimen which showed surface cracking (regardless of the bend angle) was not acceptable. Necessarily, as can be seen, many DBTT values are reported as greater than 1600°F since this was the maximum testing temperature decided upon. The second method of evaluation, which was more meaningful, compared the bend angles obtained regardless of observed surface cracking. The latter method was far more beneficial in determining the causes for high DBTT values.

The first three conditions shown in Table V represent data gathered early in the program. It was these high DBTT

values which prompted additional bend testing in an attempt to dilineate the causes of the poor observed properties. In an attempt to determine whether aluminum diffusion, or nitrogen contamination during coating adversly affects DBTT, specimens in the coated plus stripped, and simulated-coating-cycle conditions were prepared and tested. The data obtained are quite similar with regard to nitrogen analysis and DBTT and unequivocally show that the transition temperature is not affected by any chemical changes associated with the coating cycle. As was shown before, the changes in DBTT when comparing coated and bare material are due to the recrystallization which occurs due to the thermal cycle. Figures 3-35 and 3-36 show photographs of specimens with the conditions described above. It can be seen that some delamination of the substrate was noted, but no cracks were observed at the surface.

Since it was speculated that saturation of the coating with interstitials was the cause of high DBTT it was decided to expose coated specimens at 2100°F and 2400°F in an argon atmosphere to preclude contaminant pick-up. A close look at the data obtained shows a significant N_2 pick-up on a bare specimen exposed for 100 hours at 2100°F. This was due to contamination of the atmosphere, the source of which could not be ascertained It should be noted, however, that a research grade, very high purity argon was employed (2ppm N_2).

TABLE V

DUCTILE TO BRITTLE BEND TRANSITION TEMPERATURE TEST
FOR 2φ COATED AND EXPOSED Cr-5W-Y SHEET

Condition	Gas Analysis ppm (4)	Micro-Hardness VHN	Coating Thickness mils	EBMP ANALYSIS w/o	4 mils	8 mils	12 mils	16 mils	DBTT °F (1)	Comments
1. As Coated	---	Coating 662 Substrate 192	4.8	---	---	---	---	---	825	(2)
2. Coated and Exposed 2100°F/100 Hours (Air)	---	Coating 427 Substrate 190	---	---	---	---	---	---	>1600	(2)
3. Coated and Exposed 2400°F/100 Hours (Air)	---	Coating 381 Substrate 172	---	---	---	---	---	---	>1600	(2)
4. Coated and Stripped	63	196	---	Al Cr W	--- 94.4 5.7	---	---	---	800-1000	(3) Broke @ 800°F
5. Bare, 2φ Coating Cycle (Argon)	80	189	---	Al Cr W	--- 94.3 5.3	---	---	---	800-1000	(3) Broke below 800°F
6. Bare and Exposed (Argon) 2100°F/100 Hours, 2,2,2,16 Hour Cycles	883	191	---	Al Cr W	2 mils 92.7 7.6	4 mils 94.4 5.6	94.2 5.8	---	1000-1100	(3) Broke below 1000°F
7. Coated and Exposed (Argon) 2100°F/100 Hours, 2,2,2,16 Hour Cycles	83	Coating 374 Substrate 159	9	Al Cr W	15.8 79.8 4.1	13.2 82.5 4.2	--- 94.2 5.8	---	>1600	(3) Did not bend below 1250°F
8. Coated and Exposed (Argon) 2100°F/100 Hours	63	Coating 415 Substrate 177	9	Al Cr W	14.9 79.4 5.1	10.2 87.1 5.2	--- 94.6 5.4	---	>1600	(3) Bent to 105° @ 1000°F
9. Coated and Exposed (Argon) 2100°F/10 Hours	70	Coating 533 Substrate 155	7	Al Cr W	21.5 73.1 3.5	16.2 72.9 5.0	--- 94.7 5.4	---	>1600	(3) Bent to 105° @ 1400°F
10. Coated and Exposed (Argon) 2100°F/10 Hours, 2,2,2,2,2 Hour Cycles	70	Coating 670 505 Substrate 153	11	Al Cr W	36.0 60.0 3.9	20.0 76.1 4.7	10 mils 19.2 76.7 4.8	--- 94.9 5.1	>1600	(3) Did not bend
11. Coated and Exposed (Argon) 2400°F/100 Hours	130	Coating 353 Substrate 189	16	Al Cr W	7.8 85.2 4.9	7.9 86.2 5.0	6.9 87.7 5.2	--- 94.6 5.4	>1600	(3) Did not bend below 1500°F
12. Coated and Exposed (Argon) 2400°F/10 Hours	93	Coating 364 Substrate 145	12	Al Cr W	16.5 78.1 4.6	16.5 78.1 4.6	12.2 82.5 5.3	--- 94.0 6.0	>1600	(3) Bent to 105° @ 1400°F
13. Coated and Exposed (Nitrogen) 2400°F/100 Hours	11.17%	Coating ≈2200 Substrate≈1100	14	Al Cr W	---	---	---	--- 88.5 4.6	>1600	(3) Specimen broke in atmosphere furnace. ≈6.9% N_2 in solution.

(1) No Cracks Produced with a 90°-105° Angle Bend
(2) Heat #57-100 DBTT= 450°C, 37 ppm N_2
(3) Heat #67-100 DBTT = 325°C, 30 ppm N_2
(4) All analysis conducted after coating removal

FIGURE: 3-35

Cr-5W-Y DBTT SPECIMEN
COATED AND STRIPPED.
NOTE SUCCESSFUL BEND,
LACK OF ANY NITRIDE
FORMATION AND
DELAMINATION OF SUBSTRATE

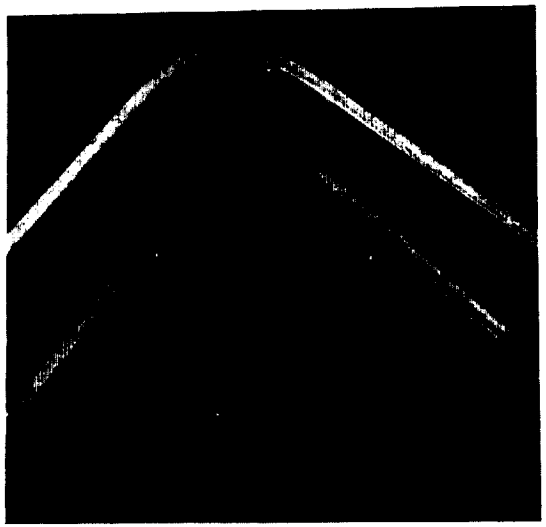

DBT 1200°F

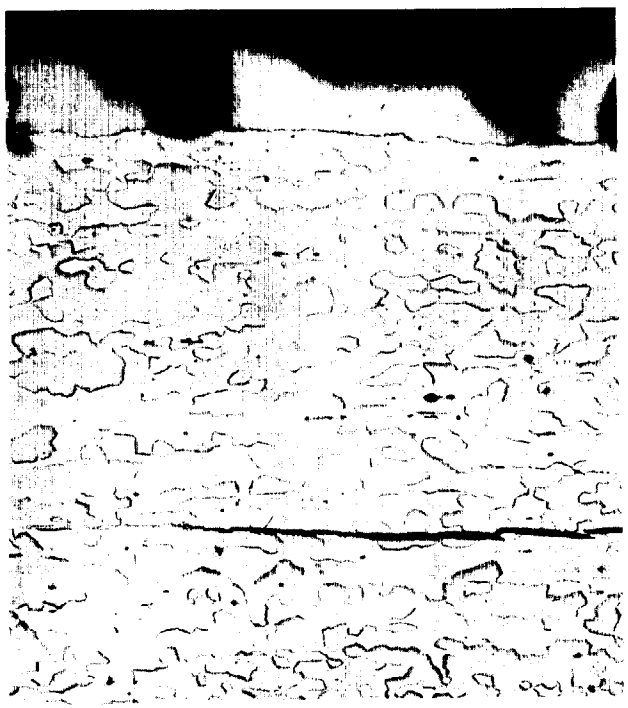

100X

DBT 1000°F

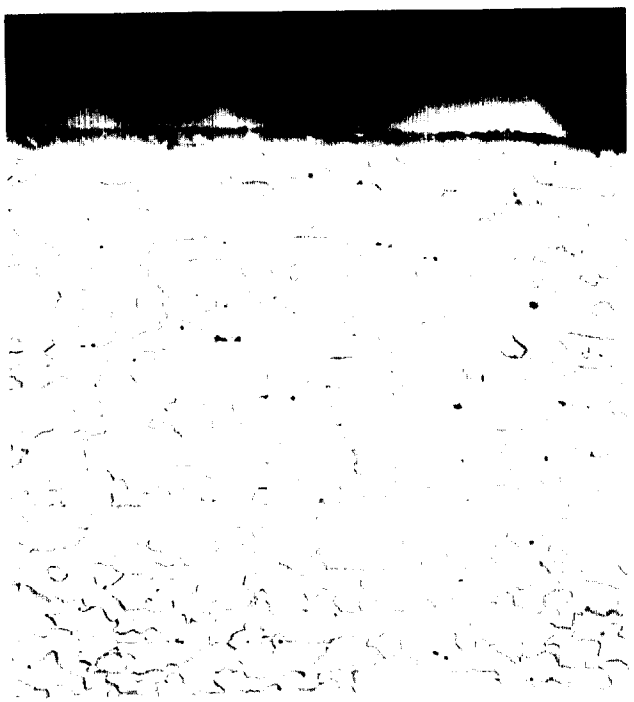

100X

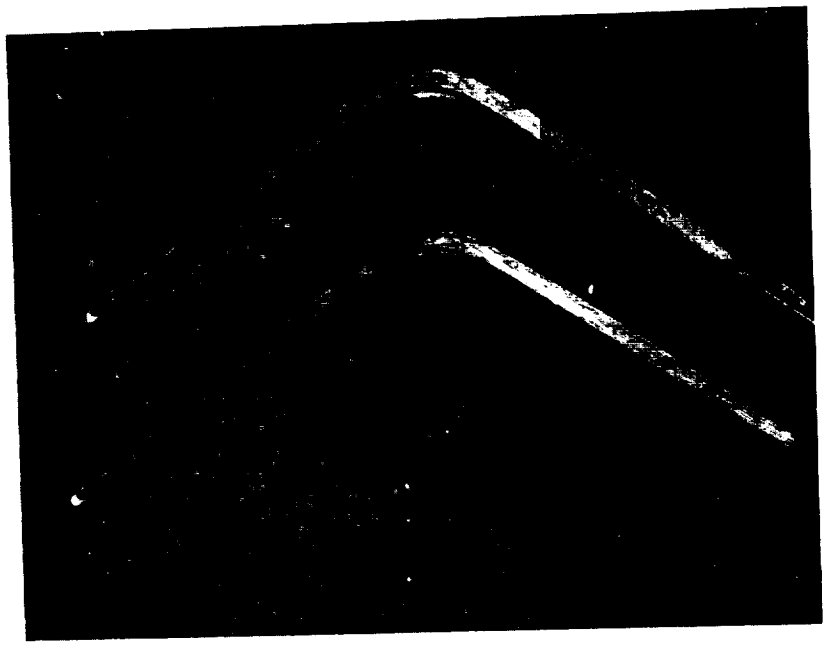

100X DBT 1100°F

FIGURE: 3-36

BARE-Cr-5W-Y DBTT SPECIMEN AFTER 2ø THERMAL COATING CYCLE IN ARGON (1800°F/10 HOURS). NOTE SUCCESSFUL DBTT AT 1100°F.

A further look at the data shows that a cyclic (2,2,2, -16) 100 hour exposure (2100°F) produces a condition (83 ppm-N , and 1250°F successful bend) significantly poorer than that seen with an iso-thermal 100 hour exposure (63 ppm) and 1000°F successful bend). The same type of results were obtained with 10 hour exposures i.e., poorer bend results with cyclic exposure at 2100°F. It also becomes obvious at this point that diffusion of aluminum into the substrate has a pronounced effect in increasing the DBTT of the coated material. Figures 3-37 through 3-41 show photomicrographs and macrographs of some of the conditions tested. Most significant in these photographs are the cracks seen extending from the coating to the substrate, and the enhanced diffusion of aluminum (into the substrate) due to the thermal cycling imposed, the surface cracking seen even under conditions where a 105° bend was obtained, and some of the fractures obtained with no bending noted.

Additional exposures were made in argon at 2400 F for both 10 and 100 hours. Significant in the results obtained was the pronounced increase in nitrogen content of the substrate after 100 hours at 2400°F. The increase seen after 10 hours was considerably smaller. The DBTT of these exposed specimens are shown in Table V and the results here, indicate that poorer results are seen with material having higher nitrogen content. Figures 3-42 and 3-43 show photo-

FIGURE: 3-37

BARE Cr-5W-Y DBTT SPECIMEN AFTER 100 HOURS AT 2100°F IN ARGON WITH A 2,2,2,16 HOUR CYCLE EXPOSURE. NOTE SUCCESSFUL DBTT AT 1000°F AND BRITTLE FRACTURE AT 800°F

DBT
800°F

100X

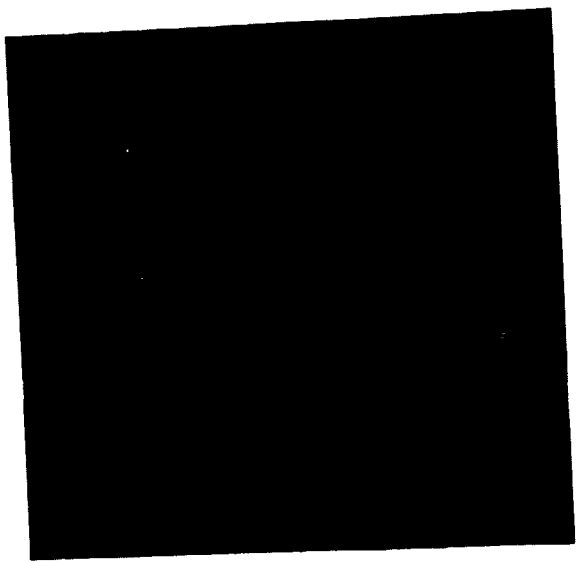

D B T
1000°F

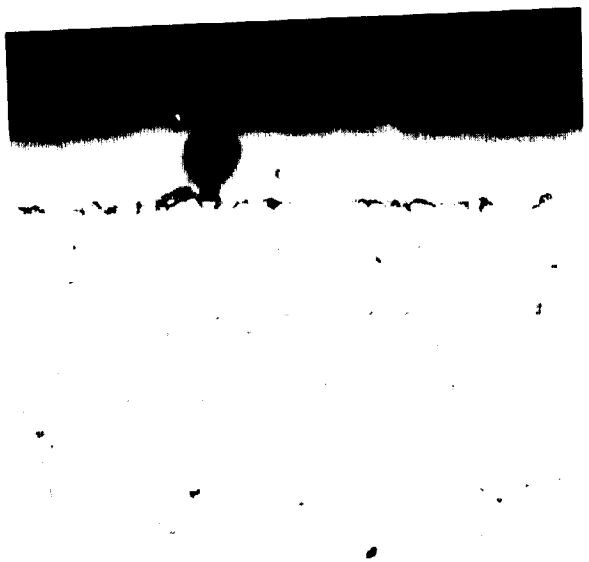

FIGURE 3-38

2ϕ COATED Cr-5W-Y DBTT SPECIMEN AFTER 100 HOURS AT 2100°F IN ARGON WITH A 2,2,2,16 HOUR CYCLIC EXPOSURE. NOTE SUCCESSFUL DBTT AT 1300°F AND 1600°F BUT WITH EXTENSIVE COATING CRACKING.

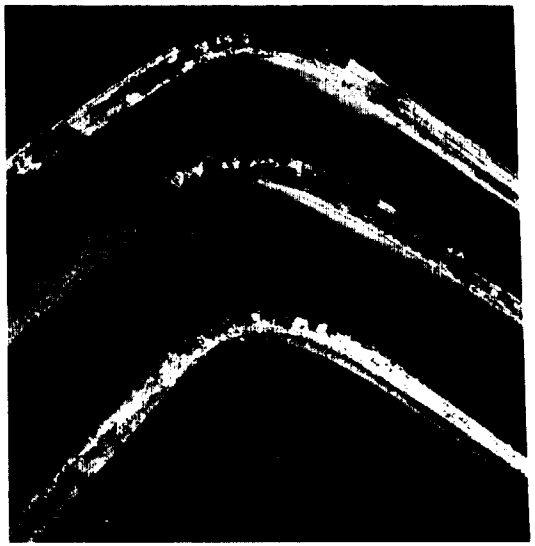

DBT 1300°F

DBT 1600°F

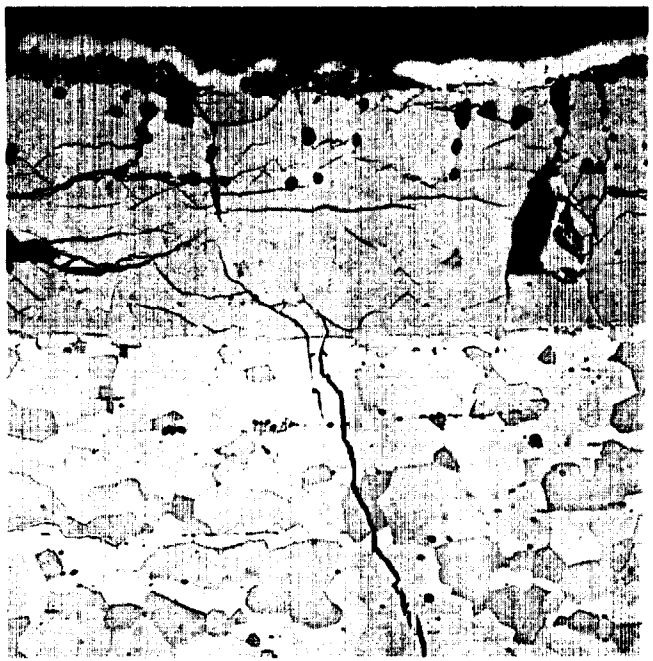

compression

tension

FIGURE 3-39

2ϕ COATED Cr-5W-Y DBTT SPECIMENS AFTER 100 HOURS AT 2100°F IN ARGON. NOTE SURFACE CRACKING.

FIGURE 3-40

2ϕ COATED Cr-5W-Y DBTT SPECIMEN
AFTER 10 HOURS AT 2100°F IN ARGON.
NOTE HIGH DBTT AND COATING CRACKING

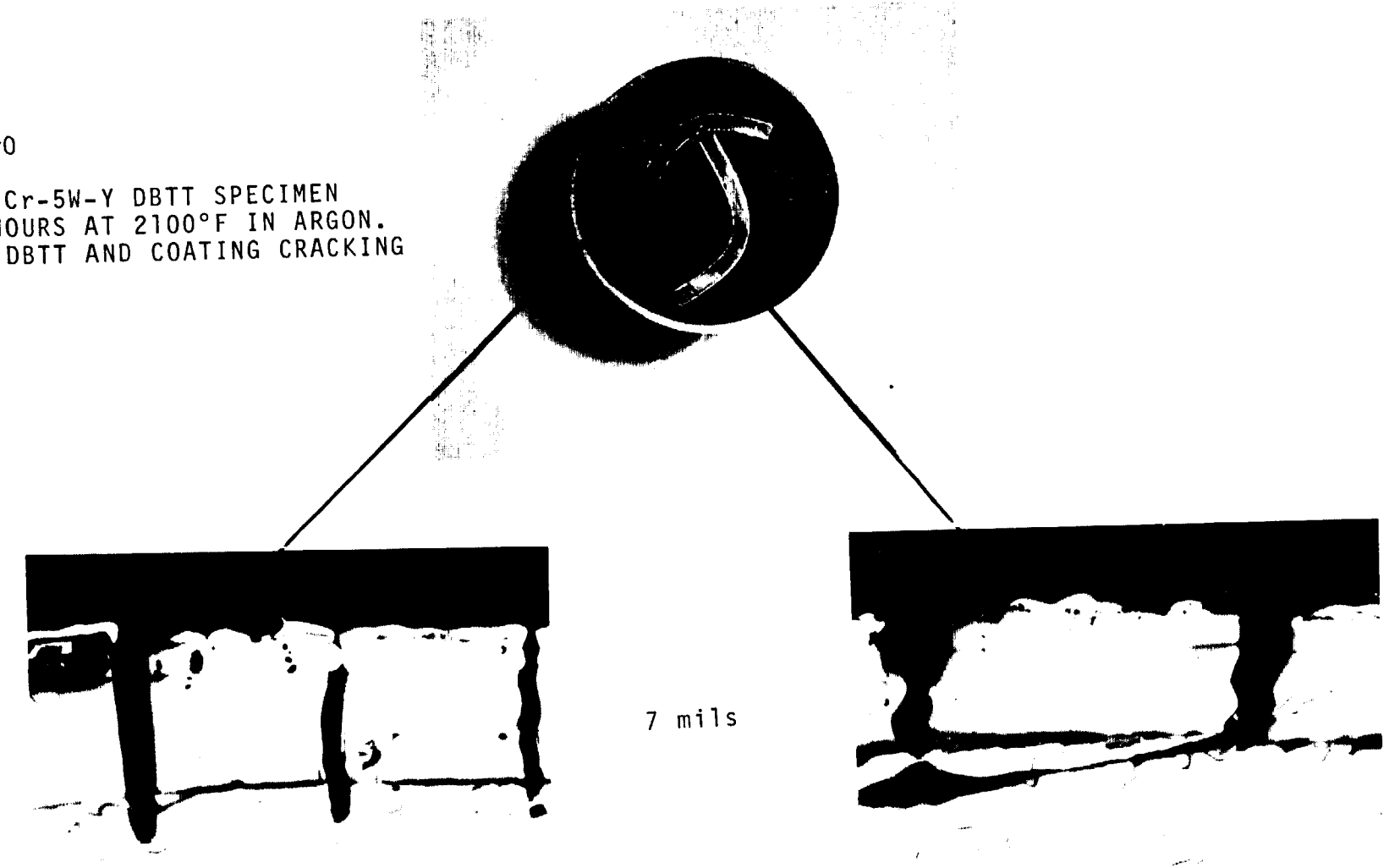

100X DBT 1500°F

100X DBT 1600°F

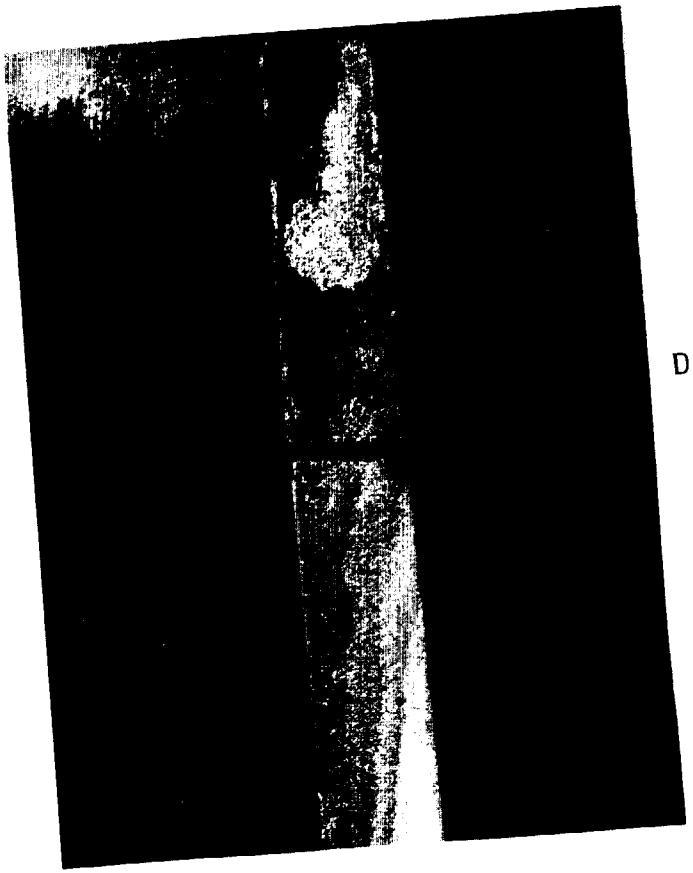

DBT 1600°F

FIGURE 3-41

2φ COATED Cr-5W-Y DBTT SPECIMEN AFTER 10 HOURS (2,2,2,2 CYCLE) AT 2100°F. NOTE SHARP NON-DEFORMED BRITTLE FRACTURE.

graphs of specimens exposed to 2400°F and bend tested.

The last exposure evaluated was under nitrogen at 2400°F for 100 hours, and as can be seen from the data, tremendous nitrogen pick-up was observed. Necessarily it can be tentatively concluded that an aluminum-base coating system owes much of its protective ability (to resist nitrogen penetration) to the formation of aluminum oxide and/or spinels of the $AlCrO_4$-type, since the absence of oxygen during this testing precluded its formation and obviously accelerated attack of the substrate (Figure 3-44).

We can, based upon all the bend data obtained, summarize the results as follows:

A. An increase in DBTT is seen by virtue of the coating cycle.

B. The increase in DBTT due to coating is caused by recrystallization of the substrate.

C. No significant nitrogen pick-up is noted after coating.

D. Softening of the substrate is noted after coating.

E. Increases ($\sim$ 500°F) in DBTT are seen on coated specimens after 2100°F exposures, with most pronounced changes seen with cyclic exposure.

F. Increases in DBTT and surfaces cracking propensity are enhanced by aluminum rather than nitrogen difussion with 2100°F exposures. Higher DBTT's are

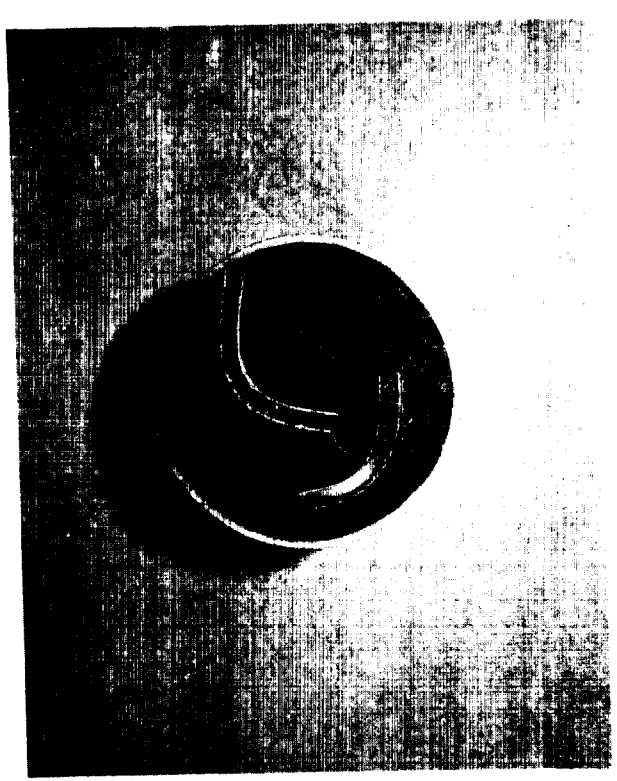

16 mils

100X DBT 1600°F

FIGURE 3-42

2ϕ COATED Cr-5W-Y DBTT SPECIMEN AFTER 100 HOURS AT 2400°F IN ARGON. NOTE SUCCESSFUL DBTT AND COATING CRACKING.

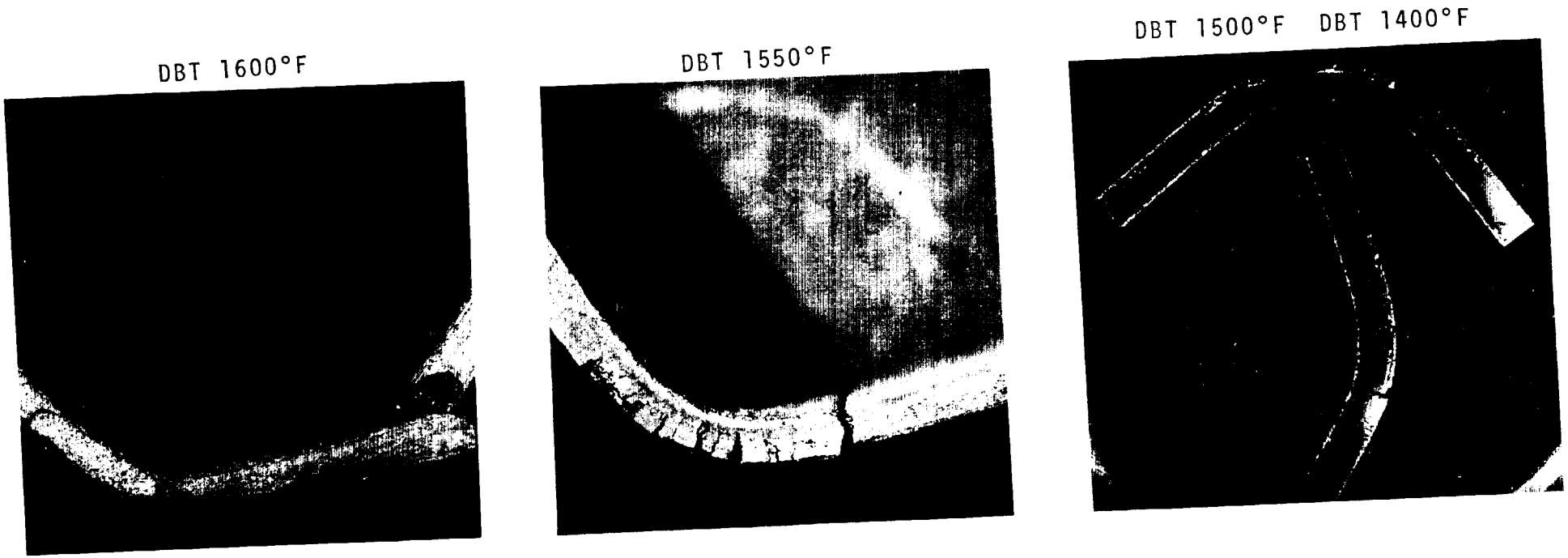

FIGURE 3-43

2ϕ COATED Cr-5W-Y DBTT SPECIMEN AFTER 10 HOURS AT 2400°F IN ARGON. NOTE EDGE CRACKING PROPAGATING FROM COATING.

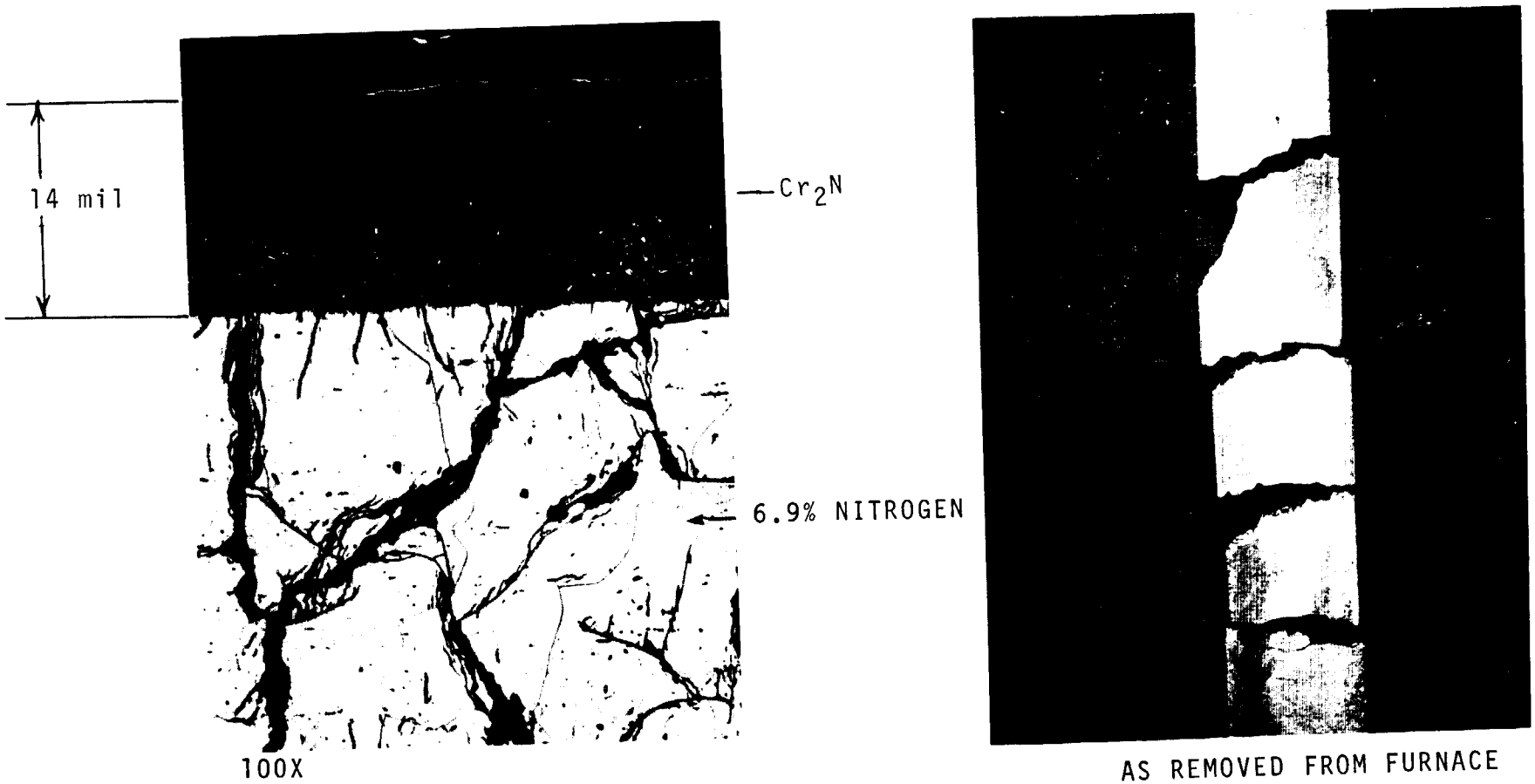

FIGURE 3-44

2ϕ COATED Cr-5W-Y DBTT SPECIMEN AFTER 100 HOURS AT 2400°F IN PURE NITROGEN. NOTE CATASTROPHIC FAILURE OF SPECIMEN DUE TO EXPOSURE ONLY IN NITROGEN. EXTENSIVE NITRIDE FORMATION WAS NOTED DUE TO ABSENCE OF ALUMINIZED PROTECTIVE LAYER.

obtained with greater aluminum diffusion.

G. In general, surface cracking per se does not preclude the attainment of reasonably good bends at 1200°F, i.e. cracking does not always propagate into the substrate.

H. Exposures at 2400°F for short times produce good (105°) bends at 1400°F, while long time exposures produce extremely high DBTT (1500°) value.

I. Even in argon atmospheres, the susceptibility to nitrogen diffusion in coated material is significant, although far less than seen with bare material. Further, the propensity toward nitrogen ingression is greater, the higher the exposure temperature.

J. Exposure at 2400°F in pure nitrogen with its attendant increase in nitrogen over that of air proved that the protection of the Cr-5W-Y alloy is attained by virtue of the formation of Al_2O_3 and $AlCrO_4$. This appears to so indicate that a pre-oxidized coated surface would behave significantly better upon exposure.

K. Coating hardness either before or after exposure is not a good measure of a system's DBTT.

This summary would indicate that an aluminum type coating on chromium base alloys shows significant promise for providing good oxidation/nitridation protection up to 2400°F. Substrate solution of aluminum, however, results in serious embrittlement and must be significantly retarded if practical use of this good protection is ever to be made.

3.4 TITANIUM-ALUMINUM SYSTEMS

3.4.1 General

As discussed briefly in the Literature Review (Section 1.2), there have been indications that the addition of certain tetravalent elements (e.g. titanium) improve the oxidation resistance of chromium. To this end it was decided to incorporate titanium in aluminum-type coatings.

3.4.2 Experimental Coating Trials and Evaluation

Table VI shows the experimental coating trials conducted on the substrate alloy. As can be seen, the co-deposition of titanium and aluminum proved to be most difficult. Figure 3-45 shows a photomicrograph of a specimen from XP19015 showing the porosity and oxides developed. It was subsequently decided to deposit the titanium and aluminum in a two step process with either the titanium or aluminum deposited first. As can be seen from Table VI, chromium was added to titanium in the pack so as to preclude the loss of chromium from the substrate upon reaction with the gaseous halide at the processing temperature. Further, the pack was pre-run at 2000°F to at least partially alloy the powder. This procedure is often employed so as to obviate powder segregation, and minimize deposition rates. As can be seen (XP19051), no coating was visible metallographically. However, a gold colored surface was visible indicating the possible formation of TiN. To minimize formation of this discolored surface, the experiment was run again

TABLE VI

TITANIUM-ALUMINUM EXPERIMENTAL COATING TRIALS ON Cr-5W-Y SUBSTRATE

XP #	PACK COMPOSITION Ti	Cr	Al_2O_3	I_2	TiH_2	PROCESSING °F/Hrs	WEIGHT CHANGE mg/cm^2	COATING THICKNESS mils	COMMENTS
19015	30%	3%Al	67%	1/4%	--	2000/10	+10.0	2.2	Heavily Oxidized and Porous Coating.
19045	37.5%	37.5%	25%	1/2%	--	2100/10	-----	---	Pre-Processing of Powder for XP19051.
19051	15%	15%	70%	1/4%	--	2000/10	+0.52	0.5	No Coating Visible. Some TiN Noted at Surface.
19063	15%	15%	70%	1/4%	2%	2200/10	+2.72	0.5-0.8	Adherent Bright Coating on Bare Substrate.
19063	15%	15%	70%	1/4%	2%	2200/10	-3.6	4.0	Adherent Slightly Oxidized Coating on Previously Aluminized Substrate.
19076	20%	20%	60%	1/4%	3%	2200/10	+12.8	0.8	Sponge Like Coating.
19085	37.5%	37.5%	25%	1/4%	--	2200/10	+10.6	0.6	Sponge Like Coating.
19092	25%	5%	70%	1/4%	--	2100/10	-----	---	Burn Out.
19097	25%	5%	70%	1/4%	3%	2200/10	-10.7	-----	No Coating.
19111	37.5%	37.5%	25%	1/4%	--	2100/10	-----	---	Burn Out.
19108	8.36% Al	22.34%	69.3%	1/4% K_2SiF_6	--	2000/10	+4.56	2.0	Tabs Were Previously Titanium Coated XP19085.
19115	37.5%	37.5%	25%	1/4%	2%	1800/10	-----	---	No Coating.
19117	37.5%	37.5%	25%	1/4%	--	2200/10	+6.93	4.0	Tabs Were Previously Aluminized In XP19102. UK.
19118	37.5%	37.5%	25%	1/4%	--	2200/40	-14.1	5.0	Tabs Were Previously Aluminized In XP19102. UK.

FIGURE: 3-45

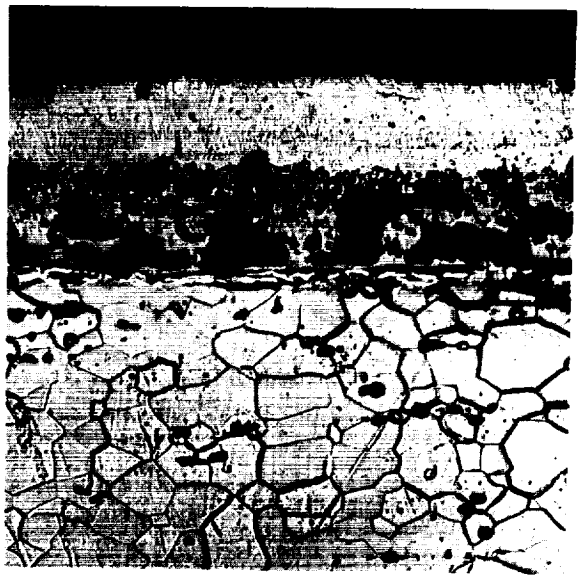

ETCH: 10% OXALIC ACID MAG: 250X

XP19015

FIGURE: 3-46

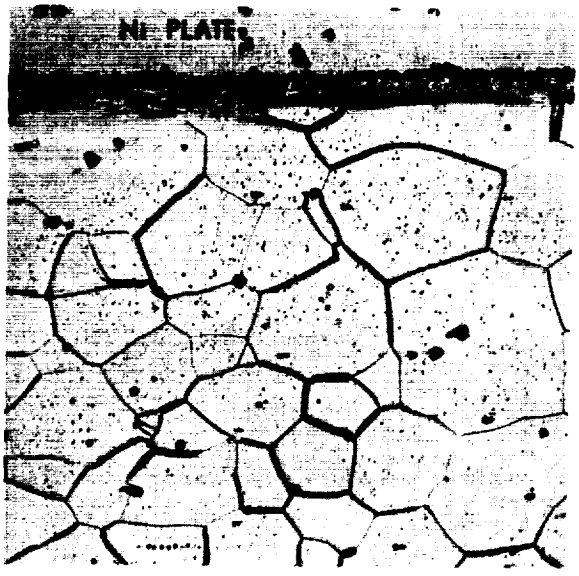

ETCH: 10% OXALIC ACID MAG: 250X

FIGURE: 3-47

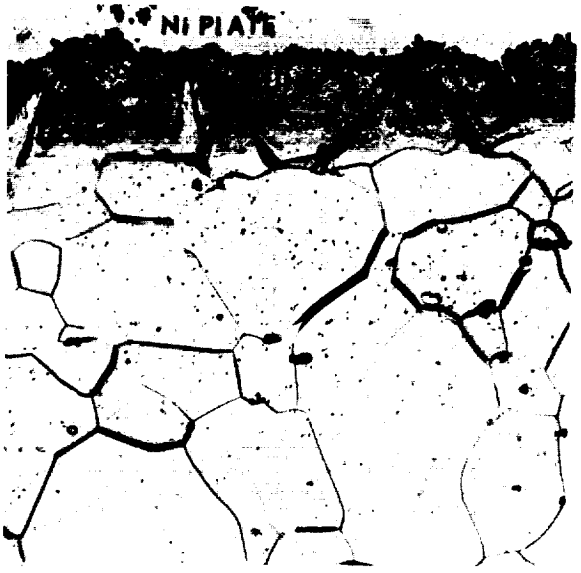

ETCH: 10% OXALIC ACID MAG: 250X

TITANIUM AND TITANIUM ALUMINUM COATINGS ON Cr-5W-Y, AS COATED. FIGURE 3-46 SHOWS TITANIUM DEPOSITED ON BARE SUBSTRATE (XP19063). FIGURE 3-47 SHOWS TITANIUM DEPOSITED ON PRE-ALUMINIZED SUBSTRATE MATERIAL (XP19063).

(XP19063) with the addition of 2% TiH_2 to the pack. Further, the processing temperature was increased to 2200°F to allow for further deposition. Concurrent with the above several specimens (pre-aluminum coated) were run to determine if titanium could be deposited in the second step of the operation. Figures 3-46 and 3-47 show photomicrographs of specimens from XP19063. It should be noted that although the coating was thicker on the pre-aluminized specimen, this specimen lost weight in the coating process. To determine if in fact titanium was deposited, a partial 2θ spectral scan (with the electron-beam microprobe) was run on the above mentioned specimen (XP19063). Figure 3-48 shows the results of the spectral scan indicating the presence of tungsten, chromium, and titanium. The presence of nickel is expected since the specimen evaluated was nickel plated. Figures 3-49 and 3-50 show electron-beam microprobe traces of the specimens from XP19063. Note the differences in the shape of the curves, diffusion depth and composition between these specimens coated in the bare condition and those in the pre-aluminized condition. Further, the possible presence of aluminum-oxide was indicated as noted by the "spike" in the traverse in Figure 3-50. Although no data is presented, short time oxidation testing at 2400°F of the titanium-aluminum coating showed poor results.

The high vapor pressure of chromium at 2200°F makes the adjustment of pack composition and processing time and temperature quite critical, as can be noted in several experiments

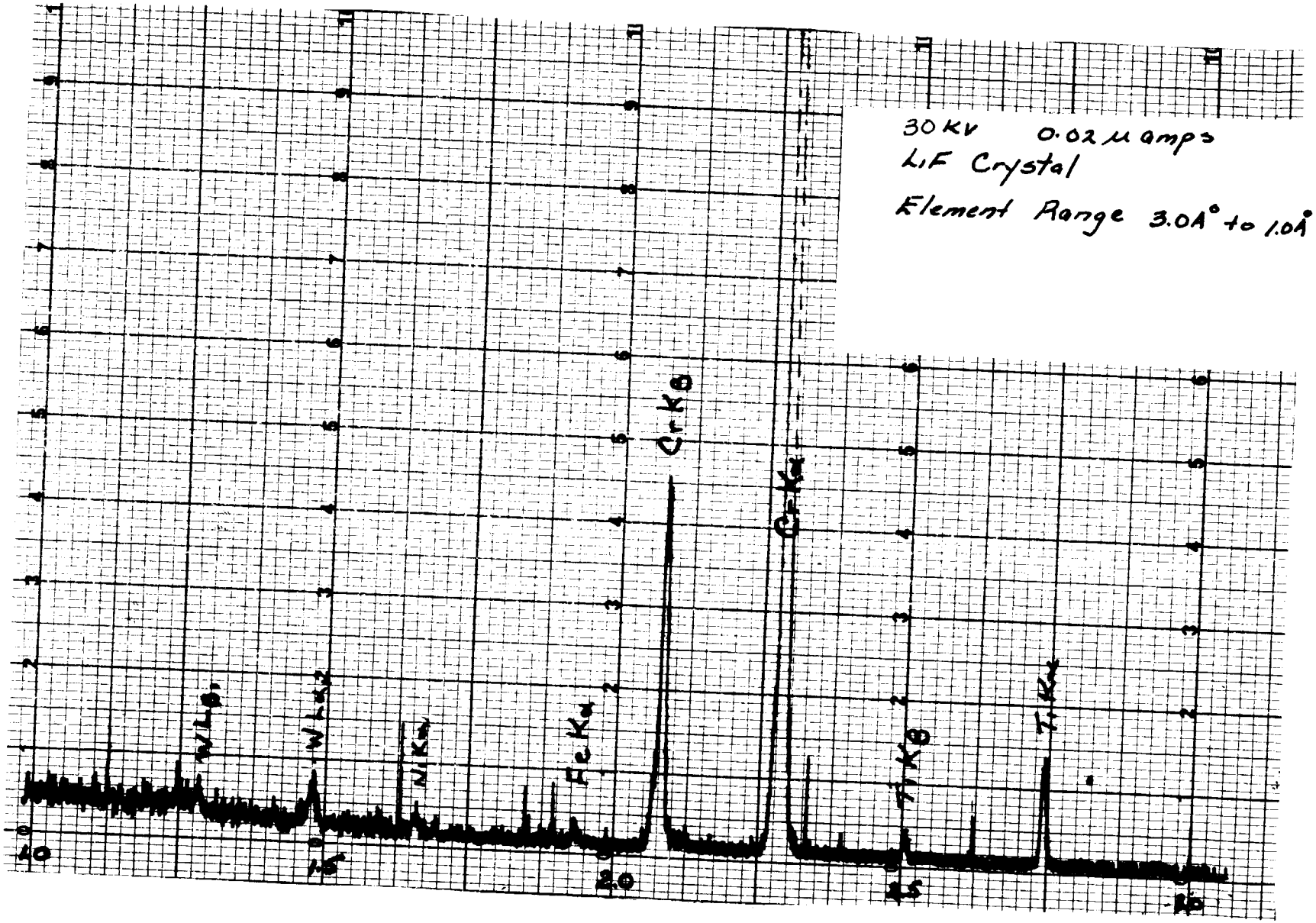

FIGURE 3-48

PARTIAL 2e SPECTRAL SCAN RUN ON SPECIMEN FROM XP19063 TO SHOW THAT TITANIUM WAS DEPOSITED.

URE 3-49

CTRON BEAM MICROPROBE
CE ON Ti COATED Cr-5W-Y
RE) SUBSTRATE (XP19063)

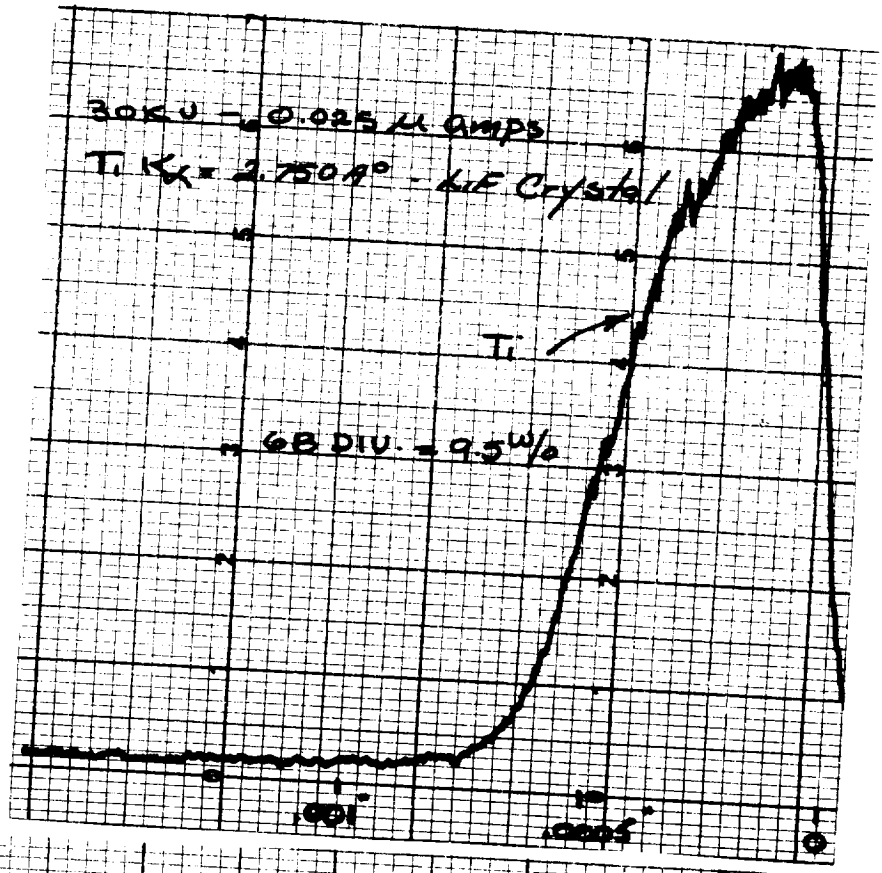

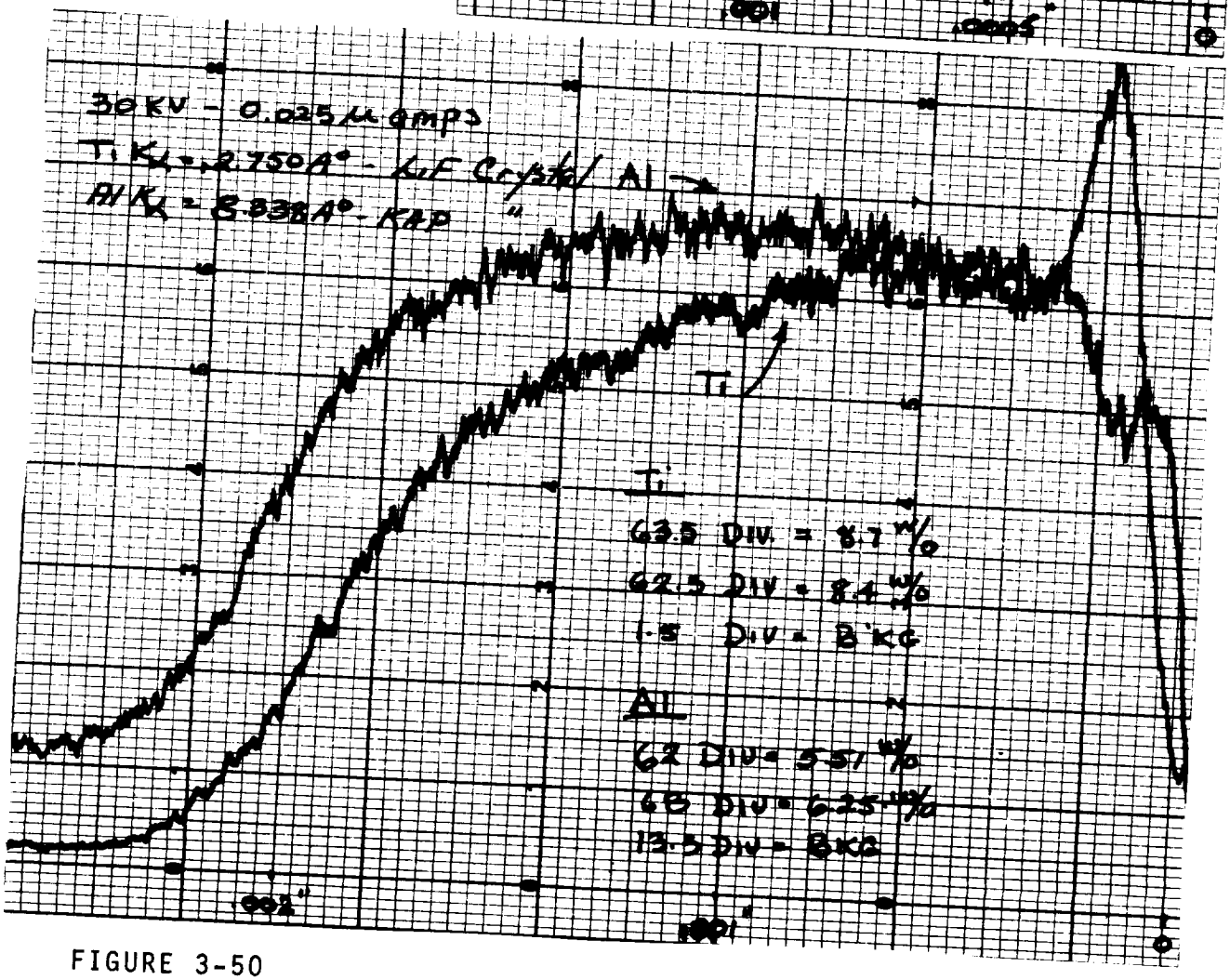

FIGURE 3-50

ELECTRON BEAM MICROPROBE TRACE ON Ti COATED (PRE-ALUMINIZED)
Cr-5W-Y SUBSTRATE (XP19063).

where a weight loss (after coating) was observed. Figure 3-51 shows a typical microstructure of Ti/Al coated Cr-5W-Y. Note that in the duplex coating the aluminum was deposited first. The "cracking" seen in the latter photomicrograph is due to metallographic polishing and was not in fact present in the as coated specimens.

A. The semi-quantitative electron-beam-microprobe traces (EBMP) illustrated in Figures 3-52 and 3-53 show the extent of titanium and aluminum diffusion as a function of time at temperature. Note that both these specimens showed titanium (peak) concentrations of approximately 10 W/o. The specimens run in XP19108 (titanized-aluminized) showed the best oxidation-nitrification resistance and although not shown, EBMP analyses indicated that the maximum concentration of this coating was 1.5 W/o titanium at a depth of 0.5 mils and decreased rapidly further inward. This would then tend to indicate that the oxidation-nitrification resistance of a titanium modified aluminum system is inversely proportional to the titanium concentration. However, it must be reiterated that although the use of titanium as a means of modifying an aluminum system appears to have deleterious effects on oxidation-nitrification resistance, a system such as those described are in fact much more resistant to attack than is the bare substrate.

B. Figure 3-54 shows three tabs from experimental runs after 100-hour exposures at 2400°F. Note the severe

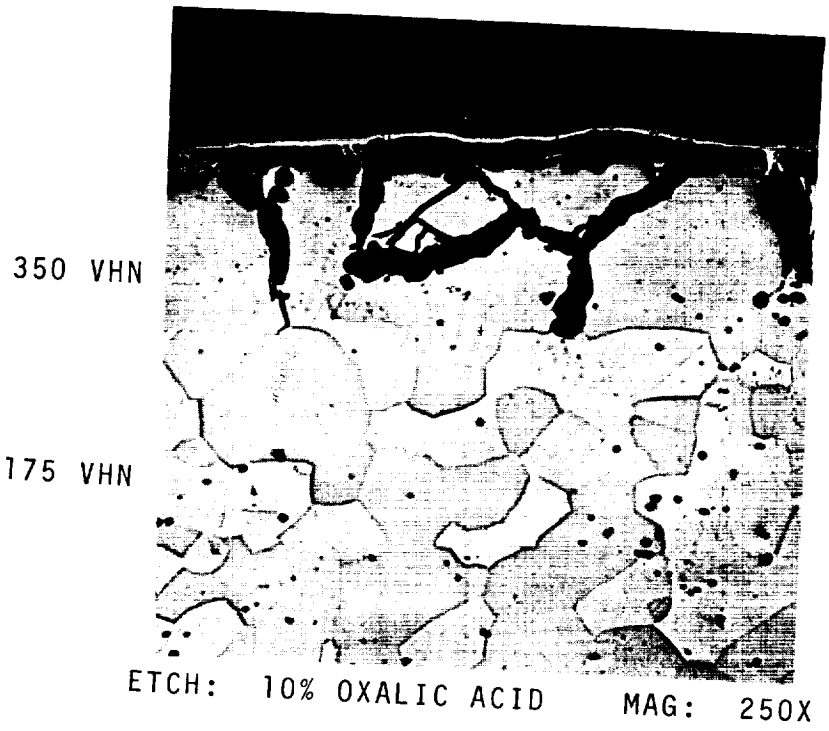

FIGURE 3-51

TITANIUM-ALUMINUM COATING ON Cr-5W-Y, AS COATED. FIGURE 3-51 SHOWS TITANIUM DEPOSITED ON PRE-ALUMINIZED SUBSTRATE (XP19102 + 19118).

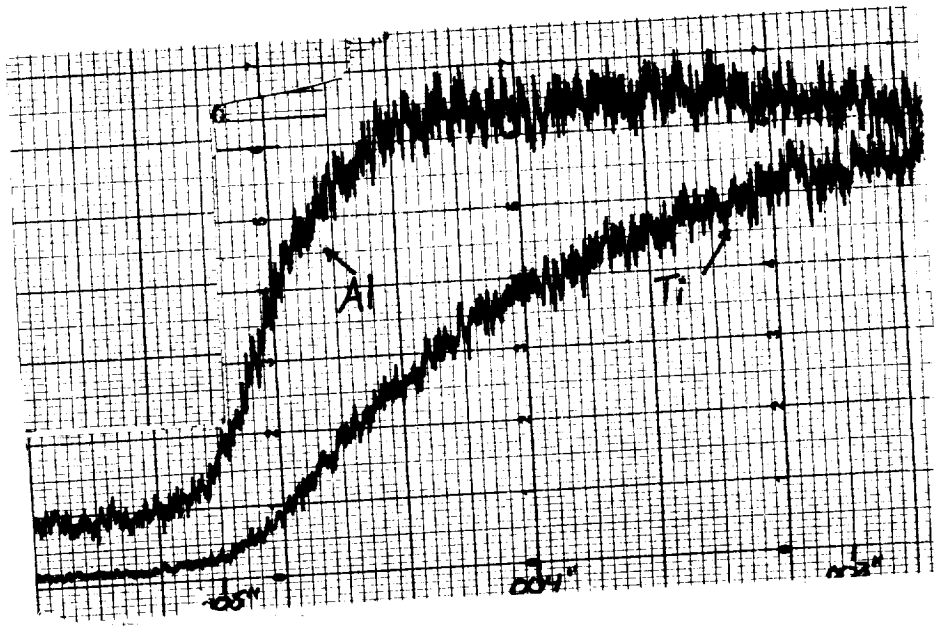

ELECTRON BEAM MICROPROBE TRAVERSE
Cr-5W-Y. SPECIMENS WERE ALUMINIZE
DEPOSITION.

FIGURE 3-52 (TOP)

XP19118. PACK CONTAINS 30% METAL
OF EQUAL WEIGHTS OF TITANIUM AND
CHROMIUM, PROCESSED AT 2200°F/40

FIGURE 3-53 (BOTTOM)

XP19117. PACK CONTAINS 30% META
OF EQUAL WEIGHTS OF TITANIUM AND
CHROMIUM, PROCESSED AT 2200°F/10

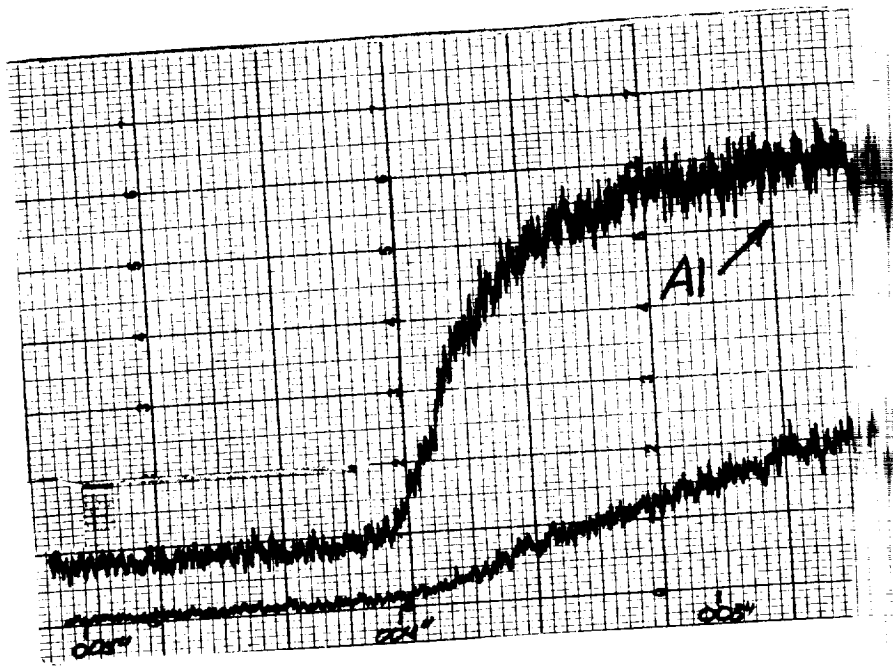

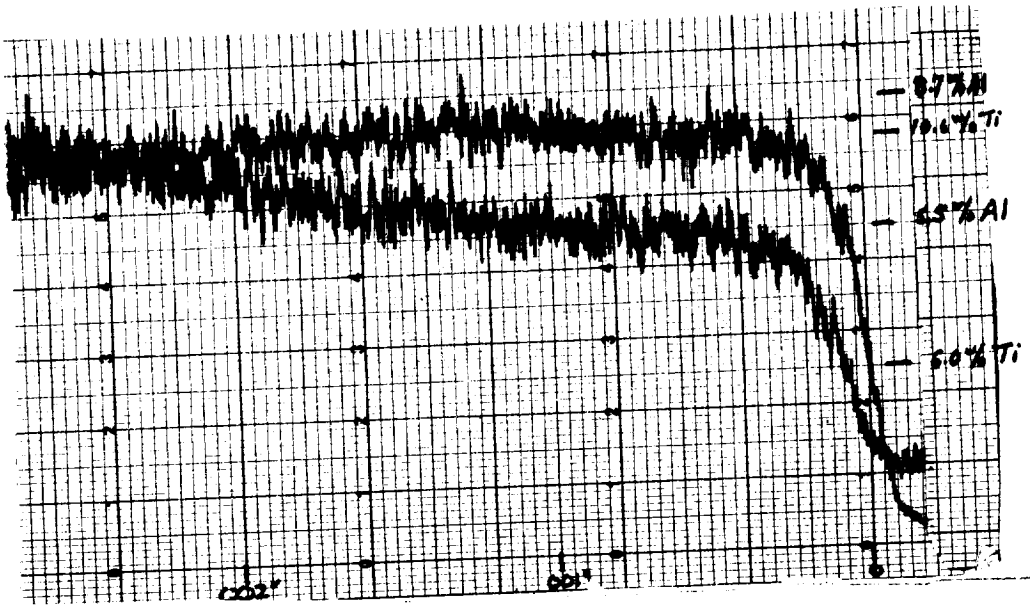

F TITANIUM-ALUMINUM COATED
PRIOR TO THE TITANIUM

.S.

RS.

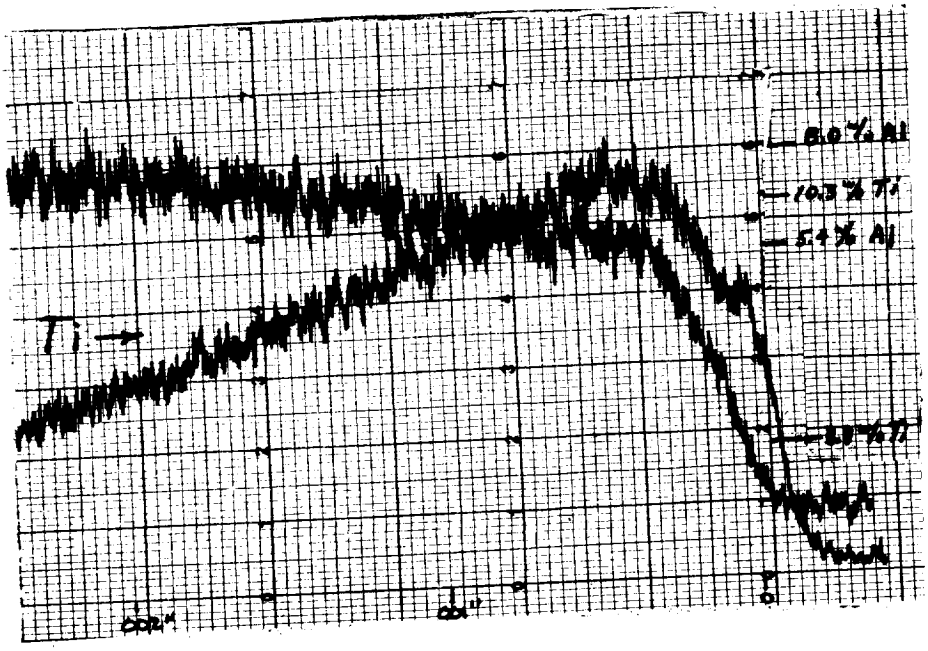

1

53-2

2400°F/100 hr's

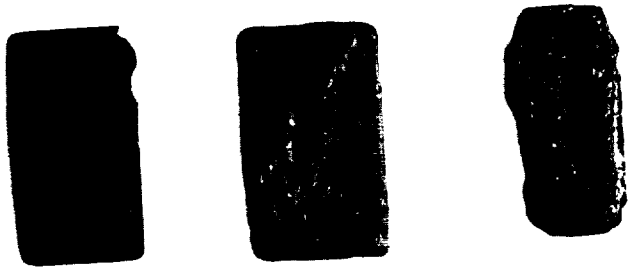

XP19108 XP19117 XP19118

~8% Ti (1) ~10% Ti ~13% Ti

(1) Values shown are for maximum concentration at surface

XP 19108

Titanium	2200°F/10 hours
Aluminum	2000°F/10 hours

XP 19117

Aluminum	2000°F/10 hours
Titanium	2200°F/10 hours

XP 19118

Aluminum	2000°F/10 hours
Titanium	2200°F/40 hours

FIGURE 3-54

TITANIUM-ALUMINUM COATINGS ON Cr-5W-Y AFTER 100 HOURS AT 2400°F. NOTE IMPROVED RESISTANCE TO ATTACK OF SPECIMEN (XP 19108) CONTAINING LEAST AMOUNT OF TITANIUM.

attack and coating spalling seen on all three specimens with the specimen from XP19108 (Ti then Al) showing the least attack.

C. Oxidation-weight change curves for several Ti/Al coating systems are shown in Figure 3-55. As can be seen from these data, the oxidation-nitrification resistance of any of these systems at 2400°F, although better than bare material, is poorer than a simple (note curve for two-phase coating) aluminum coating.

Based upon all the data obtained, it was decided that no further work on this system would be incorporated in the advanced testing. As mentioned above, it appears that the presence of titanium in an aluminum coating on the Cr-5W-Y decreases the oxidation resistance.

3.5 NICKEL ALUMINUM SYSTEM

3.5.1 General

Although the evaluation of nickel-aluminum systems was not originally called for in this program, it was felt that since Ni-Cr-Al alloys have such superior oxidation resistance, that the system warranted a cursory evaluation.

3.5.2 Experimental Coating Trials and Evaluation

A small number of experiments were conducted with the aim of depositing nickel (as a spinel former) on the Cr-5W-Y substrate

FIGURE 3-55

OXIDATION CURVES AT 2400°F FOR TITANIUM-ALUMINUM COATINGS ON Cr-5W-Y ALLOY.

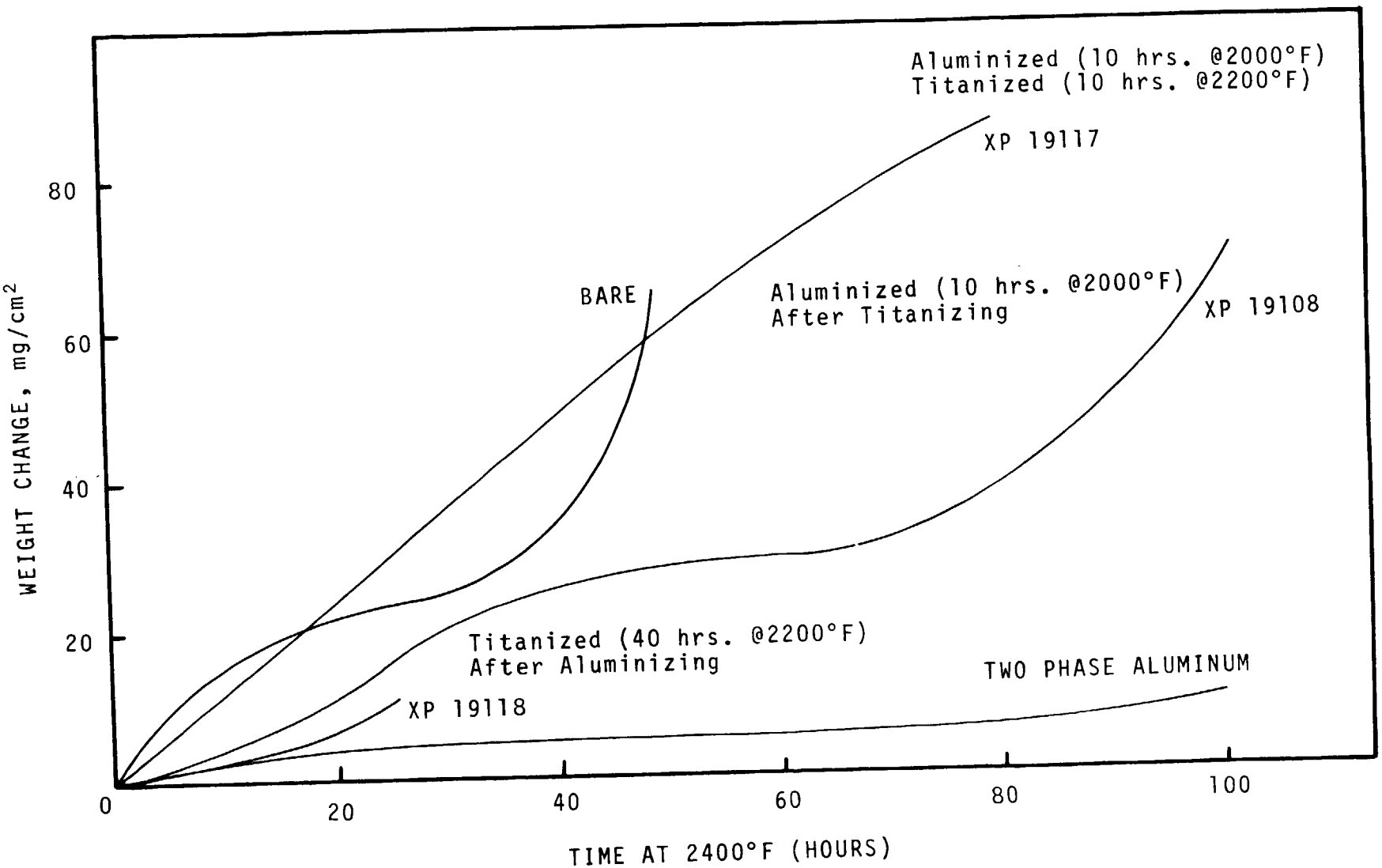

Since the possibility of accomplishing this by halide transfer appears highly improbable thermodynamically, deposition was attempted by means of a nickel-formate pack which has shown some promise in other programs. As can be seen by Table VII, no success was achieved and no further work attempted. It is, however, felt that nickel deposition might more easily be accomplished by decomposition of nickel carbonyl.

3.6 ALUMINUM SYSTEM INCORPORATING A GLASSY PHASE

3.6.1 General

In the approach to the development of coatings for gas turbine engine hot section hardware, resistance to foreign object damage (F.O.D.) has always been a subject of concern. The probability of impact damage is so high that no coating can be designed for such service without conscious considera- tion of it. Presently existing coating systems, deposited on superalloy substrates show fair ductility at service tempera- tures.

It must, however, be considered that present coating systems in commercial usage are based on superalloy substrates having moderately good, although not quite sufficient, inherent oxidation resistance. Coatings having the same degree of reliability as those presently so successful could never be considered for molybdenum substrates where an isolated pinhole might result in immediate catastrophic failure of the part.

One might reasonably expect the chromium base alloys to

TABLE VII

NICKEL-ALUMINUM EXPERIMENTAL COATING TRIALS

ON Cr-5W-Y ALLOY

XP #	PACK COMPOSITION				Process °F/hrs.	Weight Change mg/cm^2	Coating Thickness mils	Comments
	Ni Formate	Ni-Cr	Al_2O_3	I_2				
19093		50	50	1/4	2200/10			Surface Attack. No Coating.
19119	100				1650/10			Dull Silver. Pitted. No Coating.
19129	100				1750/10			Surface Attack. No Coating.
19138	100				1400/15			Surface Attack. No Coating.

fall somewhere between the superalloys and the refractory metals in sensitivity to coating defects. It is for this reason that considerable emphasis was placed on coating systems possessing either impact resistant or self-healing properties.

The glassy phase coating systems are designed to maximize the self-healing properties of the coating system. The rationale is the incorporation, within the matrix of the coating, of glassy particles or glass forming elements having softening points selected to provide viscous glasses capable of wetting and sealing defects which may be generated by impact, bending or stretching of the part in service.

3.6.2 Experimental Coating Trials and Evaluation

The program emphasis on optimization of effort on the simple-aluminum and Fe-Al systems precluded a detailed effort with this system. However, Table VIII shows the results of some of the coating trials. Figure 3-56 shows a photomicrograph of the Cr-5W-Y alloy after processing as per XP19185. It would appear that since no aluminum is present (note the EBMP analyses), the aluminizing cycle allowed for the reduction of SiO_2 to elemental silicon which subsequently diffused at 2000°F. The composition indicates the presence of Cr_2Si. Figures 3-57 and 3-58 show photomicrographs of specimens thus coated after 30 hours at 2100°F and 2400°F. Severe internal oxidation of the coating was observed with nitrogen ingression seen at 2400°F. Very erratic weight changes were observed in

TABLE VIII

EXPERIMENTAL COATING DATA OF THE ALUMINUM SYSTEMS

INCORPORATING A GLASSY PHASE

XP #	PACK COMPOSITION w/o		Processing Conditions °F/Hrs.	Weight Change mg/cm^2	Case Depth mils
19185	Slurry Coated With SiO_2 Pack In:		2000/10	10.1	2.6
	Al_2O_3	69.9			
	Cr	22.34			
	Al	8.36			
	K_2SiF_6	1/4			
19186	Si	60	2000/10	15.0	4.4
	Al	2			
	Al_2O_3	38			
	I_2	1/4			

FIGURE 3-56

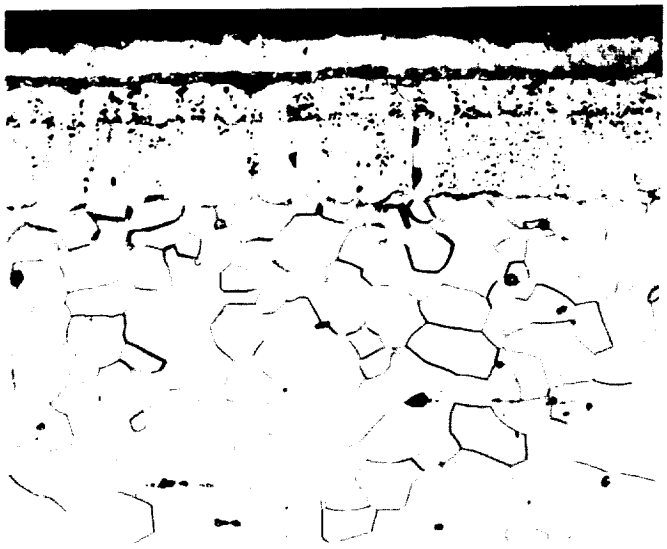

EBMP ANALYSIS

Cr	73.1	w/o
W	3.9	w/o
Al	0.0	
Si	23.0	w/o
Cr	94.9	w/o
W	5.1	w/o
Al	0.0	
Si	0.0	

ETCH 10% OXALIC ACID MAG: 250X
AS COATED

FIGURE 3-57

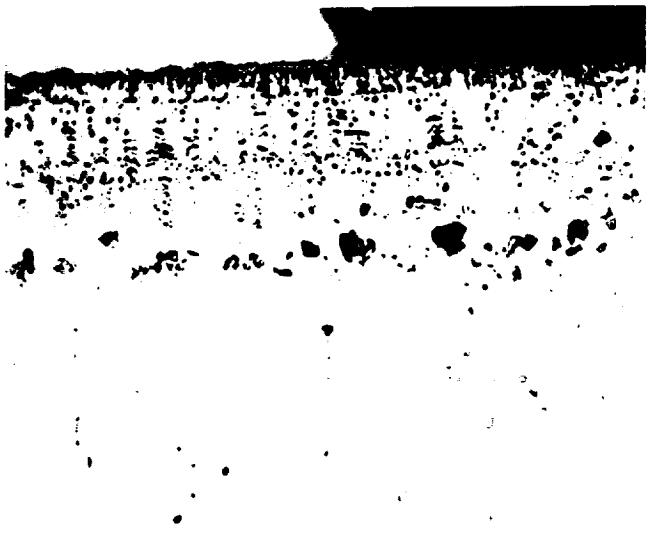

MAG: 250X
2100°F/100 HOURS

FIGURE 3-58

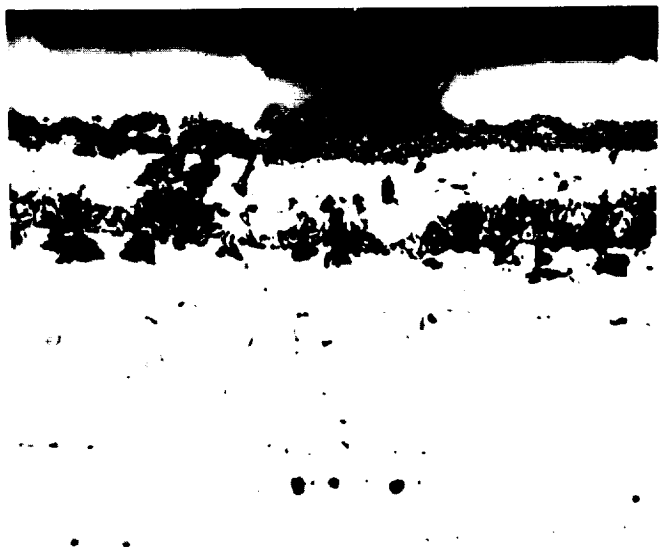

MAG: 250X
2400°F/100 HOURS

SiO_2 SLURRY-ALUMINIZED Cr-5W-Y ALLOY AS COATED AND AFTER OXIDATION EXPOSURE. NOTE EXTENT OF NITRIFICATION (3-58) AFTER EXPOSURE.

testing and thus the oxidation curves are not shown. It should be noted that the weight changes were in all cases manifested by large weight losses and gains after only short dwells at the testing temperatures. Figure 3-59 shows a photomicrograph of a specimen coated as per XP19186. It should be noted that co-deposition of Si and Al was achieved in the outer zone while the inner coating zone was quite similar to the UK coating. Oxidation tests on these specimens also showed extremely erratic results with extremely large weight changes (-60 mg/cm^2) observed. Figures 3-60 and 3-61 show photomicrographs of specimens (XP19186) after 30 hours at 2100°F and 2400°F. Note the severe oxygen attack, nitride formation and diffusion of these systems. It should be noted that although these systems did not exhibit good oxidation resistance, exposed systems did in fact show a glassy phase at the surface. Necessarily, this would indicate that a Cr-Al-Si coating could produce self-healing properties if in fact the composition were such so as to afford the desired oxidation properties.

As in the Ti-Al and Ni-Al systems, these coatings were not evaluated in the advanced testing phases, due to the less than encouraging results obtained.

3.7 ALUMINUM SYSTEMS WITH Fe-Co, Co-Ti AND Fe-Ti

3.7.1 General

It is generally accepted that the oxidation resistance of materials forming spinels at their surfaces upon exposure is superior to those forming simple oxides due to defect oxide

FIGURE 3-59

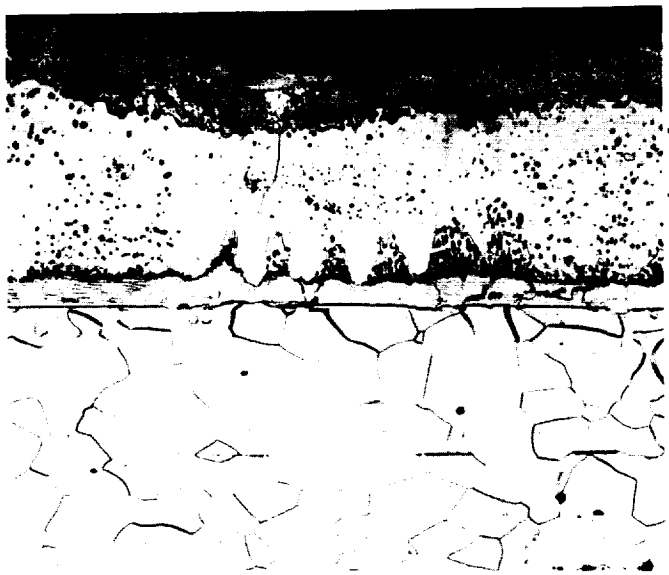

EBMP ANALYSIS

Cr	51.6	Si	37.6
Al	10.2	W	0.6
Cr	75.5	Si	20.5
Al	0.0	W	4.0
Cr	79.1	Si	0.0
Al	16.1	W	4.8

ETCH: OXALIC ACID MAG: 250X

AS COATED

FIGURE 3-60

MAG: 250X

2100°F/100 HOURS

FIGURE 3-61

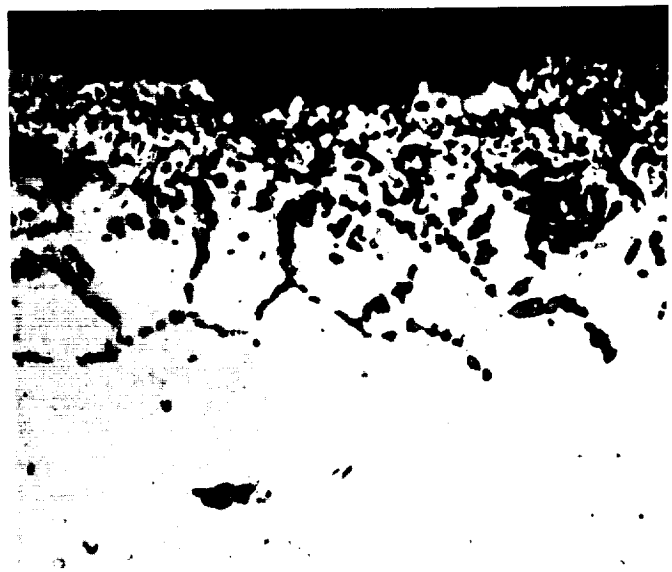

MAG: 250X

2400°F/100 HOURS

ALUMINUM-SILICON PACK COATED Cr-5W-Y AS COATED AND AFTER OXIDATION EXPOSURE.
NOTE EXTENT OF OXYGEN AND NITROGEN PENETRATION.

lattices, etc. It thus became apparent that a coating system incorporating elements which form complex spinels upon exposure might offer greater protection than one where only simple oxides form. Three complex spinel forming coating systems were to be evaluated for the Cr-5W-Y alloy, two of which contained a tetravalent element (Ti). These two latter systems (Al-Co-Ti and Al-Fe-Ti) were proposed to incorporate the benefits afforded by both tetravalent and strong spinel forming elements. Typical of some of the spinels which were expected are:

1. $FeO \cdot Cr_2O_3$
2. $FeO \cdot Al_2O_3$
3. $Fe_2 \cdot TiO_4$

It was further proposed that an Fe-Co-Al spinel would offer excellent resistance to oxidation by virtue of "sealing" the Al_2O_3 defect lattice. Three possible approaches were conceived for the deposition and/or diffusion of the above-mentioned systems as indicated below:

Type A - Whereby all the elements to be incorporated would be deposited in one process.

Type B - Whereby co-deposition of two elements would be followed by a second process to deposit the third element.

Type C - Whereby deposition of each element would be made in three separate processes.

Data gathered earlier in the program dictated that the

Type C approach, although most cumbersome, would be most easily facilitated. This was based on the fact that little or no success was achieved in attempts at co-depositing any of the elements in question. Although it is felt that co- and tri-deposition are possible, the time necessary to develop these techniques would be prohibitive. In addition, since the program was aimed at studying the effects of these elements and the feasibility of coating the Cr-5W-Y alloy, the triplex coating procedure permitted the deposition of these elements in a most efficient and expedient manner, whereby, based on preliminary data, tri-deposition was assured.

3.7.2 Experimental Coating Trials and Evaluation

Table IX shows the results of the experimental coating trials.

3.7.2.1 Al-Co-Ti

Based upon previous data on binary systems and the fact that the diffusion rate of aluminum in the Cr-5W-Y is high, it was decided to aluminize the Cr-5W-Y alloy prior to the deposition and/or diffusion of the cobalt and titanium. This was accomplished in a pack similar to that employed in the "UK" coating system, but processed at a lower temperature (1800°F) so as to compensate for the expected increase in case depth produced by the subsequent additions of titanium and cobalt. The deposition of the titanium followed by that of the cobalt produced the desired final coating alloy system. Total coating

Al-Co-Ti, Al-Fe-Ti AND Al-Fe-Co

COATING SYSTEM TRIALS ON Cr-5W-Y ALLOY

XP #	PACK COMPOSITION w/o	Processing Conditions °F/Hrs.	Weight Change mg/cm^2	Coating Thickness mils	Comments
Al-Co-Ti					
19173	8.36 Al, 22.34 Cr, 69.3 Al_2O_3, 1/4 K_2SiF_6	1800/10	2.1	1.0	
19175	25 Ti, 5 Cr, 70 Al_2O_3, 1/4 I_2	2200/25	6.85	2.1	
19176	25 Co, 5 Cr, 70 Al_2O_3, 1/4 I_2	1800/20	5.65	2.1	Inert Atmosphere Retort.
Al-Fe-Ti					
19154	25 Fe, 5 Cr, 70 Al_2O_3, 1/4 I_2	1900/20	1.98	1.0	Inert Atmosphere Retort.
19163	8.36 Al, 22.34 Cr, 69.3 Al_2O_3, 1/4 K_2SiF_6	1750/10	9.60	2.8	
19165	25 Ti, 5 Cr, 70 Al_2O_3, 1/4 I_2	2200/10	1.13	2.0	
Al-Fe-Co					
19154	25 Fe, 5 Cr, 70 Al_2O_3, 1/4 I_2	1900/20	1.98	1.0	Inert Atmosphere Retort.
19163	8.36 Al, 22.34 Cr, 69.3 Al_2O_3, 1/4 I_2	1750/10	9.60	2.8	
19178	25 Co, 5 Cr, 70 Al_2O_3, 1/4 I_2	1800/20	3.90	2.4	Inert Atmosphere Retort

NOTE: For each system, the XP #'s listed are in the chronological order of deposition for each element.

penetration was approximately 2.1 mils producing a coating which appeared to form an oxide layer on the surface and partially diffused into the substrate. Slight intergranular attack was noted near the interface of the coating which appeared to be the result of a low melting eutectic. This phenomenon was also noted on the cobalt-aluminum system which is described in a latter section.

Specimens were cyclic oxidation tested at 2100°F and 2400°F, with failure occurring at 2400°F after an exposure of 20 hours. At 2100°F slight spalling of the coating was noted, but because only modest weight gains were noted, this information did not merit termination of the test. Figure 3-62 shows the weight change-oxidation curves for this system.

Figure 3-63 shows the as deposited coating while Figure 3-64 illustrates a photomicrograph of the coating after 90 hours at 2100°F. Extensive oxidation and nitrification has occurred with almost no coating degradation evident. Table X shows the results of EBMP analyses, and it is significant to note that tri-deposition was in fact realized. Based upon these data, it was felt that no other work be attempted with this system, since it represented less protection than provided by a simple aluminum type coating.

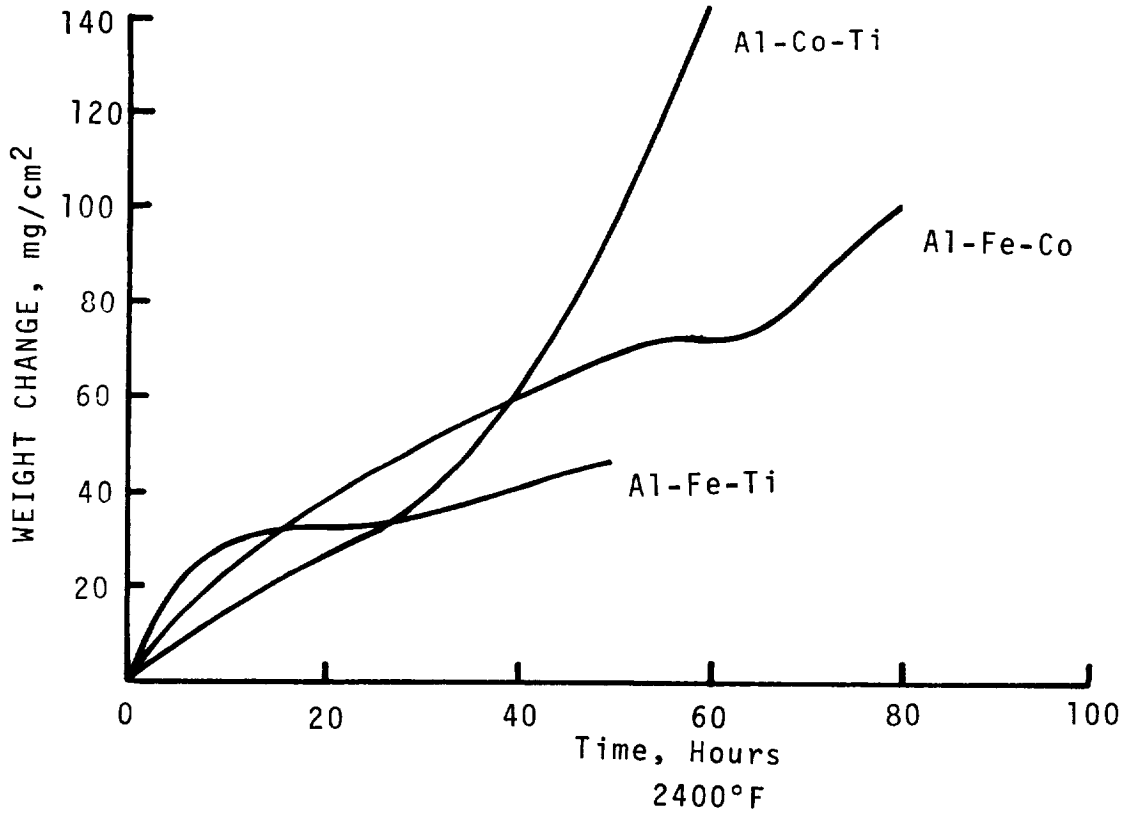

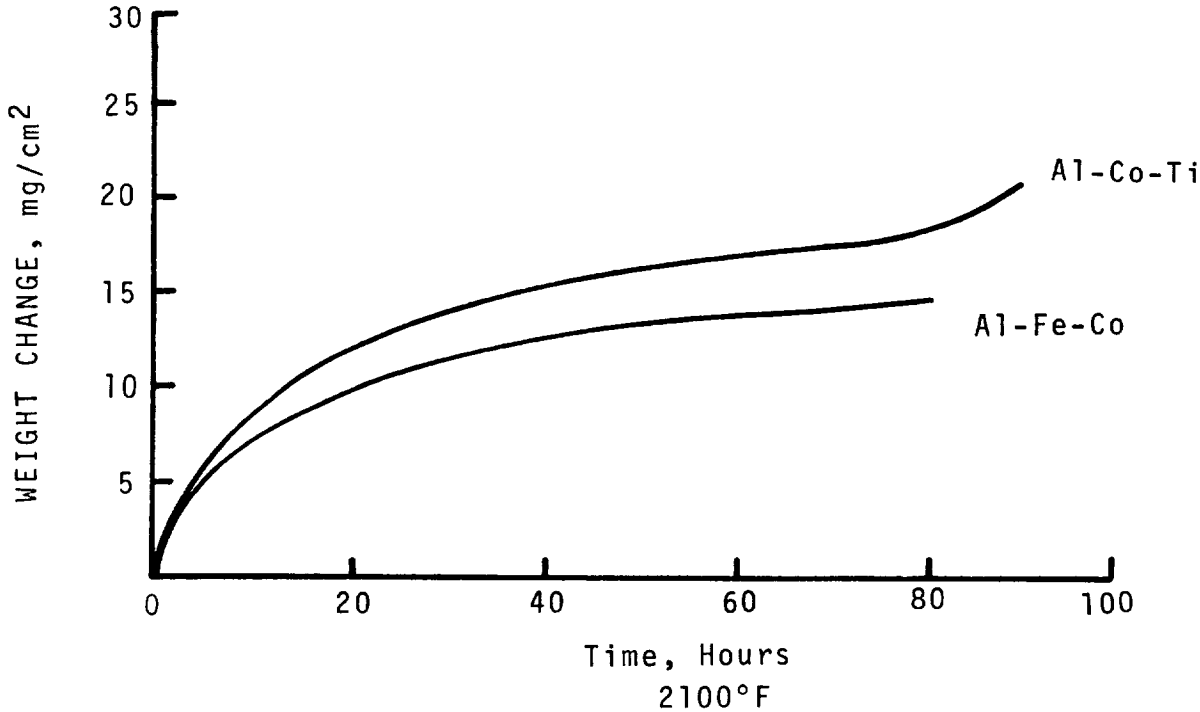

FIGURE 3-62

OXIDATION CURVES AT 2100°F AND 2400°F FOR COATING SYSTEMS AS INDICATED.

FIGURE 3-63

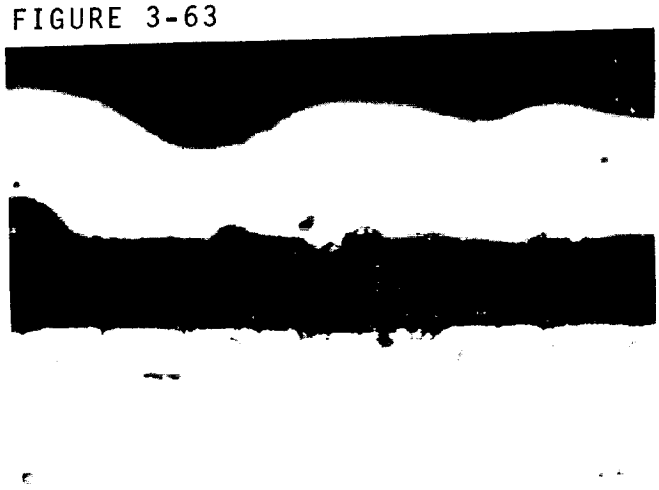

ETCH: OXALIC ACID MAG: 250X

FIGURE 3-64

ETCH: OXALIC ACID MAG: 250X

PHOTOMICROGRAPHS OF THE Al-Co-Ti COATING SYSTEM

FIGURE 3-63: AS COATED SPECIMENS
FIGURE 3-64: COATED AND EXPOSED SPECIMEN (2100°F/90 HOURS)
NOTE EXTENSIVE NITROGEN ATTACK OF SUBSTRATE

TABLE X

EBMP ANALYSIS OF THE COMPLEX SPINEL FORMING COATING SYSTEMS

System	Elements	Depth of Diffusion of Elements w/o 0.5 mils	1.0 mils	1.5 mils	2.0 mils	2.5 mils	3.0 mils
Al-Co-Ti	Aluminum	2.2	15.0	1.5	7.5	----	----
	Cobalt	1.0	1.0	1.1	-----	-----	------
	Titanium	16.0	14.8	12.0	10.0	0.0	0.0
Al-Fe-Ti	Aluminum	7.3	9.7	7.3	6.5	---	---
	Iron	23.3	25.7	24.2	15.8	14.6	----
	Titanium	49.7	31.8	27.4	20.1	0.0	0.0
Al-Fe-Co	Aluminum	5.7	4.1	3.9	3.9	---	---
	Iron	---	---	37.8	26.0	---	---
	Cobalt	4.3	3.5	2.0	1.5	----	---

3.7.2.2 Al-Fe-Ti

Although quite similar to the Al-Co-Ti system, deposition of the three elements proceeded with iron first and subsequently followed by deposition of aluminum and titanium, respectively, in separate processes. Through the course of this program, difficulty was experienced in depositing Co and Fe in halide atmospheres unless aluminum was deposited first. As can be seen from Table IX, ironizing was performed in an inert atmosphere. This has been found to be necessary to produce sound iron coatings. Figure 3-65 shows a photomicrograph of an Al-Fe-Ti coated Cr-5W-Y.

This system (Figure 3-65) produced a two phase coating which, unlike the Al-Co-Ti, was uniform and free from oxide scale and intergranular attack. Electron Beam Microprobe analysis, Table X, revealed the outer coating layer to be rich in titanium and iron (titanium 49.7 $^{W}/_{o}$, iron 23.3 $^{W}/_{o}$), with moderate percentages of aluminum. Total coating penetration was approximately 3 mils, with the iron and titanium decreasing significantly after 2 mils. Specimens were cyclic oxidation tested at 2100°F and 2400°F with failure occurring after the first ten hour cycle. Combined oxidation, nitrification and exfoliation of the coating prevented metallographic evaluation of the specimens. Figure 3-62 shows the weight change, oxidation curves for this coating alloy system.

	W/o	
Al	Ti	Fe
7.3	49.7	23.3
9.7	31.8	25.7
7.3	27.4	24.2
6.5	20.1	15.8

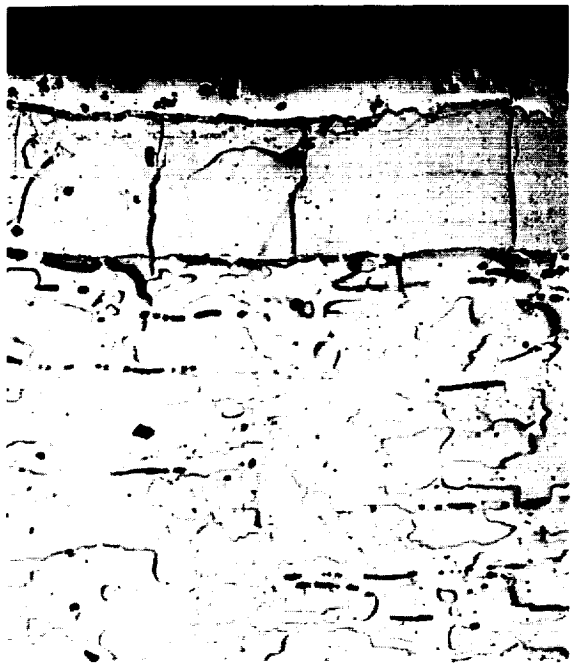

3.0 mils

ETCH: OXALIC ACID MAG: 250X

FIGURE 3-65

PHOTOMICROGRAPH OF THE Al-Ti-Fe COATED Cr-5W-Y

3.7.2.3 Al-Fe-Co

To prevent nitrogen ingression and attack of the base metal by low melting eutectics (as seen before), it was decided that the deposition of the aluminum should precede the deposition of the iron and cobalt. As previously, the powder from the "UK" coating alloy system was employed, using the same processing times and temperatures (1800°F for 10 hours); similar to what was performed on the two previously described systems. The deposition and/or diffusion of the iron and cobalt were performed in the inert atmosphere retort using the temperatures and times previously established in the systems described above. Figure 3-66 shows typical photomicrograph of the cross section of this coating alloy system. Although the Cr-5W-Y is free of attack and contamination, there appears to be an adherent oxide layer which has developed during coating on the surface of the alloy. This oxide layer has been shown to be rich in cobalt and penetrated to a depth of approximately 1.2 mils. Samples were oxidation tested at 2100°F and 2400°F with failure occurring visually (green spalling oxide) after ten hours of exposure. Oxidation test results are indicated in Figure 3-62. After exposure, specimens were examined microscopically for mode of failure. It appears that at either temperature, complete loss is evident with an oxide layer all through the surface. This appears to be Cr_2O_3 as seen in Figures

PRECEDING PAGE BLANK NOT FILMED.

3-67 and 3-68, with the 2400°F exposure exhibiting larger diffusional growth. Intergranular attack is noted in both specimens, with nitride precipitates seen within the grains at 2400°F. Both 2100°F and 2400°F exposures revealed what appear to be low melting oxides within the substrate of these specimens. EBMP analysis revealed (Table X) that Al-Fe-Co deposition was accomplished.

Based on all three systems studied, the following was revealed:

A. Tri-deposition of all elements studied was accomplished.

B. Oxide contamination was prevalent in Co containing systems, as coated.

C. No beneficial effects due to the presence of these elements (within the limits evaluated) in an aluminum coating were noted.

D. Catastrophic oxidation of these coatings was evident after 2400°F exposures.

Based upon these results, these coating systems were not taken into the advanced testing phase.

3.8 ALUMINUM-COBALT SYSTEMS

As discussed earlier, the formation of Cr_2O_3 on oxidation tested chromium does not deter further oxidation and nitrification of the

substrate material. This is due in part to the fact that Cr_2O_3 has a defect lattice structure and is not stable. It is well known that the oxidation resistance afforded by spinels (e.g. $NiO \cdot Cr_2O_3$) on the surface of many alloys is in most cases superior to that of pure oxides. This is due in part to the usual superior plasticity (1) and lattice density of these spinels. It is of interest to mention here that the superior oxidation/nitrification resistance of the program alloy (Cr-5W-Y) is in fact believed to be attributable to the formation of an Y-Cr_2O_3 type spinel on the surface of the exposed material (2).

Several experiments were conducted prior to the commencement of this contract which conclusively proved that deposition of either iron or cobalt from packs containing these elements and a halide energizer was virtually impossible. Thermodynamically the deposition of Fe or Co is not favored and the deposition experiments offer confirmation. The reactions with the halides appear to proceed as:

$$(1) \quad Cr + I_2 \rightarrow CrI_2$$

$$(2) \quad CrI_2 + Fe \rightarrow (FeCr) + I_2$$

or

$$(3) \quad CrI_2 + Co \rightarrow (CoCr) + I_2$$

(1) Journal of Electrochemical Society, E.G. Felton, 1961, Volume 108, Page 490.

(2) Corrosion Science, Seybolt, 1966, Volume 6, Pages 263-269.

The above reactions necessarily can affect a large weight change (loss) in the substrate alloy and consequently the iron and/or cobalt powder in the pack becomes coated with chromium. From these data it was decided to accomplish the deposition of aluminum coatings bearing iron and/or cobalt by one of three methods:

A. Co-deposition with aluminum.

B. Deposition from the metal halides followed by aluminizing.

C. Deposition from Fe-Cr, or Co-Cr packs followed by aluminizing.

Attempts to deposit by methods A and B met with little or no success and will be discussed below. For the purposes of clarity, the deposition of iron and cobalt will be discussed separately.

The choice of cobalt as an addition to aluminum coatings on the chromium substrate had as its foundation the same reasoning as for the choice of iron. It is well known that iron and cobalt behave alike in that both elements have strong tendencies to form spinels. Table XI shows the results of coating trials conducted on the cobalt-aluminum system. As can be noted, attempts to co-deposit aluminum and cobalt were unsuccessful. Further, the data clearly indicates that the deposition of cobalt from packs containing its iodide resulted in even more corrosive attack and lack of diffusion than seen in the iron coatings. As discussed above. the use of an argon purge was finally necessary to effect deposition without corrosive attack (i.e. by both oxygen and iodine). As in the

TABLE XI

COBALT-ALUMINUM EXPERIMENTAL COATING TRIALS ON Cr-5W-Y ALLOY

XP #	PACK COMPOSITION Co	Cr	Al_2O_3	I_2	PROCESSING CONDITIONS °F/Hrs.	WEIGHT CHANGE mg/cm^2	COMMENTS
19017	30%	3%Al	67%	1/4%	2000/10	-8.5	No Coating Deposited.
19033	10%CoI_2	--	90%		1600/10	----	Severe Surface Attack and Spalling.
19034	10%CoI_2	--	90%	1/8%	1600/10	----	" " " " "
19037	10%CoI_2	--	90%	----	1650/10	-51.0	Severe Surface Attack.
19041	5%CoI_2	--	95%	----	1750/10	-31.6	Surface Attack Noted.
19052	5%$CoBr_2$	--	95%	----	1750/10	-20.6	Intergranular Attack and Spalling.*
19065	5%$CoBr_2$	--	95%	----	1900/10	-18.9	Deposited on Bare Substrate.*
19065	5%$CoBr_2$	--	95%	----	1900/10	-29.1	Deposited on Pre-Aluminized Substrate. Coating Bright. Severe Intergranular Attack Noted In Both Cases.*
19079	5%$CoBr_2$	--	95%	----	1900/10		Heavy Oxide. Non-Magnetic.
19083	25%	5%	70%	1/4%	2200/10	-82.55	No Coating. Low Melt Phase Present. Heavy Attack.*
19084	25%	2.5%	72.5%	1/4%	2200/10	-63.34	No Coating. Low Melt Phase Present. Heavy Attack.*
19125	62.5%	12.5%	25%	1/2%	2100/10		Powder Burn Out.
19128	62.5%	12.5%	25%	1/4%	2200/10		Tabs Were Attacked.*
19132	62.5%	12.5%	25%	1/4%	2100/10	+3.32	Tabs Previously Aluminized in XP19127. Attack.
19136	62.5%	12.5%	25%	1/4%	2200/10	+28.0	Heavy Attack.*
19137	62.5%	12.5%	25%	1/4%	2200/10	-27.0	Heavy Attack.*
19144	62.5%	12.5%	25%	1/4%	1900/23	-1.94	Heavy Attack.**

* Argon
** Argon Flow

experiments conducted on iron, deposition free of contaminating effect as described above, was finally accomplished with use of a pack (XP19065) containing Al_2O_3 and $CoBr_2$. Figures 3-69 and 3-70 show photomicrographs of specimens from this experiment on both bare and pre-aluminized specimens. As can be seen in both photographs, excessive intergranular attack was noted, penetrating deep (0.003-0.006") into the substrate. A subsequent X-Ray photograph and microbrobe trace were conducted on a specimen (not pre-aluminized) to determine the approximate chemical composition of those areas attacked. Figure 3-71 shows the results of these tests indicating that this attack is quite deep and in fact cobalt rich. It should further be noted that the coating has partially separated from the substrate and contains both voids and non-metallic inclusions. Finally, the attempts at co-deposition also met with little or no success. Based on these data, all the efforts expended during subsequent work were aimed at depositing the cobalt modified system in a duplex manner. The procedures followed those employed with the previously described titanium system with the exception that in almost all cases the experiments were run under either flowing or static argon atmospheres, since all runs indicated that this deposition could not be accomplished in simple halide atmospheres. Figures 3-72 and 3-73 show typical microstructures of cobalt coated Cr-5W-Y substrate. The use of a faulty retort resulted in considerable contamination of the substrate(Figure 3-72). However, as can also be noted,some contamination and voids are also present in the specimen seen in Figure 3-73.

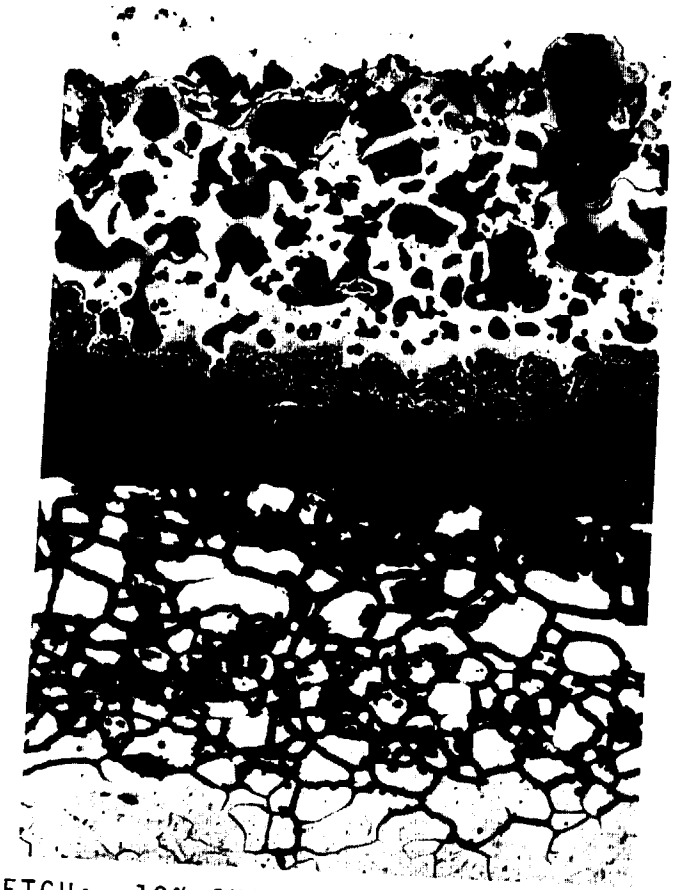

ETCH: 10% OXALIC ACID MAG: 200X

FIGURE 3-69

ETCH: 10% OXALIC ACID MAG: 100X

FIGURE 3-70

PHOTOMICROGRAPHS OF COBALT COATED (FIGURE 3-69) BARE AND PRE-ALUMINIZED (FIGURE 3-70) Cr-5W-Y SUBSTRATE. NOTE SEPARATION OF COATING AND SEVERE INTERGRANULAR (PROBABLY COBALT OXIDE) ATTACK.

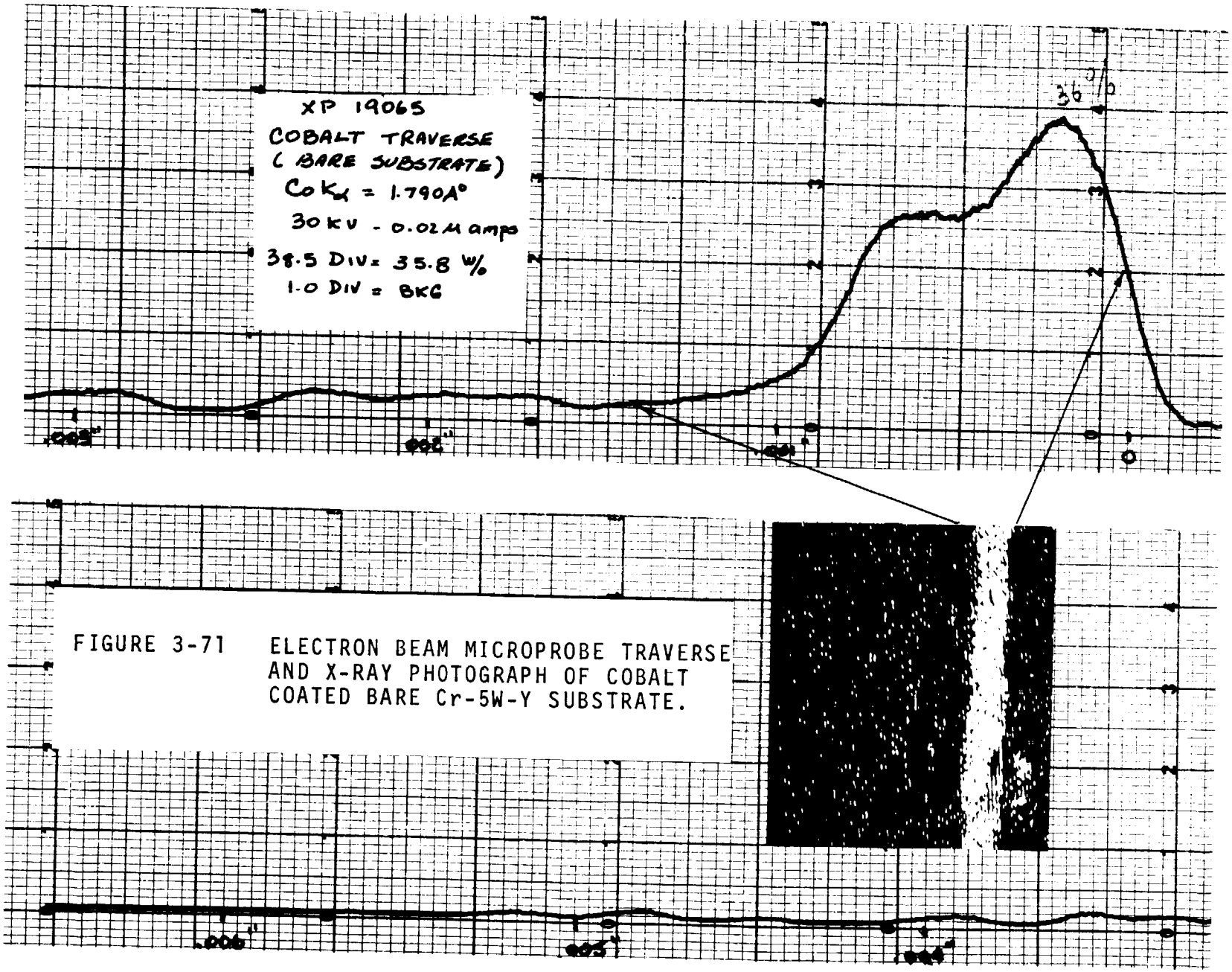

FIGURE 3-71 ELECTRON BEAM MICROPROBE TRAVERSE AND X-RAY PHOTOGRAPH OF COBALT COATED BARE Cr-5W-Y SUBSTRATE.

FIGURE 3-72

VOIDS AND HIGH COBALT CONCENTRATION AREAS

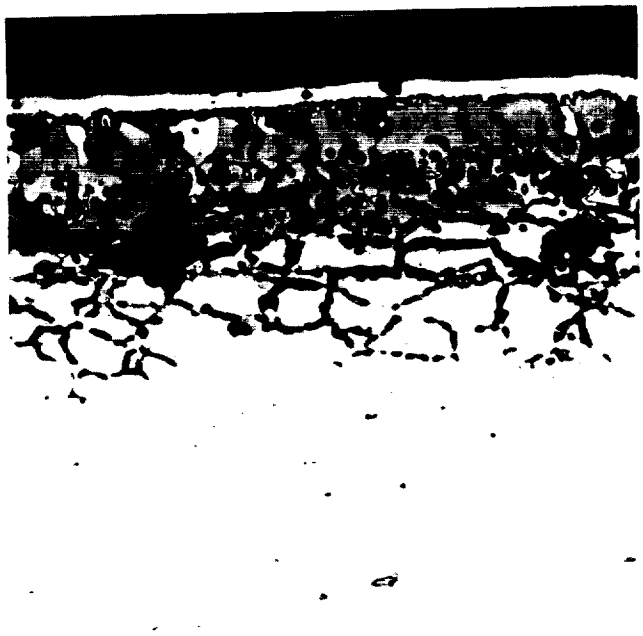

645 VHN

381 VHN

268 VHN

ETCH: 10% OXALIC ACID MAG: 250X

FIGURE 3-73

VOIDS AND HIGH COBALT CONCENTRATION AREAS

375 VHN

206 VHN

189 VHN

ETCH: 10% OXALIC ACID MAG: 250X

COBALT COATED Cr-5W-Y SUBSTRATE. NOTE EXTENT OF INTERGRANULAR ATTACK ON BOTH (FIGURE 3-72 FAULTY RETORT, FIGURE 3-73 NEW RETORT) SPECIMENS CONCOMITANT WITH SEVERE VOIDING. THE HEAVIER ATTACK NOTED ON THE SPECIMEN SEEN IN FIGURE 3-72 IS DUE TO A FAULTY RETORT. AS CAN BE SEEN FROM FIGURE 3-73 LESS CONTAMINATION HAS RESULTED WITH GOOD RETORT SEALING PRACTICE.

Some of these same described effects were found (to a slightly lesser degree) in some work on the cobaltizing of nickel base superalloys some years ago (3). In this prior work, the contamination was found to be caused by the formation of a cobalt-alloy oxide which is a liquid at the coating temperatures employed. The oxide then attacks the grain boundaries of the alloy. What has been seen in the Cr-5W-Y alloy may also be caused by the same set of conditions.

As can be noted, all the work conducted on the Co-Al system produced no one method for the efficient deposition of cobalt onto Cr-5W-Y. Further, no co-deposition technique was found to be workable. Necessarily no further work was accomplished on duplex coating since the cobalt portion of the system could not be worked out. No additional work was performed on this system nor were any tests possible.

3.9 IRON-ALUMINUM SYSTEM

3.9.1 General

The choice of iron-aluminum coating systems for evaluation had as its foundation, the following reasons:

A. Iron's ability to form reasonably "plastic" oxidation resistant spinels.

B. The known excellent oxidation resistance of of Fe-Al, Fe-Cr and Fe-Cr-Al alloys.

C. The excellent compatability between iron and chromium, since the alloy under study contained

(3) Unpublished Data, M. Negrin and A. Noetzel, Chromalloy Division, 1965

greater than 95% chromium

In order to accomplish the desired end i.e., an Fe-Al coating on the Cr-5W-Y alloy, several methods of approach were considered and evaluated as follows:

A. Deposition of iron from an iron pack (I_2 energizer) followed by aluminizing.

B. Co-deposition of iron and aluminum from an Fe-Al pack (I_2 energizer).

C. Deposition of iron from packs containing ferrous-halides (with or without elemental iron) followed by aluminizing.

D. Deposition of iron from a pack containing iron chromium (I_2 energizer) with the latter concentration being sufficient so as to preclude the "dechromizing" of the substrate alloy. As mentioned below, this "de-chromizing" is likely due to the reaction with halide of the chromium substrate at temperatures lower than that necessary for the formation of ferrous halides.

Methods A and B described above were virtually unsuccessful. However, it is felt that suitable techniques could be developed, time permitting. Method C, although partially successful in earlier experiments, proved to be non-reproducible in many aspects, e.g., weight change, corrosive attack, and surface appearance. Some of the problems were very similar to that seen with Co-Al systems.

Based upon these results, most of the coating efforts were expended with methods as described in D.

3.9.2 Experimental Coating Trials and Evaluation

Table XII shows the experimental coating trials conducted on the iron-aluminum system. Figures 3-74 and 3-75 show photomicrograph coated as per XP 19016 and 19025 showing oxide build-up at the surface. Note that the substrate in the specimen from XP 19025 has not undergone recrystallization. Subsequent to these experiments it was decided to attempt coating the substrate from packs containing ferrous halides. It was felt that the use of iron in the form (FeI_2) would preclude the formation of chromous iodide since during pack heat up, the iodide would first decompose thermally. Subsequent iron deposition would then take place and upon reaching the coating temperature, the diffusion of iron into the substrate would necessarily lower the activity of the chromium and minimize any possible weight losses due to chromium reaction with iodine. As can be seen from the comments in Table XI, only mixed success was achieved. Excessive contamination was seen on the surface of specimens from these experiments. This contamination consisted of both oxide and iodine products. To eliminate this contamination, probably caused by an inadequate purge and over-activity of the iodide, additional sets of experiments were designed using the less active bromides, and an argon purge. This procedure (XP 19052, XP 19065) was employed on both bare and pre-aluminized specimens. Figures 3-76 and 3-77 show photomicrographs from speci-

TABLE XII

IRON-ALUMINUM EXPERIMENTAL COATING TRIALS ON Cr-5W-Y ALLOY

XP #	PACK COMPOSITION Fe	Cr	Al	Al_2O_3	I_2	PROCESSING CONDITIONS °F/Hrs.	WEIGHT CHANGE mg/cm^2	COATING THICKNESS mils	COMMENTS
19004	30%		3%	67%	1/4%	1900/15	-1.6	---	No Coating Deposited.
19016	30%		3%	67%	1/4%, 1/4%$FeCl_3$	2000/10	-3.8	---	" " "
19025	15%		---	85%	1/4%	1400/10	+5.98	1.4	Coating Spalled and Heavily Oxidized.
19026	30%		3%	67%	1/4%	1400/10	+0.25	---	No Coating Visible.
19031	10%FeI_2		90%			1600/10	-----	---	Specimens Severely Attacked and Spalled.
19032	10%FeI_2		90%		1/8%	1600/10	-----	---	Specimens Severely Attacked and Spalled.
19038	10%FeI_2		90%			1650/10	-16.9	---	No Coating Deposited.
19042	5%FeI_2		95%			1750/10	-21.84	---	Heavily Oxidized Surface Noted.
19053	5%$FeBr_2$		95%			1750/10(1)	-7.3	0.5	Very Thin Coating Deposited.
19064	5%$FeBr_2$		95%			1900/10	-9.5	1.0	Deposited on Bare Substrate. Coating Bright.
19064	5%$FeBr_2$			95%		1900/10	+2.64	1.8	Deposited on Pre-Aluminized Substrate. Coating Bright.
19078(4)	5%			95%		1900/10			Heavy Green Oxide. Unable to Identify.
19081(1)	15%	15%		70%	1/4%	2200/10	+12.17		Nitride Attack.

TABLE XII (Cont.)

IRON-ALUMINUM EXPERIMENTAL COATING TRIALS ON Cr-5W-Y ALLOY

XP #	PACK COMPOSITION Fe	Cr	Al	Al_2O_3	I_2	PROCESSING CONDITIONS °F/Hrs.	WEIGHT CHANGE mg/cm^2	COATING THICKNESS mils	COMMENTS
19082(1)	15%	15%		70%	1/4%	2200/10	+9.40	2.0	Nitride Attack.
19086(1)	15%	15%		70%	1/4%	2200/10	+7.59		Nitride Attack. Slightly Magnetic.
19087(1)	15%	15%		70%	1/4%	2100/10			Powder Burn Out.
19089(1)	25%	5%		70%	1/4%	2200/10	+42.1		Nitride Attack. Non-Magnetic. Dark Green in Color.
19090(4)	25%	5%	1%	69%	1/4%	2200/10	-101.6		Nitride Attack. Slightly Magnetic.
19091(4)	25%	5%	5%	65%	1/4%	2200/10	-90.7	3.2	Nitride. Non-Magnetic.
19103(1)	25%	5%		70%	1/4%	2200/10	+6.78		Tabs Bright, Magnetic, No Signs of Nitride.
19105(1)	25%	5%		70%	1/4%	2100/10			Powder Burn Out.
19109(1)	25%	5%		70%	1/4%	2200/10			Vacuum Retort Split. Tabs Oxidized.
19110(1)	25%	5%		70%	1/4%	2200/10			Retort Was Welded. It Again Split on the Seams.
19116(1)	25%	5%		70%	1/4%	2200/10			Heavy Nitride Attack. Unable to Weigh Tabs.
19124(1)	25%	5%		70%	1/4%	2100/10			Powder Burn Out.
19131(4)	25%	5%		70%	1/4%	2200/10	+63.8		Tabs were Previously Aluminized. Heavy Nitride Layer.

TABLE XII (Cont.)

IRON-ALUMINUM EXPERIMENTAL COATING TRIALS ON Cr-5W-Y ALLOY

XP #	PACK COMPOSITION Fe	Cr	Al	Al_2O_3	I_2	PROCESSING CONDITIONS °F/Hrs.	WEIGHT CHANGE mg/cm^2	COATING THICKNESS mils	COMMENTS
19134(2)	25%	5%		70%	1/4%	2200/10	-.0011	0.8	No Nitride Layer. Slightly Magnetic.
19135(4)	25%	5%		70%	1/4%	2200/10	-.0014		No Nitride Layer. Slightly Magnetic.
19139(4)	25%	5%		70%	1/4%	2200/10	-.84		No Nitride Layer. Slightly Magnetic.
19140(2)	25%	5%		70%	1/4%	1900/10	+2.36	0.8	No Nitride Layer. Slightly Magnetic.
19141(3)	25%	5%		70%	1/4%	1900/23	+1.38	1.0	No Nitride Layer. Slightly Magnetic.
19142(4)			8%	92%	1/4%	1850/10	+2.75	5.4	2φ Aluminum Process Tabs Were Previously Ironized in XP19141.
19143(4)		22.34%	8.36%	69.3%	1/4% K_2SiF_6	2000/10	+2.76	9.4	UK Aluminum Process. Tabs Were Previously Ironized in XP19141.
19145(4)			8%	92%	1/4%	1700/10	+9.22	5.2	2φ Aluminum Process Tabs Were Previously Ironized in XP19141.
19146(4)		22.34%	8.36%	69.3%	1/4% K_2SiF_6	1850/10	+7.52	2.2	UK Aluminum Process. Tabs Were Previously Ironized in XP19141.

TABLE XII (Cont.)

IRON-ALUMINUM EXPERIMENTAL COATING TRIALS ON Cr-5W-Y ALLOY

XP #	PACK COMPOSITION Fe	Cr	Al	Al_2O_3	I_2	PROCESSING CONDITIONS °F/Hrs.	WEIGHT CHANGE mg/cm^2	COATING THICKNESS mils	COMMENTS
19147(3)	25%	5%		70%	1/4%	1750/23	+1.85	0.8	No Nitride Present. Slightly Magnetic. Dark Green.
19148(3)	25%	5%		70%	1/4%	1750/23	+1.92	0.6	No Nitride Present. Slightly Magnetic. Dark Green.
19149(4)			8%	92%	1/4%	1700/10	+7.50	2.4	2ϕ Aluminum Process. Tabs from XP19148.
19150(4)		22.34%	8.36%	69.3%	1/4% K_2SiF_6	1800/10	+13.2	5.0	UK Aluminum Process. Tabs from XP19148.

(1) Static Argon Defective Retort

(2) Static Argon New Retort

(3) Flowing Argon New Retort

(4) Conventional Pack-Cementation Type Retort

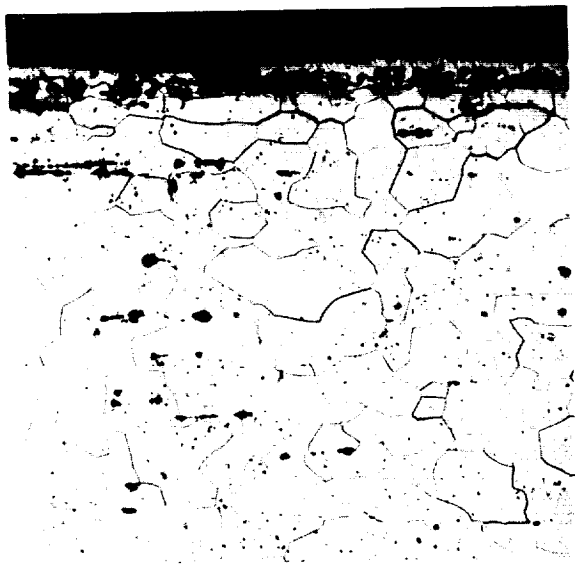

ETCH: 10% OXALIC ACID MAG: 250X

FIGURE 3-74 AS COATED

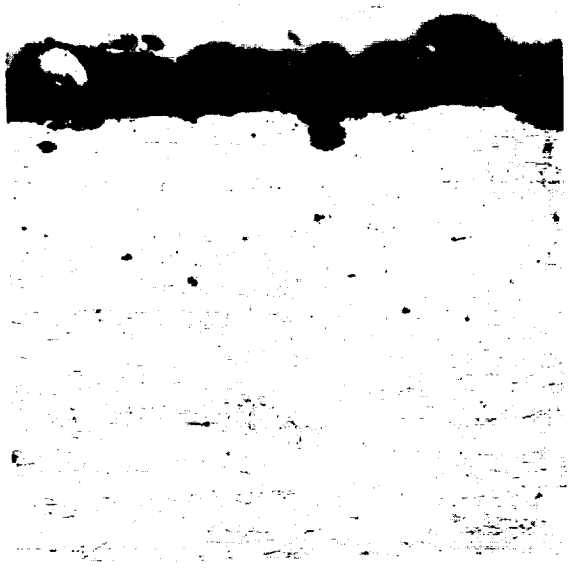

ETCH: 10% OXALIC ACID MAG: 250X

FIGURE 3-75 AS COATED

PHOTOMICROGRAPHS OF AN Fe-Al (FIG. 3-74) AND AN Fe (FIG. 3-75) COATING ON Cr-5W-Y. NOTE OXIDE BUILD UP IN BOTH CASES.

ETCH 10% OXALIC ACID MAG: 250X
FIGURE 3-76

ETCH: 10% OXALIC ACID MAG: 250X
FIGURE 3-77

PHOTOMICROGRAPHS SHOWING RESULTS OF DEPOSITION OF Fe FROM $FeBr_2$ PACKS ON BARE (FIG. 3-76) AND PRE-ALUMINIZED (FIG. 3-77) SPECIMENS. NOTE THAT COATING SEPARATION TOOK PLACE. NO ALUMINUM IS PRESENT IN THESE COATINGS.

mens run in XP19065 on bare and pre-aluminum coated tabs. It should be noted that these specimens showed excellent surface appearance and no contamination. Figures 3-78 and 3-79 show electron beam microprobe traces of specimens from XP19065, coated from a $FeBr_2$ pack on bare and pre-aluminized parts. As can be seen from Figure 3-79, deposition of iron was accomplished to a depth of 0.001 inches. Further, upon diffusion, the resulting coating contains approximately 71% iron. It can also be seen that a sharp rise in tungsten composition can be seen 0.00064-inches from the coating edge. The shape of the iron traverse (i.e., horizontal with only slight differences in composition) suggests abbreviated solubilities and thus possible intermetallic compound formation. Although not indicated on published Fe-Cr phase diagrams, there have been other (than sigma) ordered phases reported. Japanese investigators have reported the presence of an ordered Fe-Cr phase which falls within the determined composition limits in the above-mentioned specimens. Examination of the electron-beam microprobe traces in Figures 3-79 and 3-80 (pre-aluminized specimens) reveals the same trend as described above. It is of most significant importance here to note that virtually all of the aluminum coating originally present at the surface of this specimen has likely been removed by halide transfer during ironizing. Figures 3-81 to 3-84 show X-Ray photographs of the ironized (pre-aluminized) specimen discussed above, showing the distribution of

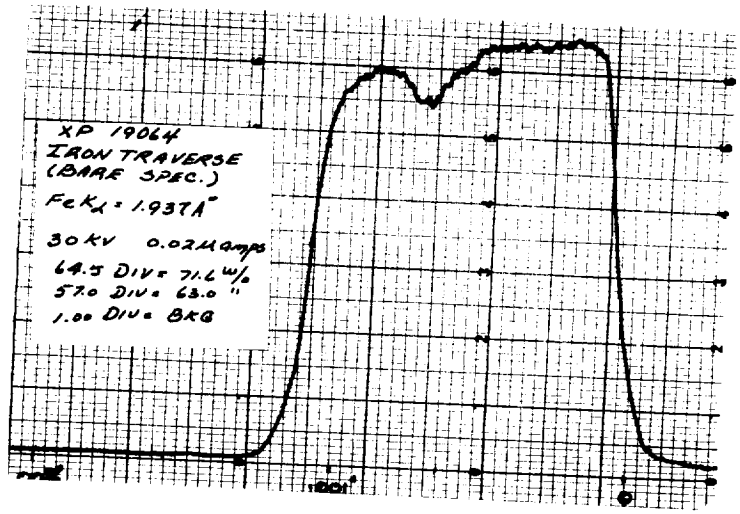

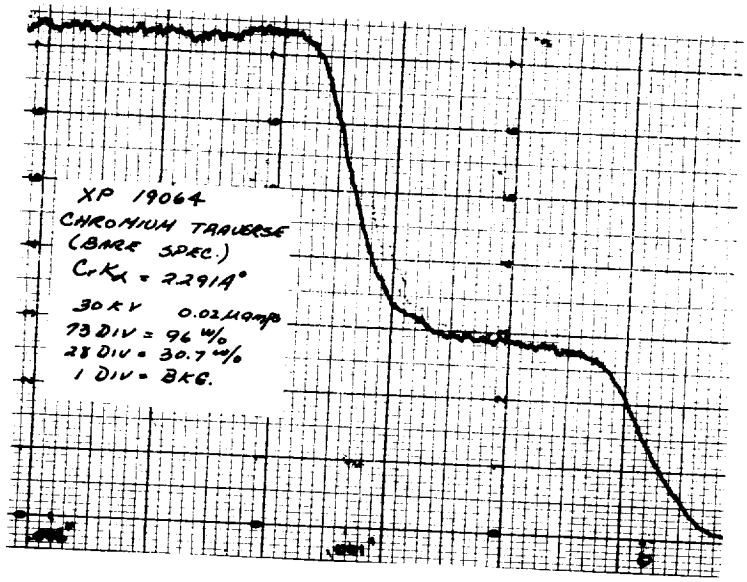

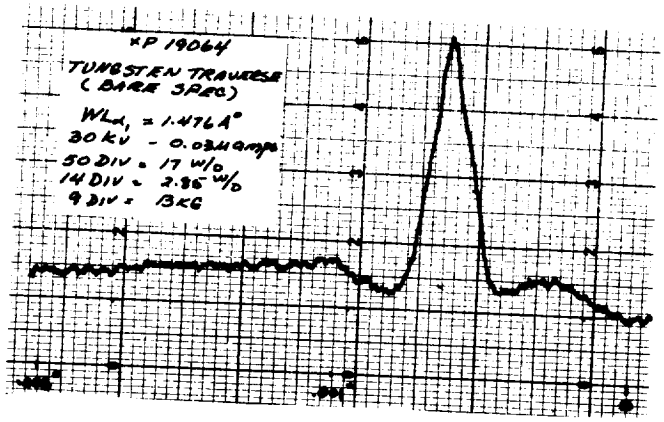

FIGURE 3-78

ELECTRON BEAM MICROPROBE TRAVERSE OF IRON COATED Cr-5W-Y. COATING DEPOSITED (XP19064) ON BARE SUBSTRATE.

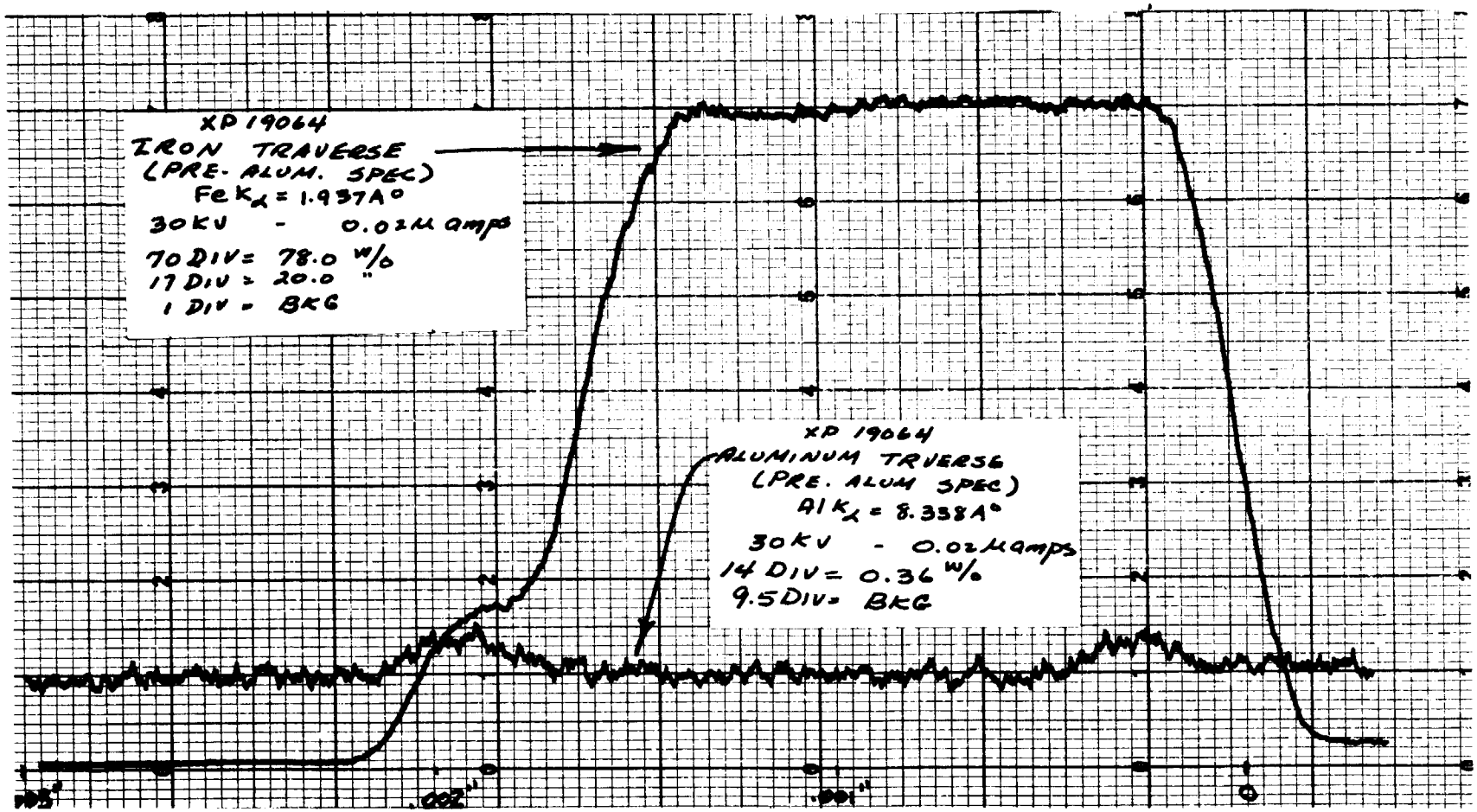

FIGURE 3-79

ELECTRON BEAM MICROPROBE TRAVERSE OF IRON COATED (PRE-ALUMINIZED) Cr-5W-Y.

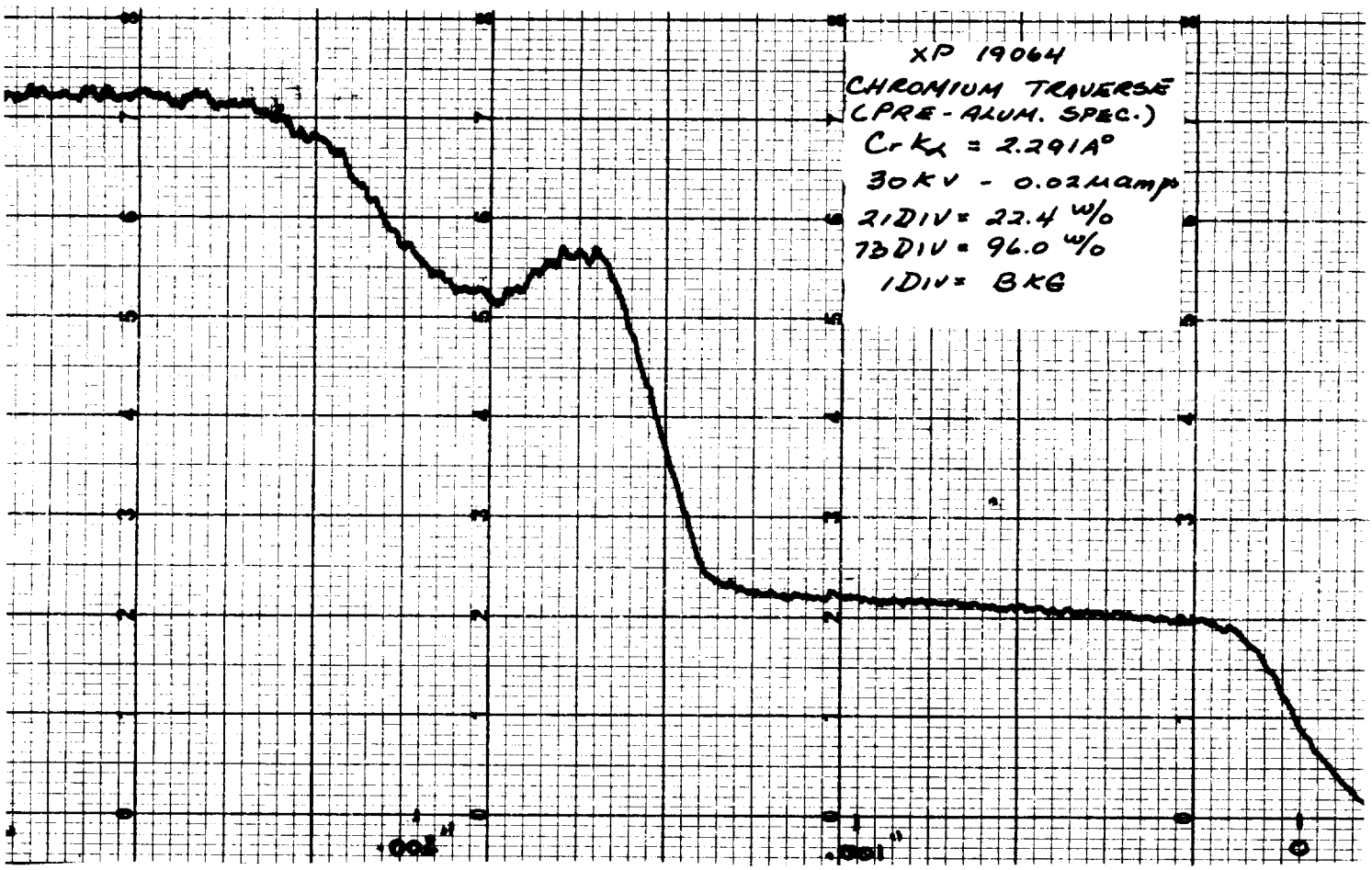

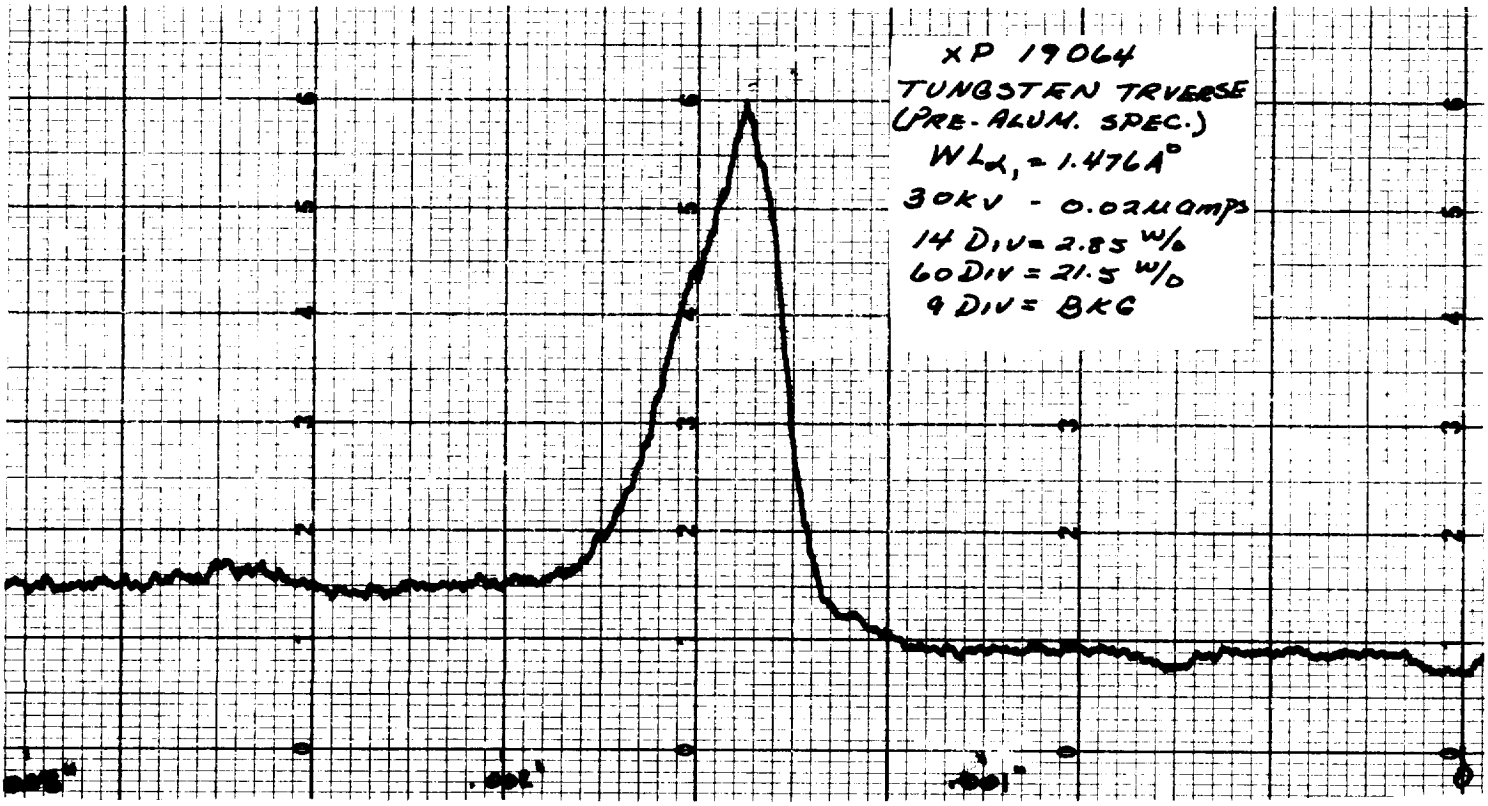

JRE 3-80 ELECTRON BEAM MICROPROBE TRAVERSE OF IRON COATED (PRE-ALUMINIZED) Cr-5W-Y.

FIGURE 3-81 ELECTRON IMAGE

FIGURE 3-82 CHROMIUM X-RAY

FIGURE 3-83 IRON X-RAY

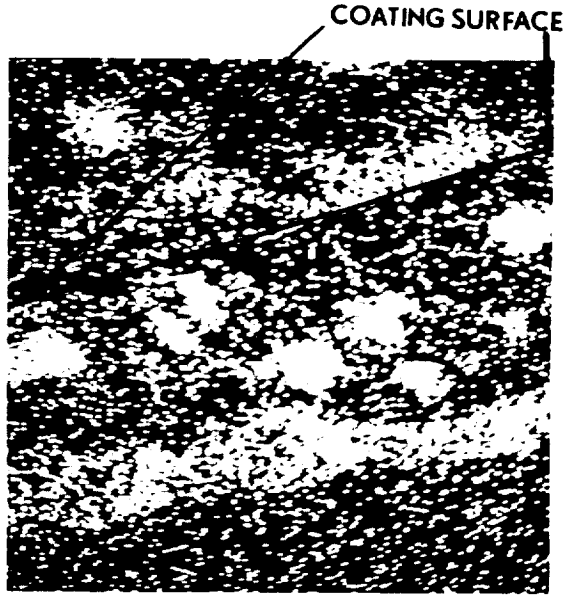

FIGURE 3-84 ALUMINUM X-RAY

X-RAY PHOTOGRAPHS (400X) OF IRON COATED (PRE-ALUMINIZED) Cr-5W-Y SUBSTRATE (XP19064). NOTE THE ALUMINUM INCLUSIONS IN FIGURE 3-74 (LARGE WHITE INDICATIONS).

iron, chromium, and aluminum. Note the inclusions present in the aluminum X-Ray photograph. These likely indicate high aluminum content and probably are in fact Al_2O_3. The same inclusions can be seen in the photomicrograph shown in Figure 3-77.

Since considerable difficulty was encountered with contamination of specimens even when run in argon, a re-check of the inert atmosphere retort was made and it showed the presence of heretofore undetectable small cracks. Although several repairs were attempted, experimental coating trials of additional specimens revealed the same corrosive attack as seen previously. Therefore, a new retort was fabricated and all ensuing experiments showed little or no corrosive attack. It should also be noted that differences were noted when comparing like experiments run in static or flowing argon atmospheres. Coatings deposited under a static argon atmosphere lacked reproducibility. Figures 3-85 and 3-86 show photomicrographs comparing the microstructures of specimens coated at 2200 F/10 hours using packs with a 5:1 and 1:1 Fe/Cr ratio respectively. Although the use of a larger iron concentration in the pack did produce a thicker coating, the appearance of voids and an oxide surface are also seen. Further, the presence of a eutectoid-like structure was seen (Figure 3-86) while Cr_2N was noted in the grain

FIGURE 3-85

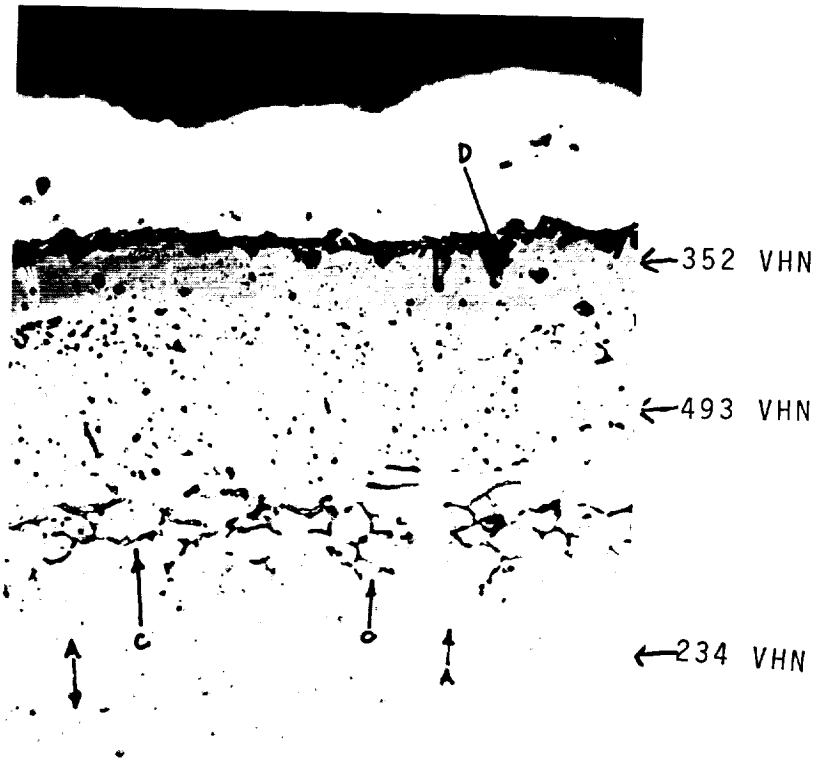

ETCH: 10% OXALIC ACID MAG: 250X

FIGURE 3-86

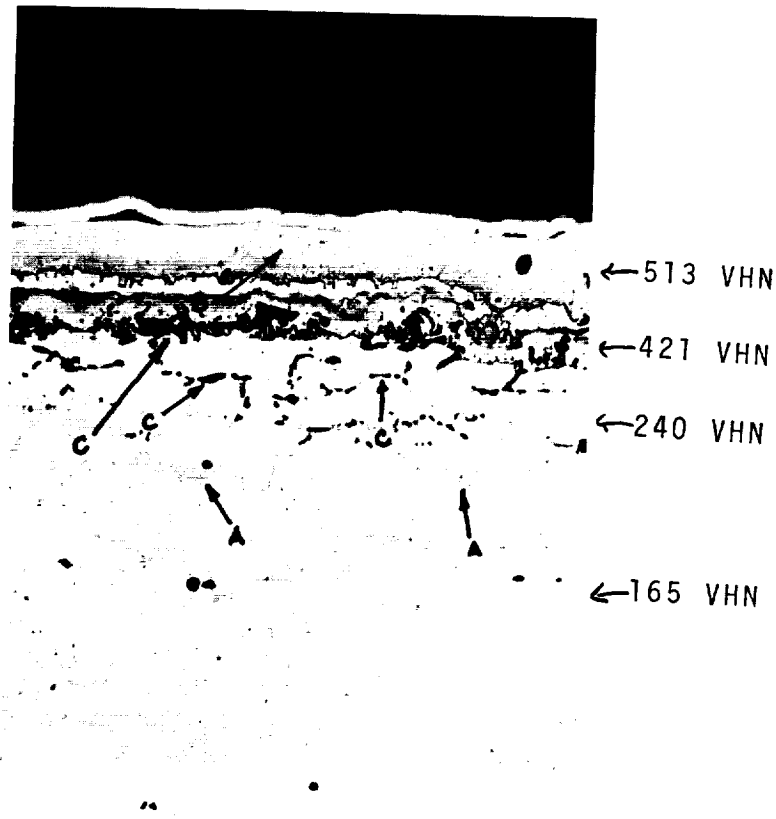

ETCH 10% OXALIC ACID MAG: 250X

IRON COATED SUBSTRATE. EXPERIMENTS CONDUCTED IN DEFECTIVE RETORT (STATIC ARGON ATMOSPHERE). DEPOSITION AT 2200°F/10 HRS. XP 19089 (FIGURE 3-85) PACK 5:1 Fe/Cr RATIO, XP 19086 (FIGURE 3-86) 1:1 Fe/Cr RATIO. ARROWS A, B, C, D SHOW Cr_2N FORMATION, Fe-Fe_4N EUTECTOID, VOIDS, AND OXIDE FORMATION RESPECTIVELY.

boundaries. These specimens were analyzed further by X-Ray diffraction and EBMP techniques and Fe_4N was in fact identified indicating the presence of the Fe_4N-Fe eutectoid. All of the nitride contamination seen in these specimens is attributed to the presence of the air in the retort, due to cracks in the retort wall.

Figures 3-87 and 3-88 show photomicrographs of specimens run in the conventional pack cementation-type retort, similar to that employed in straight aluminizing runs. The addition of aluminum to these packs was made for two reasons: 1) to determine if co-deposition is possible, and 2) to determine if the presence of aluminum will inhibit corrosive attack of the coating and substrate. As can be seen, the aluminum does in fact reduce the tendency towards corrosive attack, but voids in the coating are still prevalent. Further, as the increased hardness values seem to indicate, more aluminum was deposited on the specimen seen in Figure 3-87 (5 $^{w}/_{o}$ Al additive). In addition to the above, the acicular precipitate seen in Figure 3-88, likely of an (FeCr)N-type is not seen when the aluminum concentration of the pack is increased from 1 to 5 $^{w}/_{o}$.

As the data and photomicrographs seem to indicate, the interactions and phase relationships present in high chromium, Fe/N and Fe/N/Al bearing alloys are not fully understood, and this, then, suggests that they might

FIGURE 3-87

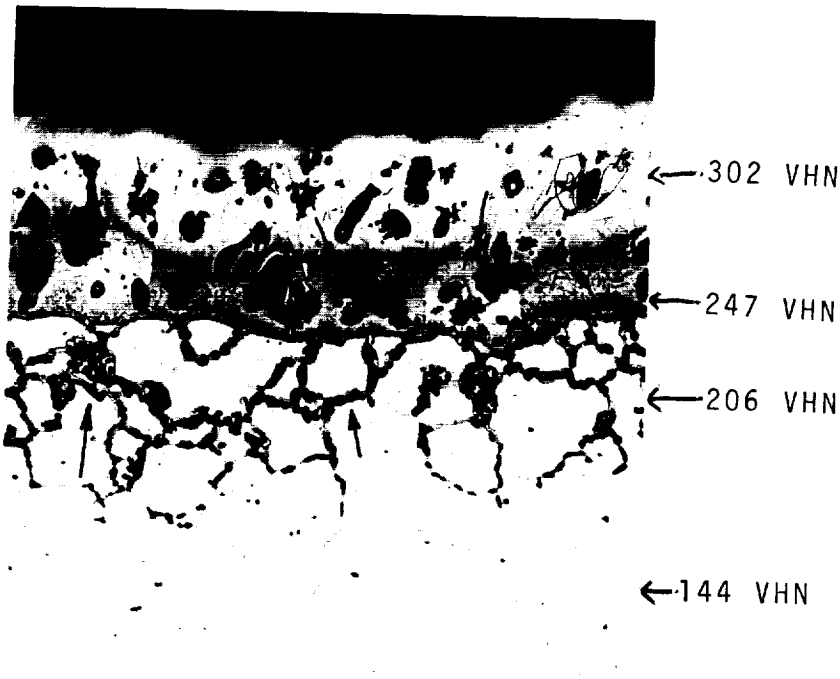

ETCH: 10% OXALIC ACID MAG: 250X

FIGURE 3-88

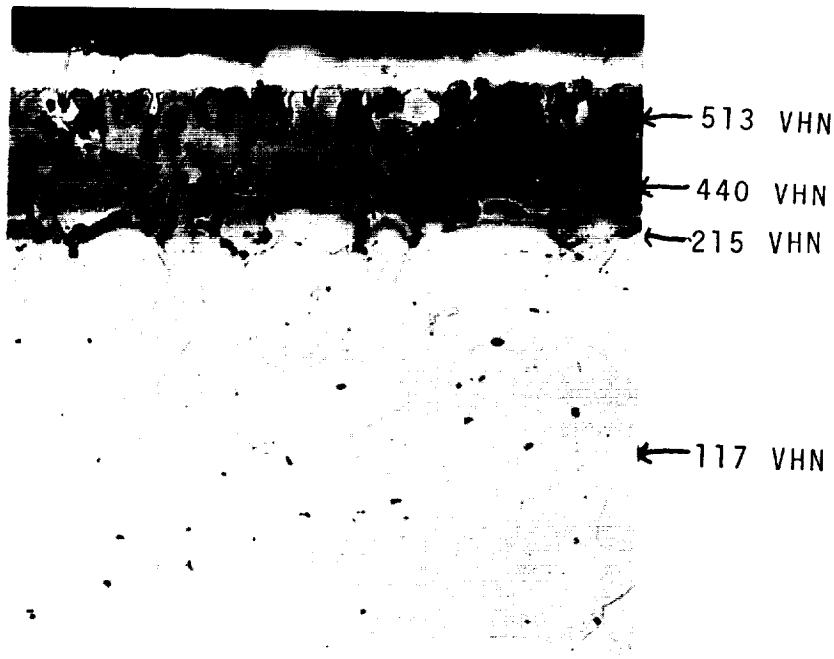

ETCH: 10% OXALIC ACID MAG: 250X

IRON COATED SUBSTRATE WITH 1 w/o (XP 19090 - FIGURE 3-87)AND 5 /o (XP 19090 - FIGURE 3-88) ALUMINUM ADDED TO 5:1 Fe/Cr PACK. NOTE LACK OF ACICULAR PRECIPITATE (ARROWS) AND INTERGRANULAR ATTACK SEEN IN FIGURE 3-88.

warrant closer scrutiny in other developmental efforts on these systems. There appears to be little pertinent information on high chromium, iron nitrogen systems available in the literature.

After a considerable difficulty was encountered with the first and defective atmosphere retort, the balance of experiments conducted employed a newly fabricated retort which employed a flowing argon atmosphere. The results of these later experiments (XP's 19141 and 19148) are also indicated in Table XII. Examination of the microstructures obtained on specimens from these runs showed that the only significant differences obtained were in the recrystallized grain size of the substrate and coating thickness. Since the differences in thickness were not too great, it was decided that the use of lower temperature-longer time ironizing (1750 F/ 25 Hrs.) as the first step in the duplex Fe/Al coating process would be best. However, some experiments were also conducted with the higher temperature processes. Since these parts, after ironizing, were to be again processed at temperatures in excess of 1750 F (during aluminizing), it was believed that the resulting substrate grain size would render the substrate too brittle to handle. Figure 3-89 represents the iron coating obtained in XP 19148 processed at 1750^{o}F. Note both the extremely low hardness values

FIGURE 3-89

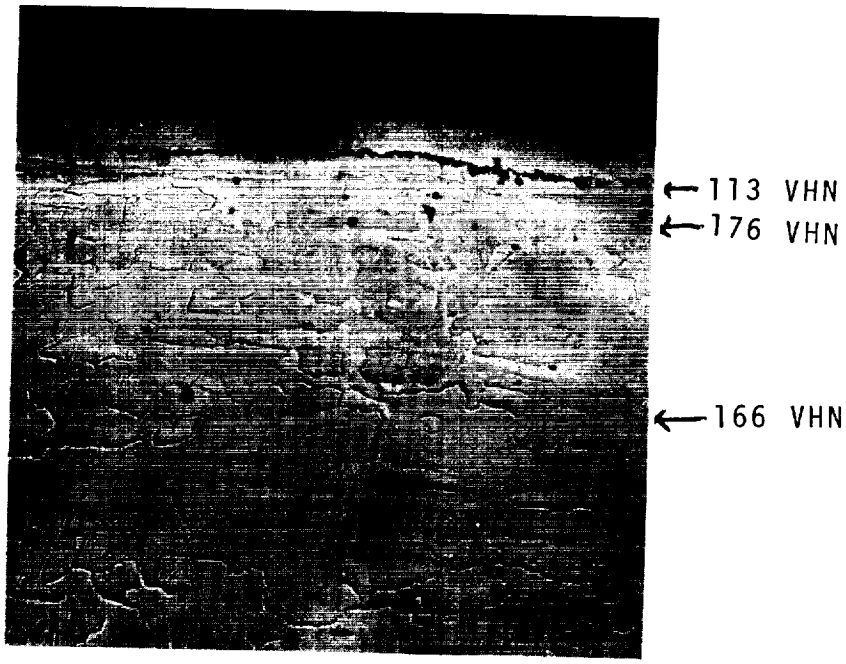

ETCH: 10% OXALIC ACID MAG: 200X

PHOTOMICROGRAPH OF IRON-COATED SUBSTRATE. PACK EMPLOYED A 5:1 Fe/Cr RATIO AND WAS PROCESSED AT 1750 F/25 HOUPS. NOTE LOW HARDNESS READINGS IN COATING AND SMALL RECRYSTALLIZED GRAIN SIZE.

of the coating and the smaller-than-usual substrate grain size obtained Figure 3-90 shows an EBMP trace of the iron-coated substrate (XP19148). Figures 3-91 to 3-93 show photomicrographs of an Fe/Al coating (XP 19148 + XP 19149) as coated and after 100 hours at 2100°F and 2400°F in oxidation. Note that the hardness of the specimen as coated (Figure 3-91) is approximately 200VHN units harder than a comparable simple solid solution aluminum coating. However, no nitride formation was noted both in the as-coated or 2100°F/100 hour (Figure 3-92) exposed conditions. Further, after the 2100°F exposure, only slight oxidation of the coating commenced.

In the 2400°F exposed specimen, considerable oxidation of the coating and severe nitride attack of the substrate could be seen. The intermediate zone of this latter specimen (403VHN) appears to be free of any nitride formation. This would tend to indicate that the coating is porous to nitrogen ingression.

As can be seen from the EBMP traverse for Fe-Al in Figure 3-94 the presence of an intermetallic phase is indicated in the first 0.0015 to 0.0020 inches of coating. The compound is probably of the (Fe-Cr), Al type. No other identification of this phase was made.

Figures 3-95 to 3-97 show photomicrographs of Fe/Al specimens as coated and after 100 hours at 2100°F and 2400°F in an oxidizing atmosphere. Although the ironizing was carried out at the same processing conditions

FIGURE 3-90

ELECTRON BEAM MICROPROBE TRAVERSE ON IRON COATED Cr-5W-Y. COATING DEPOSITED (XP19148) ON BARE SUBSTRATE

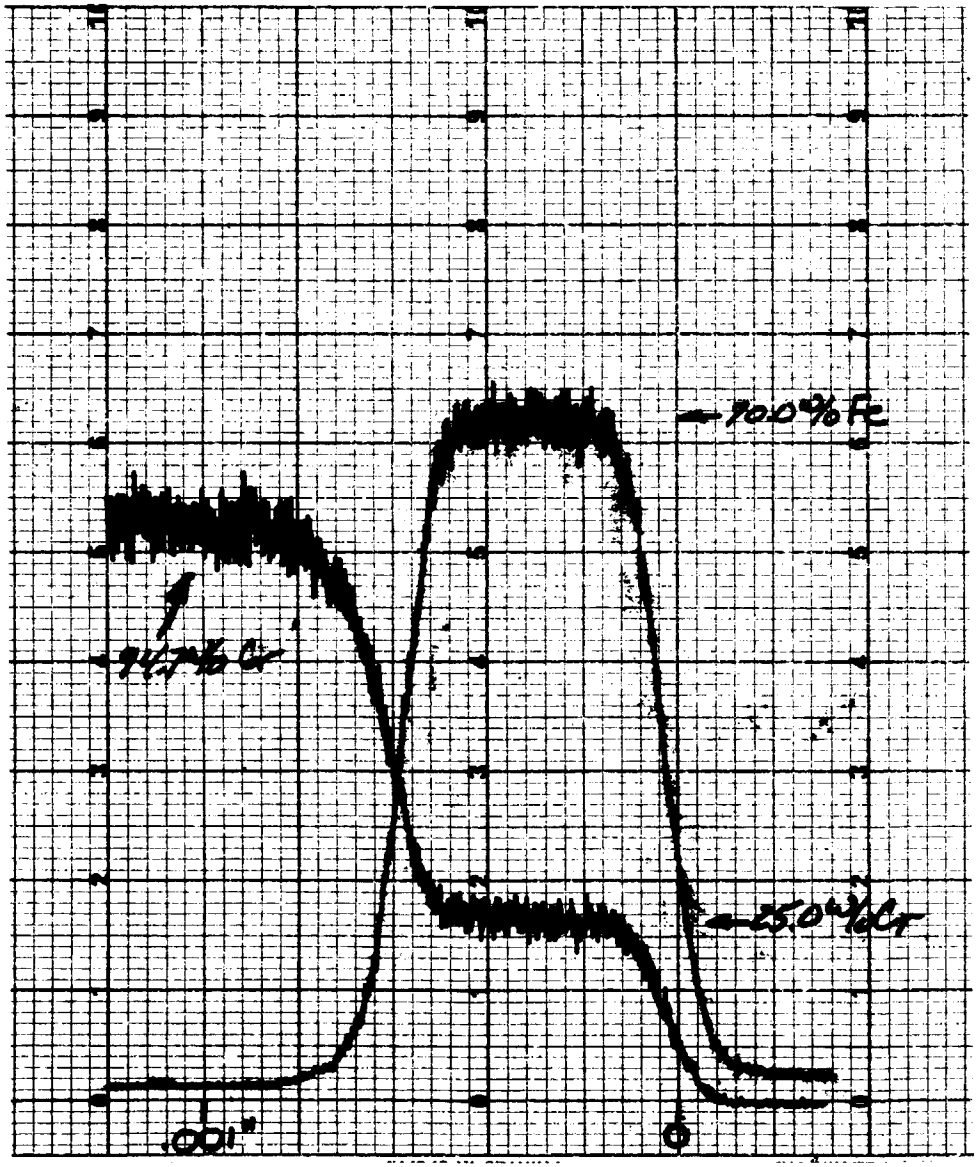

FIGURE 3-91

ETCH: 10% OXALIC ACID MAG: 200X
AS COATED

FIGURE 3-92

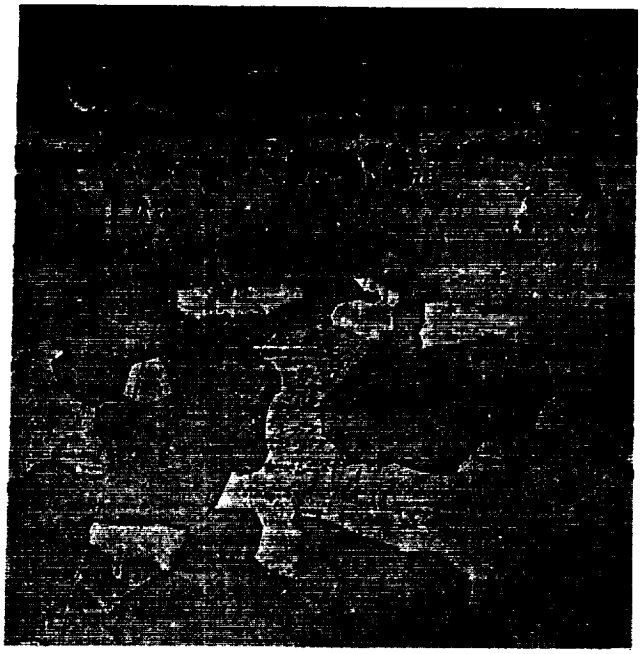

ETCH: 10% OXALIC ACID MAG: 200X
2100°F/100 HRS.

FIGURE 3-93

ETCH: 10% OXALIC ACID MAG: 200X
2400°F/100 HRS.

IRON-ALUMINIMUM COATING ON Cr-5W-Y SUBSTRATE. IRONIZED AT 1750 F/23 HRS. (XP 19148). ALUMINIZED 1700 F/10 HRS. (XP 19149) 8% Al, I, Al_2O_3 PACK. NOTE SLIGHT OXIDATION (A), HEAVY OXIDATION (B), NITRIDE FORMATION (C) AND NITRIDE-FREE ZONE (D).

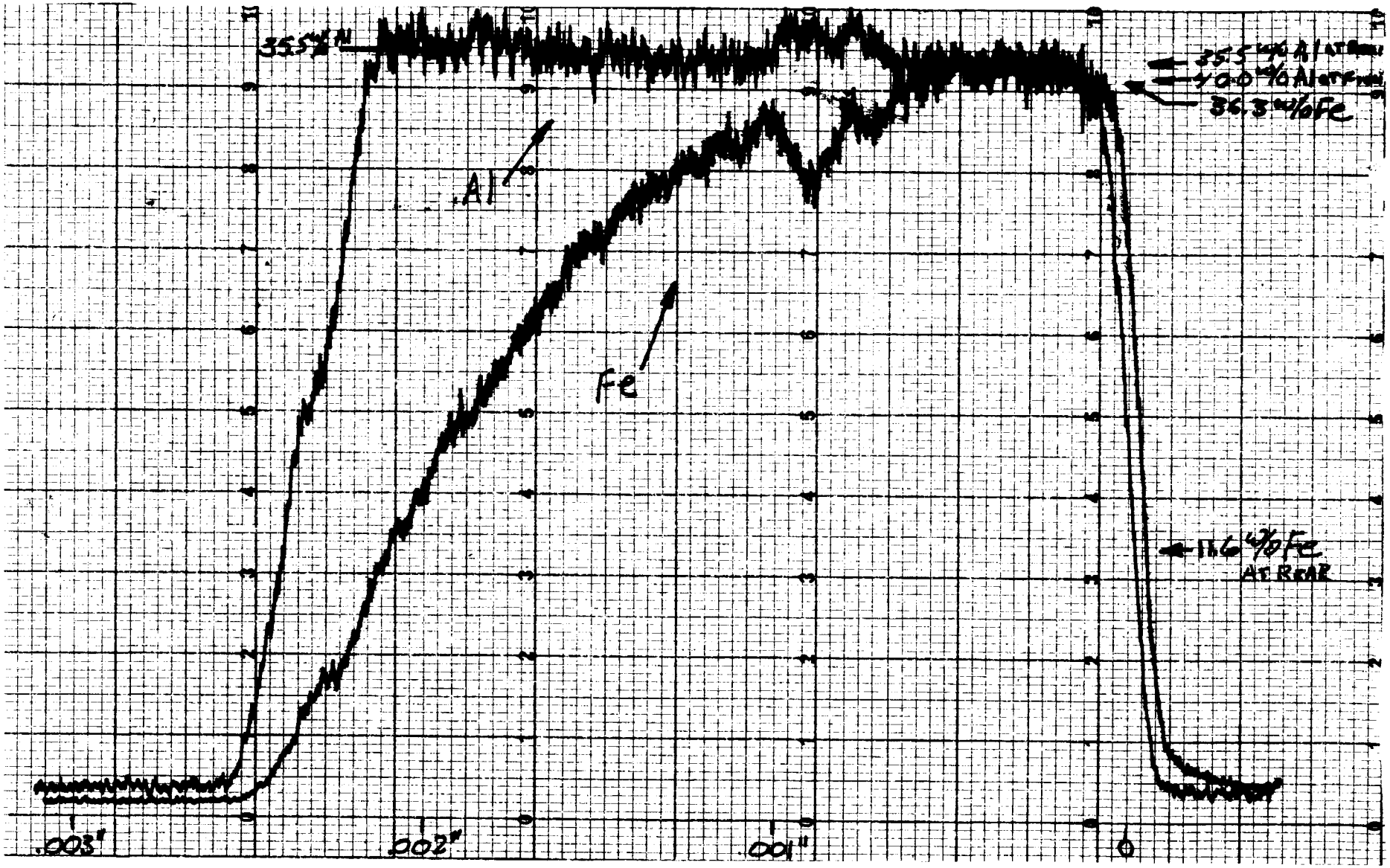

FIGURE 3-94
ELECTRON BEAM MICROPROBE TRAVERSE ON Fe-Al COATED
(2ø Type) Cr-5W-Y.

FIGURE 3-95

ETCH: 10% OXALIC ACID MAG: 200X

AS COATED

FIGURE 3-96

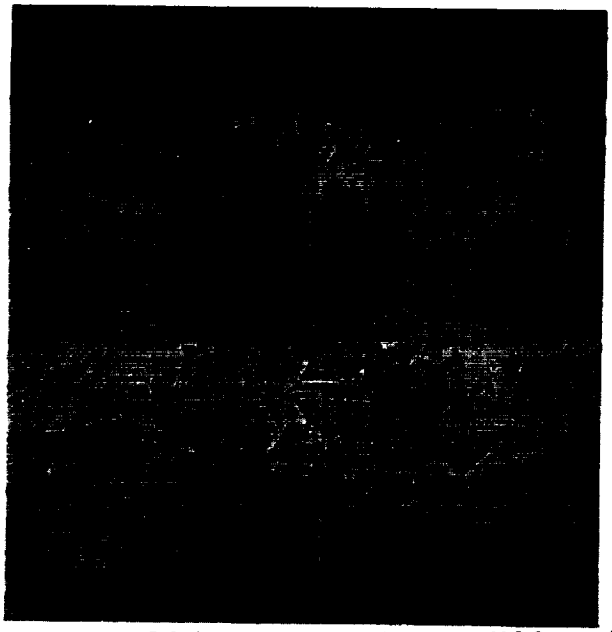

ETCH: 10% OXALIC ACID MAG: 200X

EXPOSURE TIME (2100°F/100 hrs.)

FIGURE 3-97

ETCH: 10% OXALIC ACID MAG: 200X

EXPOSURE TIME (2400°F/100 hrs.)

IRON-ALUMINUM COATING ON Cr-5W-Y SUBSTRATE. ALL SPECIMENS WERE IRONIZED AT 1750 F/23 HRS. THEN ALUMINIZED AT 1800 F/10 HRS. IN A 22% Cr, 8% Al, K SiF , Al O PACK (XP 19150). NOTE SOME OXIDATION (A) ON BOTH EXPOSED SPECIMENS, AND LACK OF NITROGEN INGRESSION.

as the previously discussed experiments, (1750°F/23 hrs.) both a different pack and processing temperature were employed for aluminizing, i.e., aluminizing was performed as per the UK-type. It should be noted that in the simple aluminum systems when employing chromium bearing packs, the coating thickness (for a given coating temperature) is always greater, the less the chromium present. However, as can be seen from the data presented, when using these two aforementioned packs on previously ironized specimens the results appear to reverse themselves somewhat, in that the chromium-bearing aluminum pack (UK) results in thicker coatings. However, this difference might be more attributable to the 100°F difference in coating temperature. It is significant to note the very high hardness values obtained on these coatings with the 2ø type and Fe-Al coating. These high hardness values appear to be indicative of intermetallic formation and it is felt that an $(Fe,Cr)_xAl_y$ compound similar to that seen in the Cr-Mn-Al $[(Cr,Mn)Al_{12}]$ system has formed. Note that although some oxidation is seen on the exposed specimen, no nitride is present in any of the conditions shown. EBMP analysis of the Fe-Al (UK type) coating described is shown in Figure 3-98. These specimens were ironized at 1750°F/23 hours followed by aluminizing under conditions similar to those employed for deposition of the

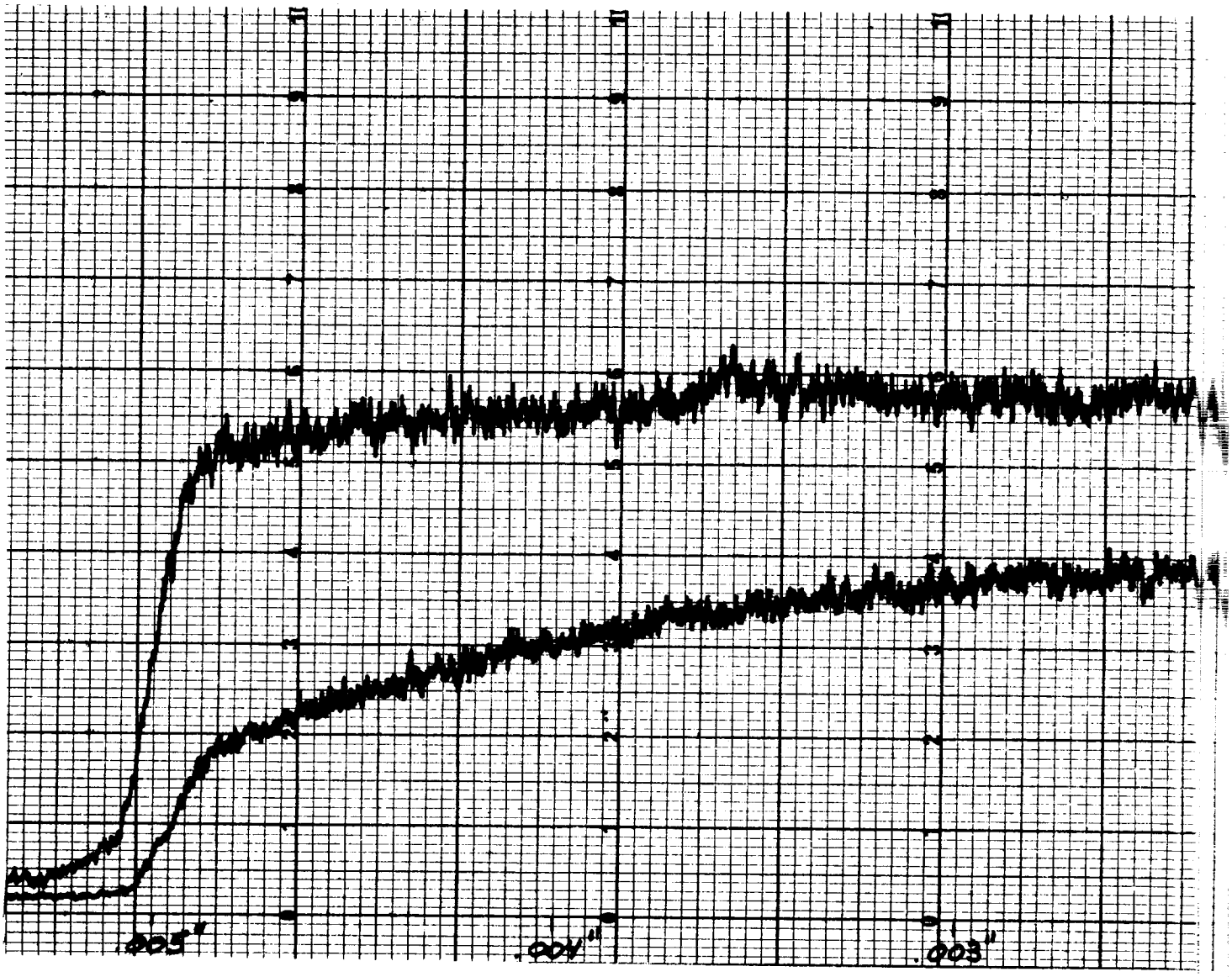

FIGURE 3-98

ELECTRON BEAM MICROPROBE TRAVERSE ON Fe-Al COATED (UK TYPE) Cr-5W-Y

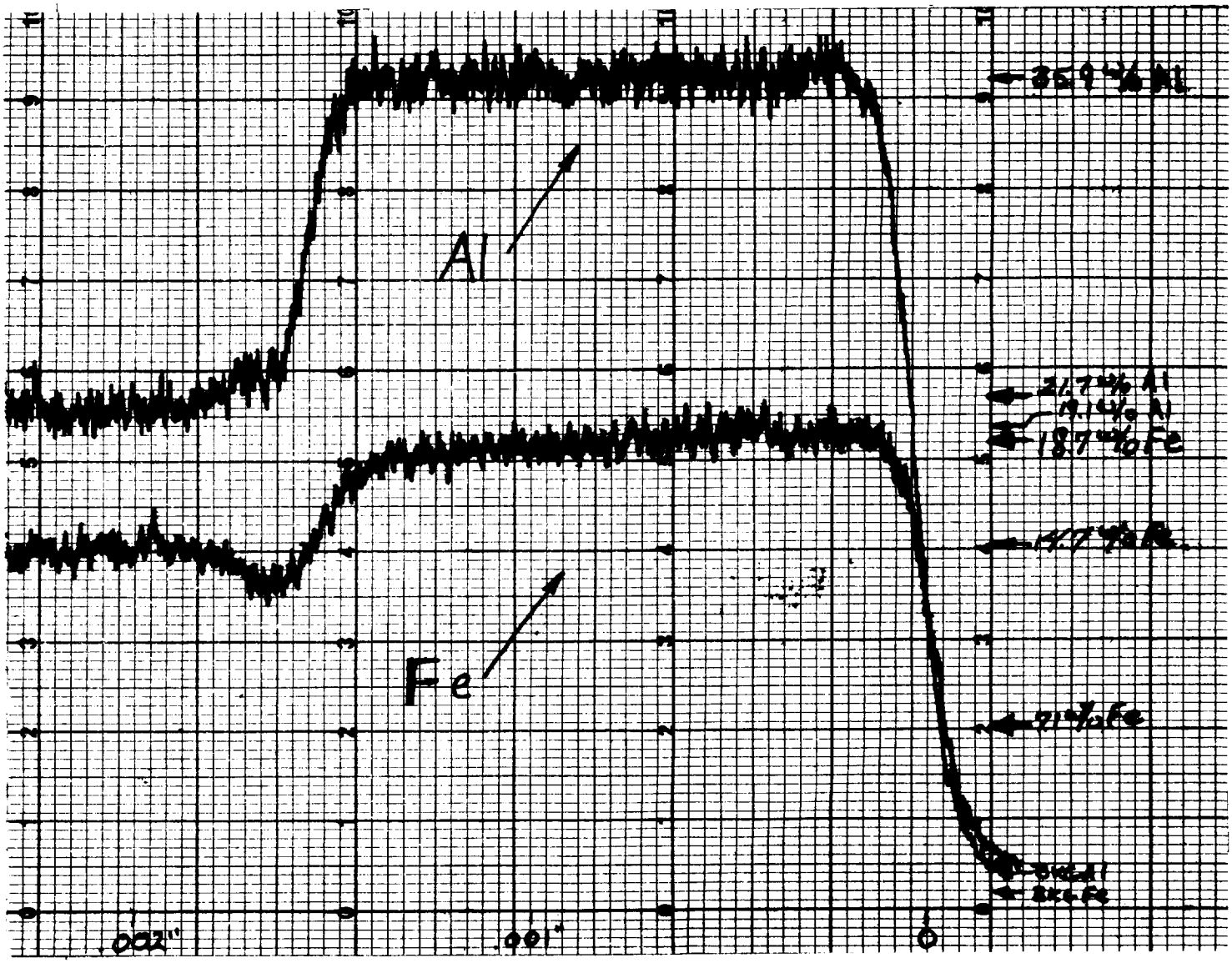
Al
Fe
35.9 % Al
21.7 % Al
9.1 % Al
18.7 % Fe
4.7 % Fe
21 % Fe
.002"
.001"
0

UK-type system. Table XII indicates these runs as XP 19148 and XP 19150.

A comparison of the two systems i.e., ironized plus UK type coated and ironized plus 2ø type coated reveals several significant facts:

A. Fe-Al(UK) coatings are two phased, thicker and have greater aluminum concentration levels than the Fe-Al (2ø) type. The coating appears to consist of an outer phase of the $(Fe_xCr_y)Al_z$ type while the inner phase appears to be also of the same type but with greater Cr-Al ratios. Necessarily one might expect this Cr-rich phase to be of higher hardness since it is known that Fe-Al intermetallic compounds are generally softer than Cr-Al types.

B. The Fe-Al(UK) coating with its larger aluminum resevoir is far more resistant to nitrogen attack but less diffusion-stable. Figures 3-99 and 3-100 show weight change oxidation curves for the Fe/Al coating systems discussed above. Based on these curves and the data previously presented, the following tentative conclusions can be drawn from these data:

a. In general the lower the ironizing and aluminizing temperatures,the better the oxidation-nitrification resistance.

OXIDATION CURVES AT 2100°F AND 2400°F FOR IRON-ALUMINUM COATINGS ON Cr-5W-Y ALLOY.

FIGURE: 3-99

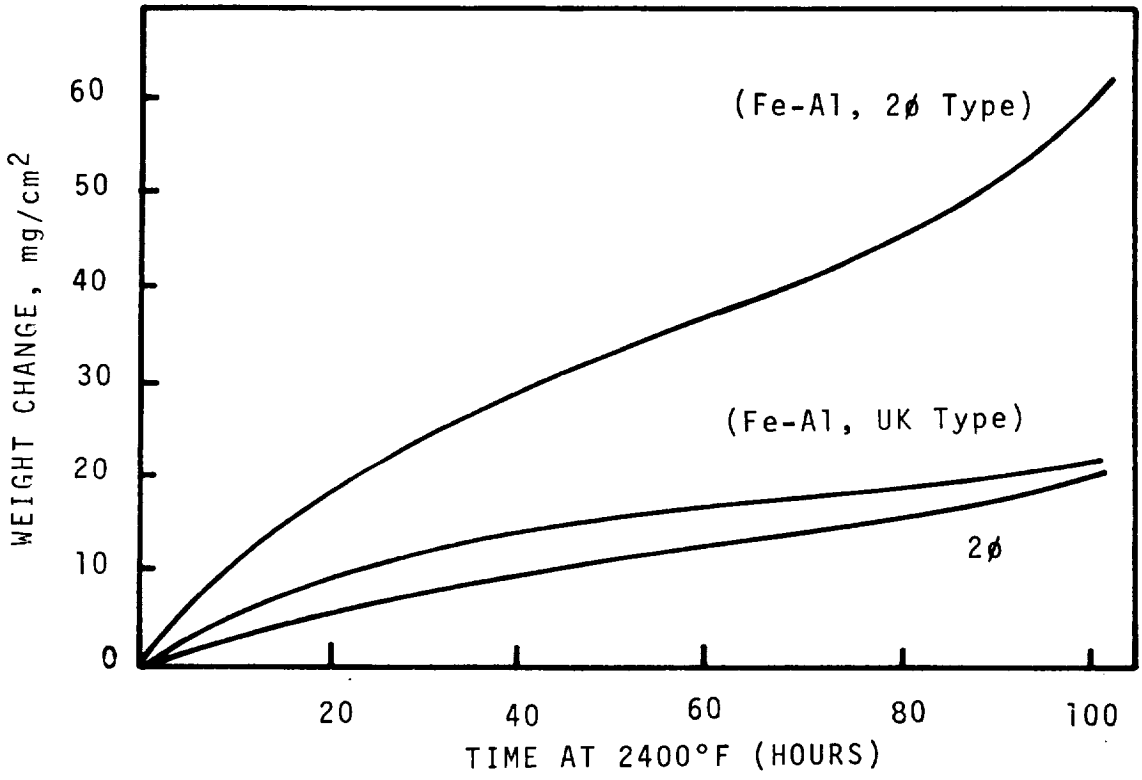

FIGURE: 3-100

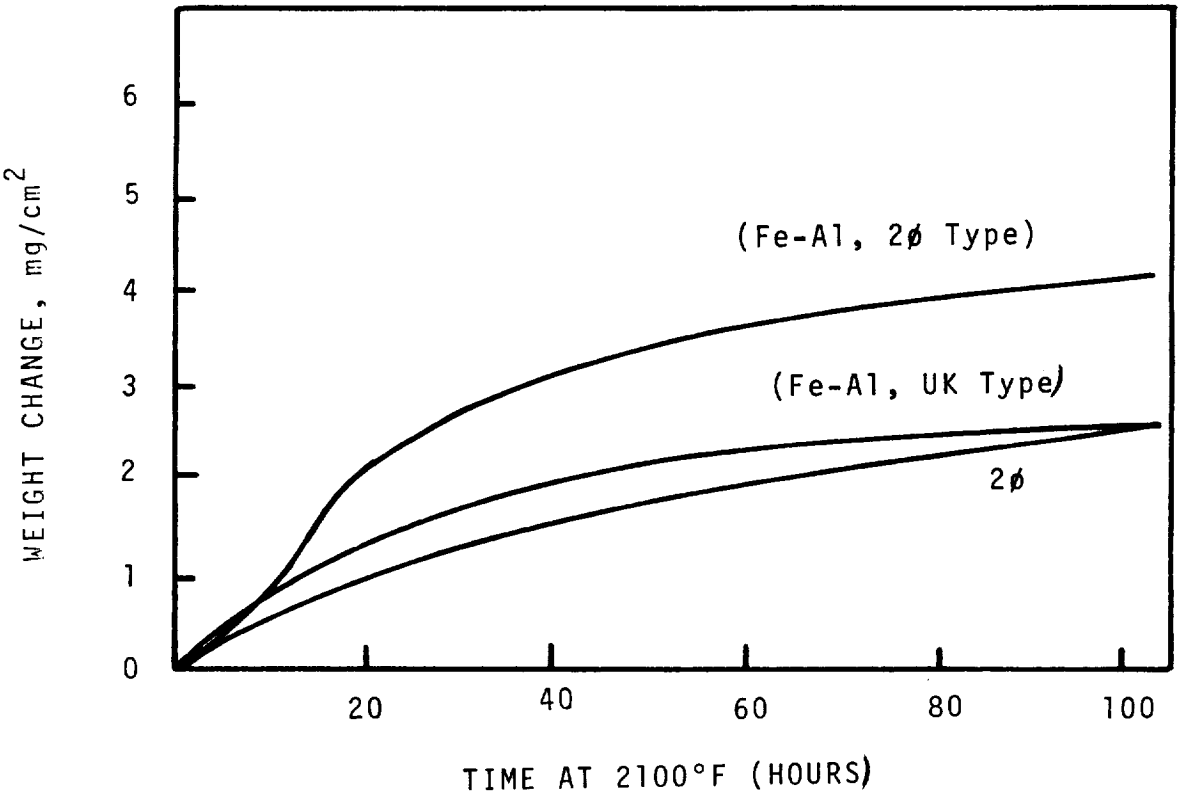

b. At comparable thicknesses, the Fe/Al and simple aluminum systems have about the same resistance to corrosive attack (100 hours exposure). The simple aluminum systems suffer from greater diffusional growth.

Based on these data it was mutually decided between cognizant Chromalloy and NASA personnel to take the Fe-Al (UK type) coating into the advanced testing phase of the program.

3.9.3 Advanced Testing and Coating Evaluation Fe-Al(UK)-Type System.

3.9.3.1 General

As mentioned above this Fe-Al(UK) type coating was taken into advanced testing and this system together with the simple aluminum (2ø) system encompassed all advanced testing. The description of the tests and the results obtained from the advanced testing phase of the program are presented below. It should also be noted that because of program and time limitations several of the advanced tests conducted on the 2ø system would not be conducted on the Fe-Al coatings.

3.9.3.2 Continuous Weight Change Oxidation

Continuous weight change oxidation data was developed for both this system at 1800 F, 2100 F and 2400 F. Figure 3-101 shows the weight change curves obtained. As described in the 2ø advance

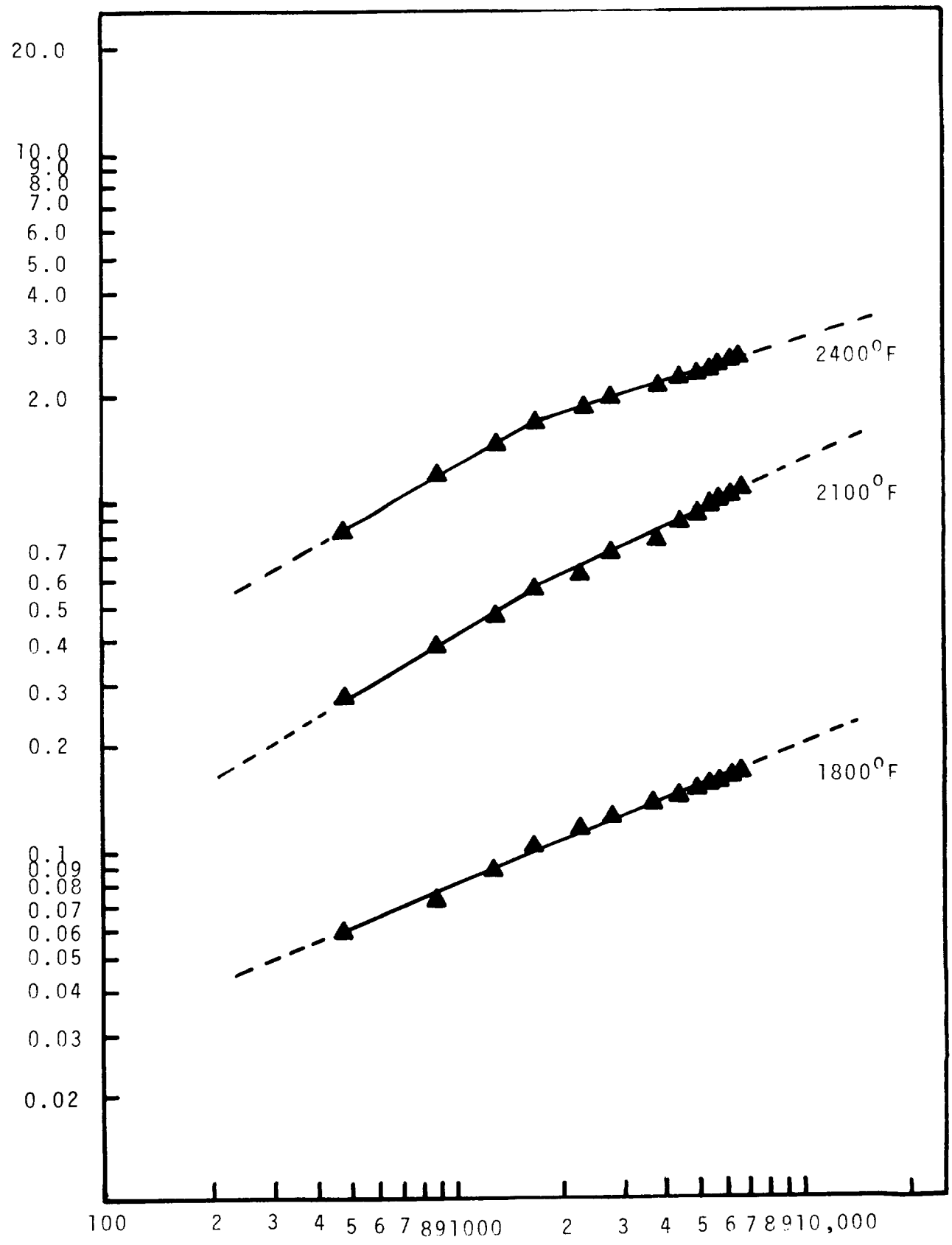

FIGURE 3-101

CONTINUOUS OXIDATION CURVES OF THE Fe-Al (UK TYPE) COATED Cr-5W-Y ALLOY EXPOSED AT 1800,2100,2400°F

testing section the most significant results seen were the decrease in oxidation rate associated with this test as compared with a cyclic test. It should further be noted that for this system the deviations from linearity of tne oxidation curves are manifested by a decrease in oxidation rate (slope of curve reduced) as compared to the 2ø simple aluminum system where the curve or rather oxidation rate increases where deviation from linearity occurs (Figure 3-27). This would seem to indicate that upon diffusion of the outer phase, homoginization occurs possibly resulting in decreased oxidation rates within the limits of time tested. It is felt that further testing would surely produce a third change in slope (increase) such that increased oxidation rates would occur.

The lesser oxidation rates seen here as compared to cyclic oxidation results are likely due to the lack of thermal shock, finite air supply etc., as described in section 3.3.3.4

3.9.3.3 Oxidation Erosion Testing

Testing was performed in an erosion rig as described in section 2.1 and in a manner similar to the testing performed on the 2ø coating. All testing on the Fe-Al coated was conducted at 2100 F as in the case of the 2ø simple-aluminum

system. The same difficulties with testing of this system were encountered as with previously erosion tested specimens i.e., difficulty in obtaining higher temperatures, specimen removal, edge cracking etc. Similarly, weight change measurements and thermal-fatigue testing were not conducted Figure 3-102 shows an Fe-Al coated specimen after 80 hours at 2100 F (XP 19184). Note the presence of white oxide on the surface of the part. Figures 3-103 and 3-104 show photomicrographs from the leading (LE) and trailing edges (TE) respectively. Although more nitrogen ingression is noted on the TE of the specimen (as in the case of the 2ø coating), both specimens show considerable oxidation attack of the coating. Figure 3-104 shows a photomicrograph of a specimen taken from a colder section of the erosion specimen. As can be seen, although no nitrogen attack of the substrate is noted, oxidation of the coating has progressed significantly. This would necessarily tend to indicate that the Fe-Al system is more deleteriously affected by erosion than is the 2ø coating system discussed in a previous section, i.e., the difference in coating life between static and dynamic testing conditions is greater for the Fe-Al coating than is the 2ø coating. It would thus appear that the higher hardness, iron containing aluminum systems are less oxidation/erosion resistant or more sensitive to high gas velocities than the softer, simple aluminum system.

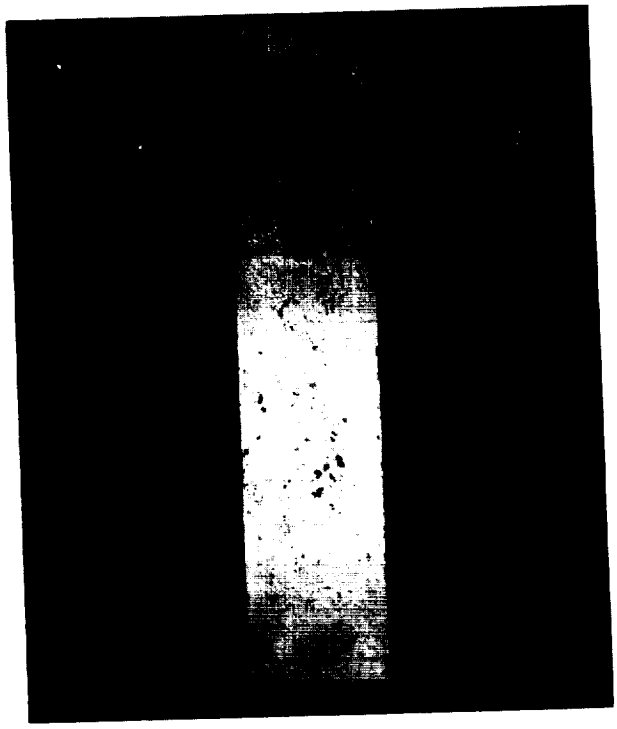

FIGURE: 3-102

OXIDATION EROSION SPECIMEN, Fe-Al COATED Cr-5W-Y, 80 HOURS AT 2100°F

FIGURE 3-103 - LEADING EDGE

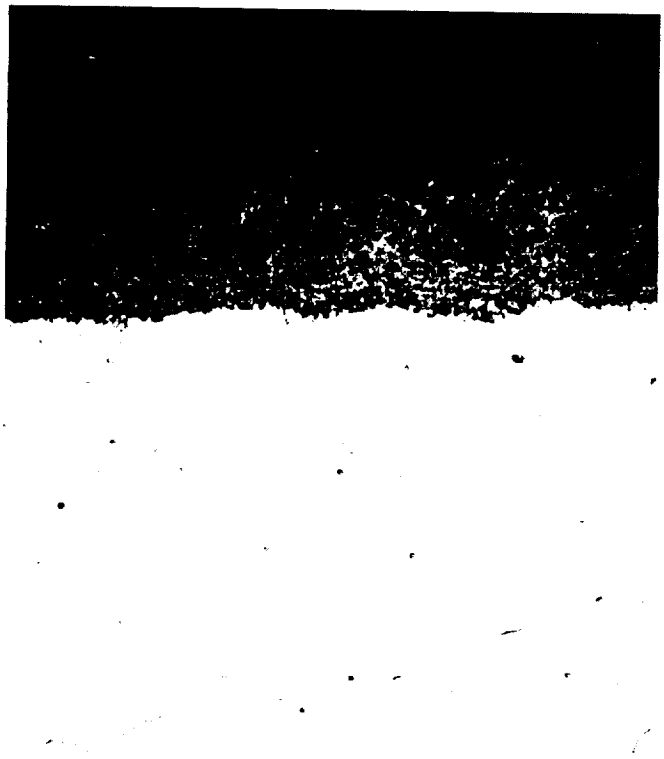

ETCH: OXALIC ACID MAG: 250X

FIGURE 3-104 - TRAILING EDGE

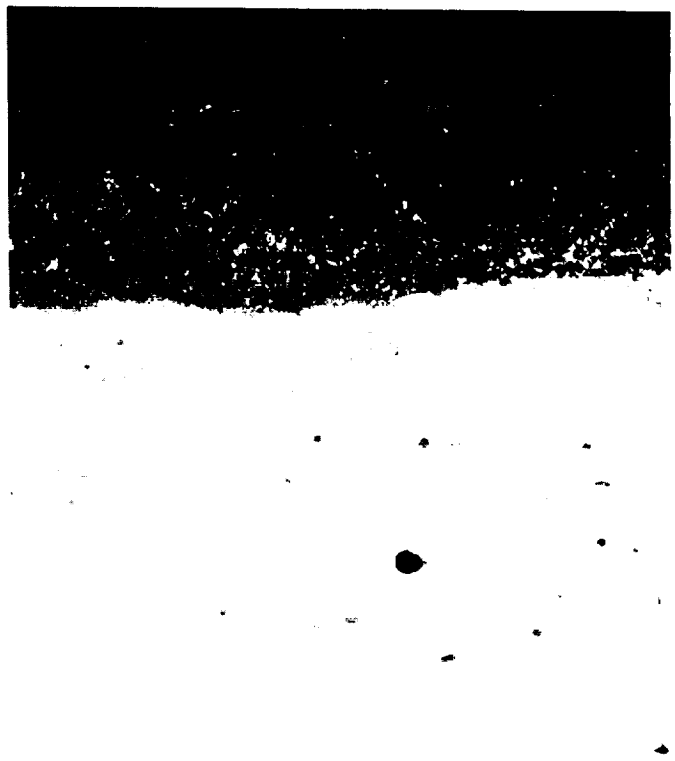

ETCH: OXALIC ACID MAG: 250X

FIGURE 3-105

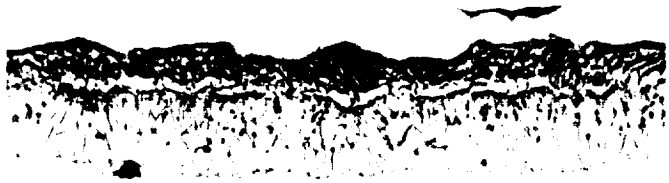

ETCH: OXALIC ACID MAG: 250X

PHOTOMICROGRAPHS OF THE Fe-Al COATED OXIDATION-EROSION SPECIMENS, 80 HOURS AT 2100°F

FIGURE 3-103 LEADING EDGE
FIGURE 3-104 TRAILING EDGE
FIGURE 3-105 COLD SECTION

3.9.3.4 Ductile Brittle Bend Transition Testing

All testing was performed according to MAB-192-M as described in section 2.7. Table XIII shows all of the data obtained in this series of tests which were designed by NASA and Chromalloy personnel to determine the changes in DBTT as a function of the following:

A. Al or nitrogen diffusion.

B. Coating thermal cycle.

C. Cyclic-thermal-stressing.

D. Oxidation Testing Thermal Cycle

As can be noted from Table XIII, several of the conditions indicated were not evaluated for nitrogen pick-up after exposure. Nitrogen analysis of these conditions were beyond the scope of the program. In an attempt to determine whether aluminum diffusion (upon exposure) or nitrogen contamination during coating adversly affects DBTT, specimens in the coated plus stripped and simulated-coating cycle conditions were prepared and tested. The data obtained are quite similar with regard to nitrogen analysis and DBTT and reveals surely that the transition temperature is not affected by any chemical changes associated with the coating cycle. The differences in DBTT between bare and coated material are due to the recrystallization of the substrate which occurs during the coating thermal-cycle.

DUCTILE TO BRITTLE BEND TRANSITION TEMPERATURE TEST

FOR Fe-Al COATED AND EXPOSED Cr-5W-Y SHEET

	CONDITION	GAS ANALYSIS ppm(2)	MICRO-HARDNESS VHN	COATING THICKNESS mils		EBMP ANALYSIS 2 mils	4 mils	6 mils	8 mils	DBTT °F(1)	COMMENTS
1.	As Coated	---	950-1026	5.0		------	------	------	-------	800°	----
2.	Coated and Stripped	93	264	---	Al	-----	-----	-----	-----	1000-1100	Did Not Bend Below 1000°F.
					Fe	-----	-----	-----	-----		
					Cr	94.1	93.6	-----	-----		
					W	5.9	6.4	-----	-----		
3.	Bare, Fe-Al Coating Cycle (Argon)	120	277	---	Al	-----	-----	-----	-----	1100-1200	Did Not Bend Below 1000°F.
					Fe	-----	-----	-----	-----		
					Cr	95.0	-----	-----	-----		
					W	5.0	-----	-----	-----		
4.	Bare and Exposed (Argon) 2100°F/100 Hours, 2,2,2,16 Hour Cycles	883	191	---	Al	-----	-----	-----	-----	1000-1100	Did Not Bend Below 1000°F.
					Fe	-----	-----	-----	-----		
					Cr	92.7	94.4	-----	-----		
					W	7.6	5.6	-----	-----		
5.	Coated and Exposed (Argon) 2100°F/100 Hours 2,2,2,16 Hour Cycles	3100	Coating 447 Substrate 264	5.8	Al	13.0	13.0	-----	-----	>1600	Bent to 105° @1500°F.
					Fe	11.6	7.4	-----	-----		
					Cr	76.6	75.0	-----	94.5		
					W	3.8	4.6	-----	5.4		
6.	Coated and Exposed (Argon) 2100°F/100 Hours	74	Coating 387 Substrate 176	5.5	Al	13.0	12.2	-----	-----	>1600	Bent to 105° @1500°F.
					Fe	9.4	7.3	-----	-----		
					Cr	73.0	75.9	94.4	-----		
					W	4.0	4.8	5.6	-----		
7.	Coated and Exposed (Argon) 2100°F/10 Hours	---	Coating 476 Substrate 240	4.5	Al	17.8	14.0	-----	-----	>1600	Bent to 105° @1400°F.
					Fe	12.5	6.7	-----	-----		
					Cr	62.3	75.1	94.9	-----		
					W	3.3	4.2	5.1	-----		
8.	Coated and Exposed (Argon) 2100°F/10 Hours 2,2,2,2,2 Hour Cycles	---	Coating 437 Substrate 210	5.8	Al	14.5	12.2	-----	-----	>1600	Did Not Bend Below 1500°F.
					Fe	11.0	8.3	-----	-----		
					Cr	71.2	74.8	94.9	-----		
					W	3.3	4.7	5.1	-----		
9.	Coated and Exposed (Argon) 2400°F/100 Hours	73	Coating 373 Substrate 230	8.5	Al	3.6	-----	3.4	-----	>1600	Bent to 105° @1600°F.
					Fe	7.3	-----	4.1	-----		
					Cr	84.2	-----	84.8	93.6		
					W	4.7	-----	5.3	5.9		
10.	Coated and Exposed (Argon) 2400°F/10 Hours	---	Coating 440 Substrate 248	5.9	Al	13.4	11.3	-----	-----	>1600	Bent to 105° @1600°F.
					Fe	9.6	8.9	-----	-----		
					Cr	73.0	75.1	94.5	-----		
					W	4.0	4.6	5.5	-----		
11.	Coated and Exposed (Nitrogen) 2400°F/100 Hours	---	Coating, Substrate 2047	8.2	Al		8 mils			>1600	Did Not Bend At Any Temperature Tested.
					Fe		-----				
					Cr		87.8				
					W		5.8				

(1) No Cracks Produced with a 90°-105°Angle Bend

(2) All Analysis Conducted After Coating Removal

All Specimens Cut From Heat #67-100 DBTT=325°C, 30 ppmN_2

Metallographic evaluation although not shown here, showed no evidences of any nitrogen - or oxygen ingression into the substrate. This information is supported by the gas analyses as indicated in Table XIII.

As mentioned in a previous section, it was speculated that saturation of the coating with interstitials was the cause of high DBTT values and necessarily it was decided to expose coated specimens at 2100°F and 2400°F in an inert atmosphere to preclude contaminant pick-up. The data reveals significant nitrogen pick-up on a bare specimen exposed for 100 hours at 2100°F. As explained in section 3.3.3.5 this was likely due to contamination of the argon employed. Most confusing of the results obtained were seen in the specimens which were Fe-Al coated and cyclic-oxidation exposed at 2100°F. Extensive nitrogen pick-up was recorded with no apparent explanation. A re-analysis for nitrogen pick-up showed the same results i.e., extremely large quantities of nitrogen diffused into the substrate. Metallographic analysis showed no evidences of nitrogen attack on any of the specimens evaluated. Micro-hardness values (264 VHN in substrate) as shown in Table XIII, also indicate that little or no nitrogen was present. Although the gas analyses were run on two separate occasions it is felt that improper preparation of the specimen occured twice. Improper

preparation, i.e., only partial removal (mechanically) of coating and/or oxide would obviously show false results due to the tremendous quantities of nitrogen in the coated surfaces after exposure. Figures 3-106 to 3-108 show photomicrographs of specimens after a successful bend test (105°) at the temperatures indicated. As can be seen, the cracks in the coating (perpendicular) to the surface appear to be the primary cause of the high DBTT. Specimens bent at temperatures less than those indicated in the above mentioned series of pictures show these cracks propagating into the substrate. It appears that this coating system although having greater diffusion stability than the 2ø system, is poorer with regards its DBTT after exposure. It is significant to also note, that the Fe-Al-coated specimen exposed to pure nitrogen showed results significantly improved over that seen with the 2ø coating. Although no successful bend tests (105°) were performed, the Fe-Al system, at least at 2400°F, shows superior resistance to nitrogen attack. Further an acicular precipitate (Figure 3-108) can be seen in this coating after exposure. This phase although extremely rich in aluminum was not clearly identified. As in the case of the 2ø coating system this Fe-Al system also owes its

FIGURE 3-106

MAG: 250X

COATED AND EXPOSED IN ARGON AT 2100°F FOR 100 HOURS

DBTT: 1500°F

FIGURE 3-107

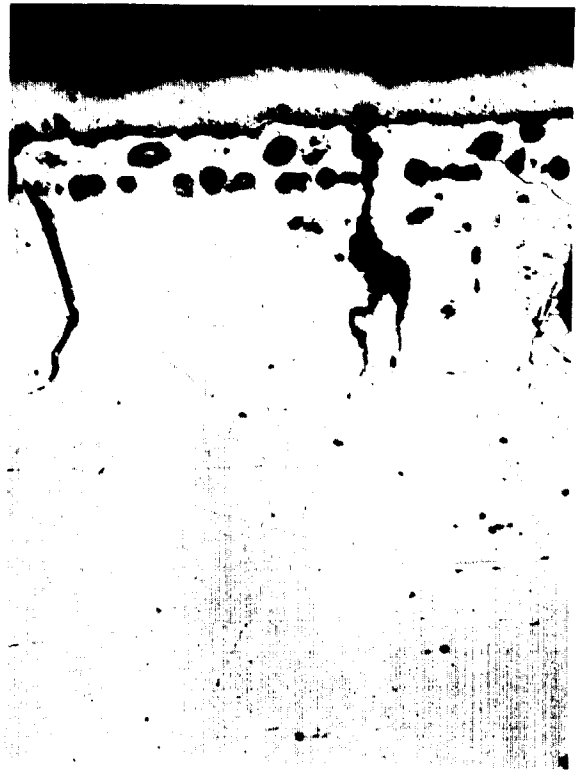

MAG: 250X

COATED AND EXPOSED IN ARGON AT 2100 F FOR 100 HOURS (2,2,2,16 HOUR CYCLE)

DBTT: 1500°F

FIGURE 3-108

MAG: 250X

COATED AND EXPOSED IN NITROGEN AT 2400°F FOR 100 HOURS

DBTT: >1600°F

PHOTOMICROGRAPHS OF THE Fe-Al COATED DBTT SPECIMENS AFTER BEND TESTING

protective abilities to the formation of oxides and/or spinels at the surface, since total permeation of these coatings is attained when oxygen is absent from corrosive environment. The high hardness values (and attendant nitride formation) seen in the pure nitrogen-exposed specimen clearly indicate the above-mentioned permeability of the coating system to nitrogen.

We can, based upon the bend data shown in Table XIII, summarize the results as follows:

A. An increase in DBTT is seen by virtue of the coating thermal cycle.

B. This coating thermal cycle caused an increase in DBTT and is attributed to the recrystallization of the substrate rather than to chemical changes.

C. No significant nitrogen pick-up is noted after coating.

D. Softening of the substrate is noted after coating.

E. Increases (500° F) in DBTT are seen after 2100°F exposures with more pronounced changes seen with either cyclic exposure or longer exposure times.

F. Increases in DBTT and surface cracking propensity are enhanced by aluminum interdiffusion rather than by nitrogen ingression for 2100°F exposures. As compared with the 2ϕ coating system, it would appear that diffusion depth in the iron aluminum system is less significant in increasing the DBTT.

G. In general, surface cracking per-se does not preclude the attainment of a successful bend but at temperatures in excess (300°F) of those seen with the 2ø simple aluminum system.

H. Exposures at 2400°F produced successful bends only in the 1500°F - 1600°F range with little differences seen between cyclic and non cyclic exposure and long (100 hours) and short times.

I. Even in argon atmospheres, the susceptibility to nitrogen diffusion of substrate coated with iron-aluminum is significant although far less than with bare material. With this system, however, little or no differences in nitrogen pick-up were seen when comparing 2100°F and 2400°F exposed specimens.

These results were different from those obtained with the 2ø system whereby higher temperatures produced greater nitrogen pick-up.

J. Exposure at 2400°F in pure nitrogen with its attendant increase in hardness and metallographic identification of nitrides proved that the protection of the Cr-5W-Y alloy is probably attained by virtue of an iron containing unidentified $AlCr_2O_4$ type of compound.

K. Coating microhardness per-se either before or after exposure is not a good indication of a systems' DBTT.

L. In general, it would appear that the Fe-Al system is somewhat superior to the 2ø system in protective ability but inferior in almost all respects with regards its DBTT.

This summary as in the case of the 2ø system would indicate that this system also shows significant promise as a means of protecting chromium base alloys from oxygen-nitrogen attack at the temperatures evaluated.

4
CONCLUSIONS

4.1 GENERAL

The following conclusions were drawn from all the work conducted to date on this program:

A. Aluminum base coatings offer a marked increase in the oxidation and nitrification resistance of the Cr-5W-Y prototype alloy evaluated.

B. Although most of the modifications studied improved the alloy's resistance to corrosive attack, a simple aluminum and Fe-Al coating offered the greatest benefit.

C. The protectiveness of the systems were directly proportional to both the concentration and depth of the aluminum present.

D. The formation of a Cr_5Al_8 intermetallic compound at the surface of a simple aluminum coating system provided the best corrosion resistance seen with simple aluminum systems.

E. Al-Co-Ti, Al-Fe-Co, Al-Co, and Al-Ti systems in the range of compositions tested showed very poor promise as oxidation-nitrification resistant systems.

F. Deposition of Co onto the Cr-5W-Y alloy proved impossible.

G. Aluminum type glassy phase coatings appear to show little promise.

H. Oxidation and nitrification of the Cr-5W-Y alloy upon coating failure appears to follow classically accepted theory.

I. Coating life appears to be quite dependent upon the type of cyclic test employed, i.e. for a given temperature, coating failure occurs in shorter times the greater the number of cycles performed. However, it should be noted that the coating life dependency on total thermal cycles increases as the test temperature increases.

J. Far shorter coating life for either simple aluminide or iron-aluminum coatings is noted under dynamic rather than static conditions.

K. For the most part, oxidation rates at 1800°F and 2100°F are parabolic with higher order rates noted at 2400°F. Further, deviations from parabolic behavior appear to be somewhat prevalent with two phase systems.

L. Visual appearance did not in fact predict coating failure. The presence of Cr_2O_3 (green) did not necessarily constitute failure, but rather some minor oxidation of the substrate. It should be noted that actual failure was considered to have occurred when catastrophic oxidation and/or nitrification took place.

M. The absence of oxygen during elevated temperature exposure results in almost catastrophic nitrification of the substrate. These data thus serve to prove that Cr/Al alloys per-se are not resistant to nitrogen attack. The oxygen is necessary so as to form at the surface a Cr-Al-O spinel type compound.

N. In the systems studied, the presence of $AlCr_2O_4$ and an Fe-Al-O type compound is responsible for protection against nitrogen attack.

O. DBTT testing showed that the degradation in properties associated with the coating cycle are due only to thermal effects, i.e. recrystallization of the substrate.

P. Upon exposure to 2100°F and 2400°F temperatures, DBTT values of coated material (Fe-Al or 2ϕ) are significantly increased.

Q. Increases in DBTT upon elevated temperature exposure appear to be primarily related to

1) Diffusion of aluminum into the substrate, and, less importantly,

2) Saturation of the coating with interstitials.

R. DBTT values for the 2ϕ coating system, in general, are lower than for the Fe-Al coating.

S. Nitrification resistance of the Fe-Al coating in air or nitrogen, especially at 2400°F, is better than the 2ϕ system.

T. Longer exposure times and/or cyclic type tests (especially for the 2ϕ system) appear to increase the DBTT values.

U. Cracks forming in the coating, perpendicular to the surface, appear at low temperatures (DBTT), and propagate into the substrate, thus yielding poor DBTT values.

5

RECOMMENDATIONS

Based on all the information developed in the course of this work, several recommendations can be made as follows:

A. A continued study of the Fe-Al system be made so as to possibly optimize the composition of this system which has shown considerable resistance to nitrogen attack.

B. A more basic study should be conducted on the effects of spinel forming elements on the oxidation-nitrification resistance of Cr-Al alloys in the range of Cr/Al composition evaluated in this program.

C. Further oxide stabilizers be added to the substrate alloy under evaluation.

D. A study of the effects of pre-oxidized (in pure oxygen) aluminum and modified aluminum coatings on the oxidation-nitrification resistance of a prototype Cr alloy.

E. An aluminum diffusion-barrier or interstitial sink type coating system be evaluated. It should, however, be noted that based on the work conducted here, a coating which in fact absorbs the interstitial elements produces high DBTT. An Al diffusion barrier approach will, however, preclude the high DBTT's associated with aluminum diffusion upon exposure.

DISTRIBUTION LIST FOR FINAL REPORTS

CONTRACT NAS3-7273

	ADDRESSEE		NUMBER OF COPIES
1.	NASA Headquarters 600 Independence Avenue, S.W. Washington, D.C. 20546 Attention: N.F. Rekos (RAP)		1
	R.H. Raring (RRM)		1
	G. Deutsch (RRM)		1
2.	NASA-Lewis Research Center 21000 Brookpark Road Cleveland, Ohio 44135 Attention: Technology Utilization Office	M.S. 3-19	1
	Report Control Office	M.S. 5-5	1
	Fluid System Components Division		
	I.I. Pinkel	M.S. 5-3	1
	P.T. Hacker	M.S. 5-3	1
	Air-Breathing Engine Division		
	J. Howard Childs	M.S. 60-4	1
	R.E. Oldrieve	M.S. 60-6	5
	Dr. W.H. Roudebush	M.S. 60-6	1
	A. Anglin	M.S. 60-6	1
	Air-Breathing Engine Procurement Section		
	John H. De Ford	M.S. 60-5	1
	Materials & Stresses Division		
	S.J. Grisaffe	M.S. 49-1	2
	G.M. Ault	M.S. 105-1	1
	R.W. Hall	M.S. 105-1	1
	J. Johnston	M.S. 49-1	1
	J.W. Weeton	M.S. 49-1	1
	J. Freche	M.S. 49-1	1
	H.B. Probst	M.S. 49-1	1
	Patent Counsel	M.S. 501-3	1
	Library	M.S. 60-3	2
3.	FAA Headquarters 800 Independence Avenue, S.W. Washington, D.C. 20553 Attention: F.B. Howard/SS-210		1
	Brig. Gen. J.C. Maxwell		1
4.	Supersonic Transport Office Wright-Patterson AFB, Ohio 45433 Attention: SESHS, J.L. Wilkins		2

		NUMBER OF COPIES
5.	NASA Scientific & Technical Information Facility P.O. Box 33 College Park, Maryland 20740 Attention: NASA Representative RQT-2448	6
6.	Aerospace Corporation P.O. Box 95085 Los Angeles, California 90045 Attention: Reports Acquisitions	1
7.	Air Force Flight Dynamics Laboratory (FDTS) Wright-Patterson AFB Dayton, Ohio 45433 Attention: SM Sgt. Jesse C. Ingram, Jr.	1
8.	AiResearch Manufacturing Company 9851-9951 Sepulveda Blvd. Los Angeles, California 90009 Attention: H.H. Block, Senior Metallurgist	1
9.	Alloy Surfaces, Inc. 100 South Justison St. Wilmington, Delaware Attention: George H. Cook	1
10.	AVCO Space Systems Division Lowell Industrial Park Lowell, Massachusetts 01851 Attention: Allan S. Bufferd	1
11.	American Society for Metals Metals Park Novelty, Ohio 44073 Attention: Dr. Taylor Lyman	1
12.	U.S. Army Materials Research Agency Watertown, Massachusetts 02172 Attention: M. Levy	1
13.	Battelle Memorial Institute 505 King Avenue Columbus, Ohio 43201 Attention: Defense Metals Information Center (DMIC) Dr. R.I. Jaffee E.S. Bartlett	1 1 1
14.	Bendix Corporation Research Laboratory Division Southfield, Michigan 48075 Attention: W.M. Spurgeon, Head, M & P Dept.	1

		NUMBER OF COPIES
15.	Boeing Company P.O. Box 733 Renton, Washington 98055 Attention: W.E. Binz, Jr. SST Unit Chief	1
16.	Bureau of Naval Weapons Department of the Navy Washington, D.C. 20025 Attention: I. Machlin C. Gilmore RRMA23	1 1
17.	Consolidated Controls Corporation 15 Durant Avenue Bethel, Connecticut 06801 Attention: J.H. O'Neill	1
18.	Corning Glass Works Corning, New York 14830 Attention: James E. Durham	1
19.	Chromizing Corporation 2100 West 139th Street Gardena, California 90249 Attention: M.R. Commanday	1
20.	City College of the City University of New York School of Engineering & Architecture Department of Chemical Engineering New York, New York 10031 Attention: M. Kolodney R.A. Graff	1 1
21.	Curtiss-Wright Corporation Metals Processing Division 760 Northland Avenue Buffalo, New York 14215 Attention: B. Triffleman	1
22.	Denver Research Institute University Park Denver, Colorado 80210 Attention: Dwight G. Moore	1
23.	Douglas Aircraft Company, Inc. Astropower Laboratory Santa Monica, California 90406 Attention: Dr. N.A. Tiner	1
24.	E.I. DuPont de Nemours & Company 1007 Market Street Wilmington, Delaware 19898 Attention: L. Monson	1
25.	Fansteel Metallurgical Corporation #1 Tantalum Place North Chicago, Illinois 60064 Attention: Dr. D.K. Priest L.M.Raring	1 1

		NUMBER OF COPIES
26.	Materials Development Dept. Turbine Operations Ford Motor Company 20000 Rotunda Drive P.O. Box 2053 Dearborn, Michigan 48123 Attention: J.A. Petrusha (Rm. E-1166)	1
27.	General Dynamics Corporation General Dynamics/Convair P.O. Box 1950 San Diego, California 92112 Attention: Dr. J. Kerr	1
28.	General Electric Company Advanced Technology Laboratories Schenectady, New York 12305	1
29.	General Electric Company Lamp Metals & Components Department Clevelani, Ohio 44117 Attention: G. Oxx	1
30.	General Electric Company Materials Devel. Lab. Oper. Advanced Engine & Technology Dept. Cincinnati, Ohio 45215 Attention: L.P. Johnke W. Chang D. Levine M. Levinstein	1 1 1 1
31.	General Motors Corporation Allison Division Materials Research Indianapolis, Indiana 46206 Attention: D. Hanink	1
32.	General Technologies Corporation 708 North West Street Alexandria, Virginia 22314 Attention: James C. Withers	1
33.	Howmet Corporation Misco Division One Misco Drive Whitehall, Michigan 49461 Attention: S. Wolosin	1
34.	Hughes Research Laboratories 3011 Malibu Canyon Road Malibu, California 90265 Attention: Rodger Turk	1

		NUMBER OF COPIES
35.	IIT Research Institute Technology Center Chicago, Illinois 60616 Attention: V. Hill	1
36.	Internation Nickel Company Paul D. Merica Research Laboratory Sterling Forest Suffern, New York 10901 Attention: Dr. F. Decker	1
37.	Ling-Temco-Vought Research Center Dallas Division P.O. Box 5003 Dallas, Texas 75222 Attention: Coating Research	1
38.	Lockheed Missiles & Space Division Dept. 52-30 Palo Alto, California 94304 Attention: R.A. Perkins	1
39.	Massachusetts Institute of Technology Department of Metallurgy Rm. 8-305 77 Massachusetts Avenue Cambridge, Massachusetts 02138 Attention: Prof. N.J. Grant	1
40.	McDonnell Aircraft Corporation Lambert-St. Louis Municipal Airport St. Louis, Missouri 63166 Attention: J.D. Culp	1
41.	Melpar, Inc. 3000 Arlington Blvd. Falls Church, Virginia 22903 Attention: H.Hahn	1
42.	Narmco Research & Development Division Whittaker Corporation 3540 Aero Court San Diego, California 92123 Attention: Dr. F.J. Riel, Technical Director	1
43.	North American Aviation, Inc. Rocketdyne Division 6633 Canoga Avenue Canoga Park, California 91303 Attention: Dr. S.D. Brown	1
44.	North Star Research and Development Institute 3100 - 38th Avenue, South Minneapolis, Minnesota 55406 Attention: M. Browning	1

		NUMBER OF COPIES
45.	Ohio State University Columbus, Ohio 43210 Attention: Prof. M.G. Fontana Chairman, Dept. of Metallurgical Eng.	1
46.	Pratt & Whitney Aircraft Division United Aircraft Corporation 400 Main Street East Hartford, Connecticut 06108 Attention: E.F. Bradley C.C. Goodrich	1 1
47.	Solar, A Division of International Harvester 2200 Pacific Highway San Diego, California 92112 Attention: A.R. Stetson J.V. Long	1 1
48.	Sylvania Electric Products Sylcor Division Cantiague Road Hicksville, Long Island, New York 11802 Attention: L. Sama	1
49.	Texas Instruments P.O. Box 5303 Dallas, Texas 75222 Attention: Materials R & D Lab	1
50.	Titanium Metals Corporation of America Technical Service 233 Broadway New York, New York 10007 Attention: W. Minkler, Manager	1
51.	TRW Inc. TRW Electromechanical Division 23555 Euclid Avenue Cleveland, Ohio 44117 Attention: J. Gadd Dr. A.S. Nemy	1 1
52.	Union Carbide Corporation Stellite Division P.O. Box 746 Kokomo, Indiana 46901 Attention: Reference Librarian	1
53.	Universal-Cyclops Steel Corporation Bridgeville, Pennsylvania 15017 Attention: C.P. Mueller	1
54.	Uiversity of California at Los Angeles Los Angeles, California 90024 Attention: Dr. G. Hoffman	1

		NUMBER OF COPIES
55.	University of Dayton Research Institute 300 College Park Avenue Dayton, Ohio 45409 Attention: John Wurst	1
56.	University of Pittsburgh Metallurgical Department Pittsburgh, Pennsylvania 14213 Attention: Dr. G.R. Fitterer	1
57.	University of Washington Ceramics Department Seattle, Washington 98101 Attention: Dr. J. Mueller	1
58.	Vitro Laboratories 200 Pleasant Valley Way West Orange, New Jersey 07052 Attention: M. Ortner	1
59.	Westinghouse Electric Corporation Research Laboratories Pittsburgh, Pennsylvania 15235 Attention: R. Grekila	1
60.	Whitfield Laboratories P.O. Box 287 Bethel, Connecticut 06801	1
61.	U.S. Atomic Energy Commission Washington, D.C. 20545 Attention: William C. Gough	1
62.	Headquarters, USAF Air Force Office of Scientific Research Propulsion Research Division Washington, D.C. 20025 Attention: Dr. M. Slawsky	1
63.	Defense Documentation Center (DDC) Cameron Station 5010 Duke Street Alexandria, Virginia 22314	1
64.	AFML Wright-Patterson AFB, Ohio 45433 Attention: N. Geyer (MAMP) Dr. A.M. Lovelace, Chief, Scientist E. Beardslee (MAAE)	1 1 1
65.	Department of the Navy ONR Code 429 Washington, D.C. 20025 Attention: Dr. R. Roberts	1

		NUMBER OF COPIES
66.	Chief, Bureau of Naval Weapons Department of the Navy Washington, D.C. 20025 Attention: RRMA-2	1
67.	NASA-Langley Research Center Langley Station Hampton, Virginia 23365 Attention: Technical Library E.E. Mathauser Irvin Miller MS 214	1 1 1
68.	NASA-Manned Spacecraft Center Structures & Mechanics Division 2101 Webster-Seabrook Road Houston, Texas 77058 Attention: Branch Chief (ES441)	1